Spatial Assessment of Boreal Forest Carbon

A DISSERTATION
SUBMITTED TO THE FACULTY OF
UNIVERSITY OF MINNESOTA
BY

Terje Kristensen

IN PARTIAL FULFILLMENT OF THE REQUIREMENTS
FOR THE DEGREE OF
DOCTOR OF PHILOSOPHY

Dr. Paul V. Bolstad, Advisor

June 2015

Acknowledgements

I would like to express my sincere gratitude to my advisor, and good friend, Professor Paul Bolstad for his endless encouragement and support. Your insight, enthusiasm, and patience were instrumental in my achievement. Our shared interests in the world around us—beyond merely my research—ensured that my PhD experience enriched me both intellectually and personally.

I would also like to thank my experienced committee members: Professor Alan Ek, Dr. Randy Kolka, and Dr. Charles Perry. Your invaluable guidance and input throughout this process greatly contributed to my dissertation. In addition, I would be remiss without sharing my humble appreciation for the two people who put me on this track to begin with—Professor Mikael Ohlson and Professor Erik Næsset. I am thankful for the opportunity to have worked in this field and for your continued commitment to my research over the years. Moreover, I was fortunate to have the financial support of several great institutions including the Norwegian University of Life Sciences, Fulbright Foundation, Norwegian Research Council, and Torske Klubben Minneapolis.

Last, but certainly not least, I would like to offer my heartfelt thanks to my parents. None of this could have been attained without your unconditional love and encouragement. Your unwavering support has been my crutch throughout this process, and this degree is as much yours as it is mine.

i

Abstract

The ability to accurately map and monitor forest carbon (C) has gained global attention as countries seek to comply with international agreements to mitigate climate change. However, attaining precise estimates of forest C storage is challenging due to the inherent heterogeneity occurring across different scales. To develop cost-effective sampling protocols, there is a need for more unbiased estimates of the current C stock, its distribution among forest compartments and its variability across different scales. As a contribution to this work, this dissertation used high-resolution field measurements of C collected from different forest compartments across a boreal forest stand in South East Norway.

In the first paper, we combined the use of airborne scanning light detection and ranging (lidar) systems with fine-scale spatial C data relating to vegetation and the soil surface to describe and contrast the size and spatial distribution of C pools across the forest. We found that predictor variables from lidar derived metrics delivered precise models of above and belowground tree C, which comprised the largest of the measured C pool in our study. We also found evidence that lidar canopy data correlated well with the variation in field layer C stock. By using topographical models from lidar ground returns we were able to establish a strong correlation between lidar data and the organic layer C stock at a stand level. In the search for an effective tool to measure and monitor forest C pools, we found the capabilities of lidar to map forest C encouraging.

In the second paper, we used a geostatistical approach to analyze the fine-scale heterogeneity of the soil organic layer (forest floor) C storage. Our results showed that the C stocks were highly variable within each plot, with spatial autocorrelation distances < 3 m. Further, we established that a minimum of 20 to 25 inventory samples is needed to determine the organic layer C stock with a precision of ±0.5 kg C m^{-2} in inventory plots of ~2000 m^2.

In the third paper, we investigated how the short-range spatial variability of organic layer C affects sampling strategies aiming to monitor and detect changes in the C stock. We found that sample repeatability rapidly declines with sample separation distance, and the *a priori* sample sizes needed to detect a change a fixed change in the organic layer C stock vary by a factor of ~4 over 15 to 125 cm separation distance. Unless care is taken by the surveyor to ensure spatial sampling precision, substantially larger samples sizes, or longer time intervals between baseline sampling and revisit are required to detect a change.

In the final paper, we utilized the nested sampling protocol to investigate the spatial variability of organic layer C across different scales and incorporated inventory expenses in the development of a cost-optimal sampling approach. Because precise estimates are costly to obtain, it is of great interest for surveyors to develop cost-efficient sampling protocols aimed at maximizing the spatial coverage, while minimizing the estimate variance. We found that the majority of the estimate variance is confined within

small subplots (100 m^2) of the forest (25 km^2), emphasizing the importance of considering the short-range variability when conducting a large-scale inventory. Further, this chapter demonstrated how optimal allocation of sampling units (plot, subplot and sample) is not only a function of the variance component within that dimension, but also changes with the sampling unit costs and the acceptable margin of error. We found that the costs of conducting an organic layer C inventory could be reduced by more than 60% by increasing the inventory uncertainty from ±0.25 Mg C ha^{-1} to ±0.5 Mg C ha^{-1}. Finally, we established that sampling costs can be reduced with as much 80% by conducting a double sampling procedure that utilizes the correlation between organic layer C stock (r = 0.79 to 0.85) and measurements of layer thickness.

Table of Contents

Chapter 3: Spatial variability of organic layer thickness and carbon stocks in mature boreal forests stands – Implications and suggestions for sampling designs

Chapter 4: Relocation of paired samples: Implications for soil C monitoring

Chapter 5: Optimum sampling allocation: Reducing the costs of organic layer C stock inventories in boreal forests using a double sampling approach

List of Tables

List of Figures

Chapter 1: Introduction

1.1. Boreal forests carbon

Boreal forest covers over 1.2 billion ha^{-1} representing ~30% of all the Earth's forests (FAO, 2006). Two thirds of the boreal forests are situated in Eurasia, with >20% in Russia alone, and the remaining third in Canada and northern United States (Bradshaw et al., 2009). Although boreal forests are characterized by relative simple vegetation with few dominant species, the composition is a result of complex dynamics between climate, topography, geology, and disturbances (Soja et al., 2007). As a result of these interactions, boreal forests are the largest reservoir of terrestrial carbon (C) and a vital net sink in the global C cycle (Bonan, 2008). It is estimated that boreal forests alone is responsible for ~22% of the global residual terrestrial CO_2 uptake between 1900 and 2007 (Pan et al., 2011). This circumpolar region is of particular interest because it is situated at latitudes expected to undergo great climatic change in the coming decade (Chapin et al., 2000; Nabuurs et al., 2007), possibly altering the C sink strengths and current C stock (Koven, 2013; Kurz et al., 2008; Soja et al., 2007). Today most studies exploring the role of boreal forests in the global terrestrial C cycle rely on simulations (Baritz et al., 2010; Kurz et al., 2008), but because limited empirical data is available we currently have inconsistent mechanistic models with coarse resolution and a high degree of uncertainty (Ortiz et al., 2013; Pan et al., 2011). If we are to resolve conflicts in these

models, and later verify the hypothesis on feedbacks between forest processes and the atmosphere, we need more observations from local stands integrated with tools that may be employed over larger areas. In addition, developing the capabilities of estimating and verifying changes in forest C at the field level may be of substantial monetary value under international C trading regimes (Poussart et al., 2004).

While widespread attention has been given to methods and tools for mapping and monitoring the C storage in trees (Hudak et al., 2012; Stephens et al., 2012), less is known about the role of the understory vegetation and C storage in soils. Although the understory vegetation usually contains a relatively small portion of the forest C stock at a given time, it may produce as much as 10 to 35% of the total annual input of organic litter to the soil (Havas and Kubin, 1983; Muukkonen and Mäkipää, 2006). Despite being a key component in the boreal forest C cycle (Nilsson and Wardle, 2005), it is often left out of forest C models due to the lack of empirical evidence (Liski et al., 2002).

Boreal forest soils represent a large C pool characterized by high spatial and temporal variations (Callesen et al., 2003; Häkkinen et al., 2011). Of particular interest is the top soil organic layer, as it is believed that the most rapid and profound changes in soil C will occur here (Gaudinski et al., 2000; Trumbore, 2009). This is due to the tight coupling between soil processes and properties of vegetation structure (Hogberg and Read, 2006; Wardle et al., 2004; Wardle et al., 2012). The complex configuration of the organic layer C pool is not a result of linear and additive sets of causes, but is instead

affected by a range of interrelated environmental variables, each with a number of potential effects, making precise mapping and monitoring of organic layer C a formidable task. To avoid considerable uncertainty in C estimates it is essential to consider the spatial dependency of soil properties, meaning that proximal measurements tend to have more similarities than distant ones (Post et al., 2001). Although there is a general awareness that robust planning of soil C inventories requires some explanatory data on the spatial variability when developing sampling protocols (Lark, 2012), most earlier surveys, which form the basis of most meta-studies and modeling efforts, have been conducted under the assumption of random spatial variability. Consequently systematic biases have likely been introduced in many regional and national estimates (Ortiz et al., 2013).

1.2. *Rationale of study*

The efficiency, accuracy, and cost of estimating and monitoring forest C can be considerably improved by developing sampling protocols guided by statistical, operational and site-specific conditions. One promising method for mapping forest C stocks is airborne laser scanners, and in particular light detection and ranging (lidar). Lidar measures the elapsed time between the emission of a pulse of laser light and the reflected wave of energy back to the sensor (Lefsky et al., 1999). Because the waveform is proportional to energy reflected from vegetation at various heights, processed lidar data provides a three-dimensional description of forest structure. Lidar has already

3

demonstrated a great potential for forestry purposes, such as precise estimates of above and belowground biomass (Hudak et al., 2012; Lefsky et al., 1999; Næsset and Gobakken, 2008; Stephens et al., 2012). Lidar can therefore be used to comply with various international conventions such as the Kyoto Protocol to the United Nations Framework Convention on Climate Change (UNFCCC). Some countries, such as New Zealand, already use lidar in an operational forest C inventory system as part of their commitment to the Kyoto Protocol (Beets et al., 2010; Stephens et al., 2012). Since lidar-derivable forest properties, such as volumetric measurements, species composition, and topographical features, have all been linked to understory vegetation and organic layer C in earlier ecological studies (Hansson et al., 2011; Hogberg and Read, 2006; Stendahl et al., 2010), lidar data may contain valuable information about structures affecting the C stocks of several forest compartments. Albeit a few studies have attempted to use lidar data for other purposes than mapping standing biomass, no study has yet explored the multi-purpose potential of lidar data for mapping multiple forest C compartments.

Similarly, there is need for direct quantification on the amount and spatial variability of organic layer C stocks (Baritz et al., 2010; Ortiz et al., 2013). Knowledge of the magnitude of organic layer C variability across different scales can ensure unbiased investigations, and assist future surveys in optimally allocating sampling efforts. Despite the importance of considering spatial variability in C estimates, data with high spatial resolution on the organic layer C stock in boreal forests remains scarce. Two studies

4

conducted on managed young and middle-aged forest stands in Finland did produce strong spatial dependencies in the first few meters for soil C in the organic layer (Häkkinen et al., 2011; Muukkonen et al., 2009). However, due to the confounding effects different management practices have on soil attributes, spatial assessments of C in soils from actively managed forests are problematic (Finer et al., 2003; Hedde et al., 2008; Schulp et al., 2008). More information about the variability in undisturbed soils is therefore required.

Organic layer C estimates with acceptable levels of uncertainty commonly require a large number of observations (Birdsey, 2004), making the costs associated with such measurements high (Mäkipää et al., 2008). Soil C measuring and monitoring programs face a critical dilemma when implemented: maximizing the estimate precision and spatial coverage of the C inventory while minimizing the sampling effort (de Gruijter, 2006). The surveyor must therefore decide on the number of observations required and how to optimally distribute the sampling effort to minimize the estimator variance, or where resources are limited, determine the degree of accuracy possible under the given resource constraints (Peltoniemi et al., 2004; Post et al., 2001; Ståhl, 2004). As most expenses in soil C assessments occur during sample collection and laboratory analysis (Mäkipää et al., 2008; Singh et al., 2013), substantial cost-reduction may be possible by incorporating knowledge about spatial variability when distributing sampling units across the area of interest. A second approach to improve the economic feasibility of soil C inventories and

verification protocols is to incorporate a double sampling strategy, collecting data on an inexpensive auxiliary variable highly correlated to the principal variable of interest (Cochran, 1977). However, the potential cost-benefits of a double sampling strategy for organic layer C measurements have not yet been assessed in detail.

1.3. *Dissertation goals and objectives*

The overarching goal of the work in this dissertation is to advance our understanding of the spatial distribution of organic carbon (C) stocks across boreal forests ecosystems. The work quantifies organic C storage in different forest compartments, assesses the variability across different scales, and explores the main challenges we are facing when aiming to precisely estimate and monitor changes in forest C stocks.

Chapter 2 of this dissertation aims to provide a foundation for future research concerning the use of airborne small footprint scanning lidar for assessing and monitoring boreal forest C. To analyze this relationship we combine lidar with fine-scale spatial C data to describe and contrast the size and spatial distribution of C pools in multilayered boreal forests plots. The main goals of Chapter 3 are to assess and quantify the short-range variability of organic layer C in undisturbed boreal forest soils and provide references against which subsequent and future sampling schemes may be evaluated. In Chapter 4, we discuss how the observed spatial variability in organic layer C affects sampling protocols aimed at detecting changes in the C stock. The chapter assesses the implications of short-range variability on paired sampling requirements, and explores the

trade-offs between relocation accuracy and time between baseline measurements and revisit.

Finally, Chapter 5 provide a case study for optimizing sampling in organic layer C inventories across a forest by setting out methods and showing the considerations under which such studies should be conducted. It also incorporates a simulation on how expenditures affect optimal allocation of sampling units, and investigates the cost-efficiency of a double sampling approach, using measurements of organic layer thickness as an auxiliary variable.

Chapter 2: Airborne lidar as a tool for mapping above and belowground carbon pools in boreal conifer stands

Terje Kristensen[a*], Erik Næsset[b], Mikael Ohlson[b], Paul Bolstad[a], Randall Kolka[c]

[a] Department of Forest Resources, University of Minnesota, 115 Green Hall, 1530 Cleveland Ave. N., St. Paul, MN 55108, USA

[b] Department of Ecology and Natural Management, Norwegian University of Life Sciences, P.O.Box 5003, 1432 Ås, Norway

[c] USDA Forest Service, Northern Research Station, 1831 Hwy 169 East, Grand Rapids, MN 55744, USA

Summary

A large and growing body of evidence has demonstrated that airborne scanning light detection and ranging (lidar) systems can be an effective tool in measuring and monitoring above-ground forest tree biomass. However, the potential of lidar as an all-round tool for assisting in assessment of carbon (C) stocks in soil and non-tree vegetation components of the forest ecosystem has been given much less attention. Here we combine the use airborne small footprint scanning lidar with fine-scale spatial C data relating to vegetation and the soil surface to describe and contrast the size and spatial

distribution of C pools within and among multilayered Norway spruce (*Picea abies*) stands. Predictor variables from lidar derived metrics delivered precise models of above- and below-ground tree C, which comprised the largest C pool in our study stands. We also found evidence that lidar canopy data correlated well with the variation in field layer C stock, consisting mainly of ericaceous dwarf shrubs and herbaceous plants. However, lidar metrics derived directly from understory echoes did not yield significant models. Furthermore, our results indicate that the variation in both the mosses and soil organic layer C stock plots appears less influenced by differences in stand structure properties than topographical gradients. By using topographical models from lidar ground returns we were able to establish a strong correlation between lidar data and the organic layer C stock at a stand level. Increasing the topographical resolution from plot averages (~2000 m^2) towards individual grid cells ($1m^2$) with distinct sampling points did not yield consistent models. Our study demonstrates a connection between the size and distribution of different forest C pools and models derived from airborne lidar data, providing a foundation for future research concerning the use of lidar for assessing and monitoring boreal forest C.

2.1.   Introduction

The boreal forest is a vital net sink in the global carbon (C) cycle, being responsible for ~22% of the global residual terrestrial CO_2 uptake between 1900 and 2007 (Pan et al., 2011). The boreal forest zone is of particular interest because it is

situated at latitudes undergoing great climatic stress, possibly altering its current role as a C sink (Nabuurs et al., 2007). Most studies exploring the role of boreal forests rely on simulations (Baritz et al., 2010; Kurz et al., 2008), but limited empirical data even in regions subject to intense investigation, result in models with coarse resolution and a high degree of uncertainty. To improve estimates and model accuracies of C stocks and fluxes, more direct observations from local stands are needed. Accurate reporting of the C stocks in forested ecosystems is also a requirement for countries ratifying the Kyoto protocol to the United Nations Framework Convention on Climate Change (UNFCCC). To monitor, report, and verify C stocks, there is a need for repeatable, cost-effective remote sensing methods to estimate above- and below-ground biomass components over large areas. Airborne scanning light detection and ranging (lidar) systems have been acknowledged to have a strong potential for monitoring C pools (Ahern et al., 1998).

Lidar measures the elapsed time between the emission of a pulse of laser light and the reflected wave of energy back to the sensor. The waveform is proportional to the amount of reflectance of vegetation at various heights as the pulse travels through the canopy towards the ground. Systems recording the entire waveform is becoming more common, but most airborne scanning lidar systems used for operational purposes have to date mainly been discrete return systems by which a maximum of 4 to 5 individual echoes typically have been recorded for each pulse. When the ground is determined from the last return, time is converted to distance giving discrete vertical measurement

(echoes) of the forest. After the lidar data have been processed, lidar provides a three-dimensional description of the structure of the forest. Airborne lidar is usually integrated with a high precision Global Navigation Satellite System (GNSS), which records the position of the platform so each echo can have a position accuracy of < 0.1 m (Ahokas et al., 2003). The technology has been widely used for forestry purposes, generating data on stem volume (Holmgren, 2004; Næsset, 1997b), canopy height (Magnussen et al., 1999; Næsset, 1997a; Næsset and Økland, 2002), and basal area (Holmgren, 2004; Næsset, 2002). Because these biophysical properties are closely associated to tree biomass, which can be computed by allometric equations, studies have successfully demonstrated the use of lidar for both above- and below-ground biomass estimates (Næsset and Gobakken, 2008). Thus, tree biomass data derived from airborne lidar can be used to comply with various international conventions requiring reports on C storage in trees. For example, New Zealand uses lidar in an operational forest C inventory system as part of their commitment to the Kyoto Protocol (Beets et al., 2010; Stephens et al., 2012).

Boreal forest soils represent a large C pool characterized by high spatial and temporal variations (Callesen et al., 2003; Häkkinen et al., 2011), making accurate assessments of soil C expensive and labor intensive (Mäkipää et al., 2008). For purposes such as investment planning in forest C offset projects, the variability and rate of soil C accumulation and storage is a major challenge. Because the loss of value is often smaller than the cost of accurate measurements, offset projects regularly ignore potential C

credits from this compartment (Pearson et al., 2007). Of particular interest for C mapping is the organic layer of boreal forest soils, as it is believed that the most rapid and profound changes from a changing climate will occur here, due to the tight coupling between soil processes and properties of vegetation structure (Wardle et al., 2012; Yarwood et al., 2009). Although lidar cannot provide direct measurements of soil C , it delivers accurate measurements of stand structure properties such as volumetric forest properties (Holmgren, 2004; Holmgren et al., 2003; Kankare et al., 2013) and species composition (Holmgren et al., 2008; Ørka et al., 2009), which all have been linked to the organic layer C stocks and fluxes in earlier ecological studies (Hansson et al., 2011; Hogberg and Read, 2006; Stendahl et al., 2010). A particularly promising aspect of small footprint laser data, compared to other remote sensing imagery such as optical sensors (Mulder et al., 2011), is the ability to map topographical features with high detail (Hyyppä et al., 2008). Local topography have been acknowledged to be a strong predictor for accumulation of C in top soil horizons (Seibert et al., 2007; Simonson, 1959), and surveyors have utilized digital elevation maps (DEM) from remote sensing as auxiliary information in mapping organic layer C (Seibert et al., 2007; Thompson and Kolka, 2005).

Trees and forest soils have received widespread attention for their role and importance in C cycling, but less is known about the role of the forest understory vegetation. Although usually containing a relatively small portion of the forest C stock at

a given time, understory vegetation can produce as much as 10 to 35% of the total annual input of organic litter (Havas and Kubin, 1983; Muukkonen and Mäkipää, 2006). Despite being a key component in the forest C cycle (Nilsson and Wardle, 2005), it is often left out of forest C models due to the lack of empirical evidence (Liski et al., 2002). The productivity of the understory vegetation is strongly associated with light availability, which in turn is a result of the above-ground dynamics such as species composition (Barbier et al., 2008), development phase (Pase and Hurd, 1958), and time since local disturbances (Alaback, 1982). Above-ground features, such as canopy structure can be precisely computed from the use of lidar (Korhonen et al., 2011). Compared to conventional optical remote sensing such as Landsat, returns from lidar have the advantage of mapping three-dimensional surface structures, which includes information on surfaces below canopies, such as the understory vegetation. Thus, recent studies have successfully used structural parameters from lidar as proxies for understory light availability (Alexander et al., 2013) and to map understory species abundance and distribution (Hill and Broughton, 2009; Martinuzzi et al., 2009; Nijland et al., 2014; Peckham et al., 2009).

Despite an urgent need of more information about forest C pools and efficient methods for monitoring and sustainable management, no studies have yet attempted to employ secondary information from lidar, such as canopy gap structure, non-canopy echo densities, and ground echoes (topographical features) to model the C stock in multiple

forest compartments. The objective of the present study was to explore the effectiveness of using airborne small footprint and discrete return lidar to estimate C stocks in living forest compartments and the soil organic layer in multilayered boreal conifer stands. The focus was on identifying lidar derived variables which may have potential for future prediction models in forest C assessments. Furthermore, we also investigate the scale effects of the relationships between lidar variables and field measurements. To enable a quality assessment of how lidar copes with the natural heterogeneity, all stands used in this study are mature, multilayered boreal spruce forests, which have not been impacted by any form of forest practices in the last century (Lie et al., 2012).

2.2. Methods

2.2.1. *Study area*

Eight circular study plots with a 50 m diameter (~2000 m^2) were positioned in mature and multilayered spruce forests in the Årum – Kapteinstjern area, located approximately 35 km north of Skien in Telemark County, SE Norway (Fig. 1 and Table 1). Six of the eight plots were selected randomly, i.e. four were positioned by random in the forest landscape SW of the lake Årumvannet, and two were randomly positioned adjacent to the forest landscape near Lake Kapteinstjern. Here, were also two plots located subjectively to cover the occurrence of the red-listed lichen *Usnea longissima*, see lichen study by Lie et al (2009). The area is considered situated in the border of the south – middle boreal vegetation zone (Moen, 1999). Climate is oceanic (Moen, 1999),

with an annual mean temperature approx. 3.3°C, and average extreme temperatures 14.5°C in July and -7°C in January. Annual precipitation averages 1120 mm, with a high of 115 mm in July, and a low of 60 mm in February. The study plots are located between 470 and 600 m above sea-level. The forests belong to the *Picea - Vaccinum myrtillus* type (Cajander, 1949; Kielland-Lund, 1981), which are the most abundant forest type in NW Europe. The forests are dominated by Norway spruce (*Picea abies* (L.) Karsten), but scattered occurrences of Scots pine (*Pinus sylvestris* L.) and birch (*Betula pendula* Roth and *B.pubescens* Ehrh.) are common.

The understory vegetation in the area is characterized by European blueberry (*Vaccinium myrtillus),* feather mosses (in particular *Pleurozium schreberi* and *Hylocomium splendens),* Green peat moss (*Sphagnum girgensohnii*) and Common haircap moss (*Polytrichum commune*). There is usually a distinct height difference between the overstory and understory vegetation in these forests, making these stands suitable for investigating the understory layer separately. The soils in this area are mesic to mesic/moist podzols, nutrient poor with a low pH (Nielsen et al., 2007). Spatial properties of the organic layer in these study plots are examined in Kristensen et al. (2015 – *in review*). General characteristics of the study plots are shown in Table 1, and Molinari et al. (2005) and Bjune et al. (2009) provide information about the Holocene history of the forest stands.
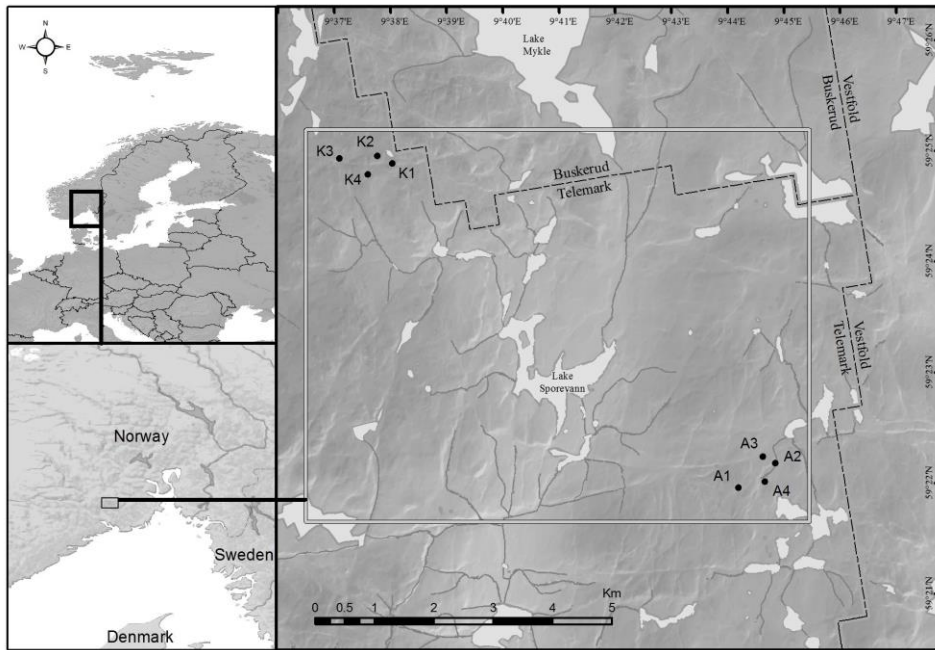
Figure 1. Location of the study plots in a boreal forest landscape in SE Norway. Plots labeled (K) are located close to the small lake Kapteinstjern, and plots labeled (A) are located SW of the lake Årumsvannet.

Table 1. General properties of study plots.

Stem density, stand age and basal area were determined from field measurements, while Aspect was computed from lidar echoes.

	Plot[†]							
	A1	A2	A3	A4	K1	K2	K3	K4
Latitude	59°36'63'	59°36'99'	59°37'10'	59°36'73'	59°41'55'	59°41'67'	59°41'64'	59°41'39'
Longitude	9°73'50'	9°74'59'	9°74'24'	9°74'26'	9°63'35'	9°62'92'	9°61'79'	9°62'61'
Altitude (m.a.s.l)	572	516	520	522	643	649	615	641
Stem density (ha^{-1})	351	611	688	652	270	484	479	565
Stand age (yrs.)	115	121	146	143	190	183	155	188
Basal area (m^2 ha^{-1})	30	26	20	20	24	28	28	17
Aspect	NW	NE	N	N	S	N	S	SE

†Plot A1 through A4 is located in Årum (A), while plot K1 through K4 is located in the Lake Kapteinstjern area.

2.2.2. Field data acquisition and preparation

To estimate standing biomass using traditional field methods we divided the trees into two classes, under and above 1.3 m tall. All trees above 1.3 m within each plot were measured for diameter at breast height (dbh) using a caliper. Then 20 trees were selected using a relascope (Bitterlich, 1984), a technique which selects trees with a probability proportional to their basal area. The selected trees were then measured in height using a Vertex hypsometer. Based on the 20 sample trees from each plot, height-diameter regression models were developed for each specific plot and species (Norway spruce, Scots Pine and deciduous spp.):

$$h = \alpha + dbh\beta + \varepsilon \qquad\qquad\qquad (1)$$

where α is the species-specific constant, dbh is the diameter at breast height, and β the plot specific regression coefficient, which in these plots ranged from 0.82 to 0.90, ε is a normally distributed error term. Basal area was calculated for all trees > 1.3 m.

Above-ground biomass was estimated on an individual tree basis as the sum of biomass components of stem with bark, branches, foliage, stumps. Each component was estimated using species-specific allometric models with dbh and height as independent variables (Marklund, 1988). Tree biomass is mainly a function of dbh and not height (Korsmo, 1995; Payandeh, 1981), but because higher stand densities generally results in more stem growth and less branch biomass (Kozlowski and Pallardy, 1997), we included height in our equations. Below-ground tree biomass (roots > 2 mm) was calculated using

18

equations developed by Petersson and Ståhl (2006) which are built upon data from Marklund (1988) using dbh only. To estimate C storage in tree compartments we followed the established practice of assuming 50% C content in tree biomass (Chapin et al., 2011; Kolari, 2004). Total plot estimates of above- and below-ground tree C stock was computed as the sum of all individual trees within each plot. Tree cores were extracted using an increment borer and individual tree age was later determined in the laboratory by analysing the growth rings.

Young tree saplings < 1.3 m were measured for height, before sixteen randomly chosen saplings on each plot were harvested. After being oven-dried (Thermax Series TS8000) at 65°C to a constant mass, the weights were used to develop a regression model for sapling biomass. The C content in this compartment was assumed to be 50%.

For our investigation of the understory vegetation and top organic layer, each plot was divided into a systematic grid containing 73 sampling points (625 cm^2), with a distance between each point being 5 m in both north-south and east-west directions (Fig. 2). All field layer vegetation (shrubs and herbaceous plants) within the quadrat was clipped at a ground level. The biomass is considered as the field layer compartment from the clip plots. For the purpose of this study, the C stock in saplings is analyzed separately and not as a part of the field layer compartment. We have based the divisions of the different compartments on traditional a priori grouping defined by discrete and measureable biological trait differences (Reich et al., 2001).

19
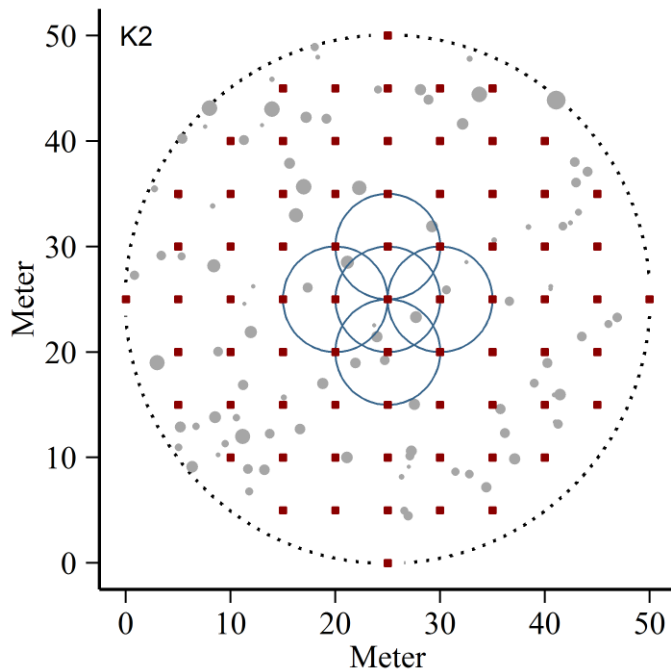
Figure 2. Sampling strategy for the eight boreal forest plots used in this study. Filled squares represent 73 sample points for field layer vegetation, mosses and the organic top soil layer. Filled circles indicate location of standing trees. Stand density measures were calculated at a plot scale (dotted circle) and in subplots with a radius of 5 m around for each of the 73 sampling points (full circles). For illustration purposes only five of the density circles are displayed.

Separate samples of both moss and soil organic layer were collected from the center of the quadrat using a cylindrical steel corer (d = 56 mm). Mosses are considered separately from field layer. However, the term understory encompasses field layer, saplings and mosses. The soil organic layer consists of the F (O_e) and H (O_a) horizon,

20

partially decomposed matter and well-decomposed organic matter, down to the mineral soil boundary. The boundary between the organic horizons and mineral soil is sharp and clear visually due to the low faunal mixing of decomposing litter in these forests. Since root biomass is estimated from the above-ground data, living roots (> 2 mm) were excluded from the soil sample to avoid any double counting. After collection, all samples were stored in separate paper bags and dried in room temperature (15 to 20°C).

Individual coordinates for each tree and field samples were acquired using two differential global positioning systems (GPS) and global navigation satellite systems (GLONASS) 40-channel dual-frequency survey grade receivers (Topcon Legacy) as field and base units. We established ground truth coordinates for the plot center and each sample collected at the end of centerlines. The distance between the plots and the base station was less than 10 km.

All samples were dried to constant mass in a drying oven at 65°C for 6 to 24 hours. Samples were then weighed again to determine dry content. To determine C concentration (C_c), samples were grounded to a size of < 100 μm using a ball mill, before the homogenized mixture was analyzed using a VarioMax EL CHN analyzer with a TCD detector (Elementar Analysensyterne GmbH, Hanau, Germany). The analysis was conducted at the Skogforsk (Ås, Norway) commercial laboratory and complied with ISO 9000 certified methods. The stock of C was estimated by multiplying the sample weight of the organic material (per unit area) with the C_c derived from the sample material.

2.2.3. Lidar data acquisition and processing

A Piper PA31-310 aircraft flying approximately 500 m above ground carried the ALTM 3100C (Optech, Canada) scanning lidar system. The pulse frequency was 100 kHz with an average pulse density of 4.5 ($\pm$ 0.8) m^{-2}. Pulses with scan angles exceeding 15° were excluded from the data. After lidar data acquisition, standard filtering procedures were used (Næsset, 2004) considering only the first and last echoes. Planimetric coordinates and ellipsoidic heights were computed from processing first and last echoes. Ground echoes were extracted from the last echo data by filtering out local maxima representing echoes from vegetation. From the planimetric coordinates and height values of each ground point retained from the last echo data, a digital elevation model (DEM) was rendered using a thin plate spline interpolation on 1m grid cells. The smoothing parameter (λ) for the interpolation was determined by generalized cross validation (Wahba, 1990). To avoid any edge effects in the DEM, the interpolation was conducted on a dataset including ground returns up to 10 m outside the plot window. The expected ellipsoidic height accuracy of the DEM is approximately 25 cm (Næsset and Gobakken, 2008).

For estimation of the living C stock (trees and understory vegetation), first and last echoes were spatially registered to the DEM according to their coordinates. The height of each individual echo (point) was then computed by subtracting terrain surface height from the first echo height. Because first echoes from tree canopies have shown to

22

be more stable than last echoes across different lidar configurations and flying heights (Næsset, 2004), we only used first echoes in the tree biomass estimates. However, for understory biomass predictions, both first echoes and combined first-last echoes were considered. Non-ground echoes from outside the plot windows were excluded from further analysis and lidar metrics were aggregated in bins representing each plot.

2.2.4. *Statistical analysis of field data*

All statistical analyzes were carried out with the software package R, version 3.0.2. (R Core Team, 2013). Standard statistical methods were used describe central trends and spread, without considering the spatial nature of the data. One-way analysis of variance (ANOVA) was used to determine if there were any statistically significant differences between means or distributions. Statistical significance was accepted at the $\alpha = 0.05$ level. Associations between parameters were described using Pearson's, Spearman rank correlation coefficient or least squares regression.

After determining the spatial properties the stems, each sample point was tested against a number of point measurements relating to the spatial configuration of stems. A nearest neighbor distance analysis was used to determine the distance from each of the sampling points to the surrounding trees. After proximity was determined we computed stem density (n m^{-2}), basal area density (m^2 m^{-2}) and above-ground biomass density (kg m^{-2}) in a radius of 5 m from each of the sampling points (Fig. 2). As sampling points close to the plot boundaries can be affected by trees outside the observation window, the

23

nearest neighbor analysis was also used to identify points positioned closer to the plot window than the given radius. These samples were excluded from further analysis to avoid errors caused by edge effects. Tree density data was evaluated against each C compartment on all eight plots using a linear regression model.

To investigate the influence of trees on the spatial characteristics of understory vegetation and organic layer C stock we used a two-step approach. First, we quantified the spatial pattern of trees using a univariate second-order analysis, Ripley's K(r) (Ripley, 1977). This function has the advantage of characterizing the spatial structure at different ranges simultaneously (Cressie, 1993), and is commonly used in ecological plant modeling studies (Dale, 1999). K(r) represents the expected number of stems in a circle with radius r centered at an arbitrary point divided by the intensity (λ) of the pattern. Isotropic edge correction was applied to get an unbiased estimator of the function (Goreaud and Pélissier, 1999; Ripley, 1977).

$$\hat{K}(r) = \lambda^{-1} \sum_i \sum_{j \neq i} \omega(l_i, l_j)^{-1} \frac{I(d_{ij} < r)}{N} \qquad (2)$$

where λ is the density of stems per unit area, d_{ij} is the distance between the ith and j^{th} points, and $I(x)$ is the indicator function. Edge correction is provided by the weight function $\omega(l_i, l_j)$ which gives 0 if stems i and j are more than distance r apart, otherwise it uses the inverse fraction of a circumference centered in i. The function was transformed with $\hat{L}(r)$ to linearize the K function and stabilize the variance (Besag, 1977). This gives

$L(r) = 0$ under a null hypothesis of complete spatial randomness, which corresponds to a Poisson pattern (CSR) (Besag, 1977; Goreaud and Pélissier, 1999):

$$\hat{L}(r) = \sqrt{\frac{\hat{K}(r)}{\pi}} - r \qquad\qquad (3)$$

Deviations of from the expected value, was tested at $L(r) - r = 0$ at distances up to 12 m. Significance was evaluated by comparing the observed data with critical values derived from 1000 Monte Carlo simulations of a null model.

2.2.5. *Modeling forest carbon stocks using lidar*

A total of 83 vegetation metrics were derived from the lidar echoes and divided into two categories, above and below 1.5 m, representing the overstory and understory vegetation (*Appendix Table A1*). From the overstory echoes standard metrics of overstory canopy heights (h) were computed. According to results in Næsset (2004) and Næsset and Gobakken (2005) the 95th percentile is found to be more accurate than maximum heights. Canopy densities (cd) were computed as the proportion of first echoes for ten intervals representing proportions of echoes from the lower canopy limit (1.5 m) up to the 95th percentile, including the mean, maximum, standard deviation and coefficient of variation (CV). Since understory conditions, such as light admittance, not only depends on the canopy right above the point of interest, we computed additional canopy densities for each plot containing buffer areas from 2 to 10 m (in 2 m intervals) outside the original plot window. Although data on the canopy density distributions are useful for individual

25

plot measurements, they are not as well suited for direct comparisons between plots. To evaluate differences in canopy characteristics between plots, we therefore computed canopy distribution for five fixed stratum bin heights (*Appendix Table A1*).

To explore the use of lidar data in mapping and quantifying understory biomass we computed understory metrics using both combined echoes and first echoes only. Two filters were applied; Filter1: including all non-ground echoes up to 1.5 m, and Filter 2: non-ground echoes 0.2 m to 1.5 m. From these four datasets (combined echoes using filter 1, combined echoes using filter 2, first only using filter 1 and first only using filter 2) we first estimated the understory intensity (U_i) as the proportion of non-overstory echoes above the given threshold. U_i is given as a fraction of the effective area covered divided by the total plot area. Second, metrics of understory heights (U_h) which includes quantiles equivalent to the 0, 10,...90th percentiles, mean, maximum, standard deviation and coefficient of variation were computed. Third, the distribution of understory echoes was classified in three separate height bins (Filter 1: 0 to 0.5 m, 0.5 to 1 m, 1 to 1.5 m, Filter 2: 0.2 to 0.5 m, 0.5 to 1 m and 1 to 1.5 m).

To further inspect the relation between overstory and understory biomass, we delineated the area into canopy or canopy gaps. Several different methods have been proposed to define forest canopy from lidar data (Gaulton and Malthus, 2010; Vehmas et al., 2011). Here we mapped the canopy at 1 m^2 raster resolution, classifying each cell depending on if the cell contained echoes from the overstory or not. The pixel-based class

information was then mapped with the field sampling points to determine the sample class (canopy or canopy interspace) of each individual sample. The classification of sampling points was quality controlled by using a nearest neighbor analysis to determine distance to nearest stem. Points were excluded from this analysis if: (1) classified as canopy interspace, but located < 0.5 m from the nearest stem, or (2) classified as under canopy, but located > 5 m from the nearest stem. Overall, a total of 14 sampling points were disqualified due to classification discrepancies. Averaged across all plots, 45% of the samples (min 37%, max 53%) were classified as under canopy across all plots.

Nine spatial covariates were computed from the DEM by considering a square kernel composed of nine grid cells with 1 m raster map resolutions. The following covariates were used in the model selection procedures at both plot and point scale: elevation, slope, aspect, northness (cosine of aspect), eastness (sin of aspect) (Stage, 1976), surface curvature (Zevenbergen and Thorne, 1987), topographic position index (TPI) (Guisan et al., 1999), terrain ruggedness (TRI) (Riley et al., 1999) and topographic wetness index (TWI) (Beven and Kirkby, 1979; Gessler et al., 1995). At a plot scale, TPI was computed relative to the surrounding 100 m. TPI is an estimate of the relative topographic position of a given point as the elevation difference between this point and the mean elevation within a set neighborhood. Positive TPI values indicates that the plot was located higher than the surrounding landscape, and negative values indicating that the plot was situated lower than the surrounding landscape. Plot values were found by

averaging all cells located inside each plot, while covariates for individual sampling points were extracted from the corresponding cell.

We analyzed the use of lidar metrics against field data on several different levels: (1) Stepwise multiple regressions (Eq. 4) were used to examine how the variability of C stocks in of forest compartments (mean plot values of above-ground tree, belowground tree, field layer, mosses and organic layer) at a plot level can be explained using combinations of lidar metrics as predictor variables, (2) we determined the correlation between point specific topographical values derived from lidar correlated with individual samples of field layer, mosses and organic layer C stocks for each plot and in an overall model. Assumptions of linearity, independence of errors, homoscedasticity, and normality of residuals were controlled for using standard statistical methods. Residuals deviating more than ± 3 SE was assumed registration errors and excluded for further analysis. To control collinearity among the selected models, any model with variance inflation factor (VIF) larger than 5 was rejected. The goodness of fit was evaluated by root mean square error (RMSE), adjusted R^2 and residual studies.

$$y = b_0 + b_1 x_1 + b_2 x_2 + \varepsilon \qquad\qquad (4)$$

where y represents the selected forest C pool, b_0 is the constant; b_1, b_2 represents the regression coefficients of the best fit model; x_1 and x_2 are explanatory lidar variables representing metrics of overstory, understory or local topography, and ε is a normally distributed error term.

2.3. Results

2.3.1. Carbon pools

Total measured C stocks summed for all forest compartments in the eight study plots ranged from 72.85 to 147.39 Mg C ha^{-1} (Fig. 3). From 48 to 59% of the C stock was found in the above-ground tree component, 19 to 23% was located in the tree roots, while 2 to 3% in the understory compartment, composed of field layer vegetation, saplings and mosses. The organic layer contained 16 to 31% of the measured C stock in these forests.
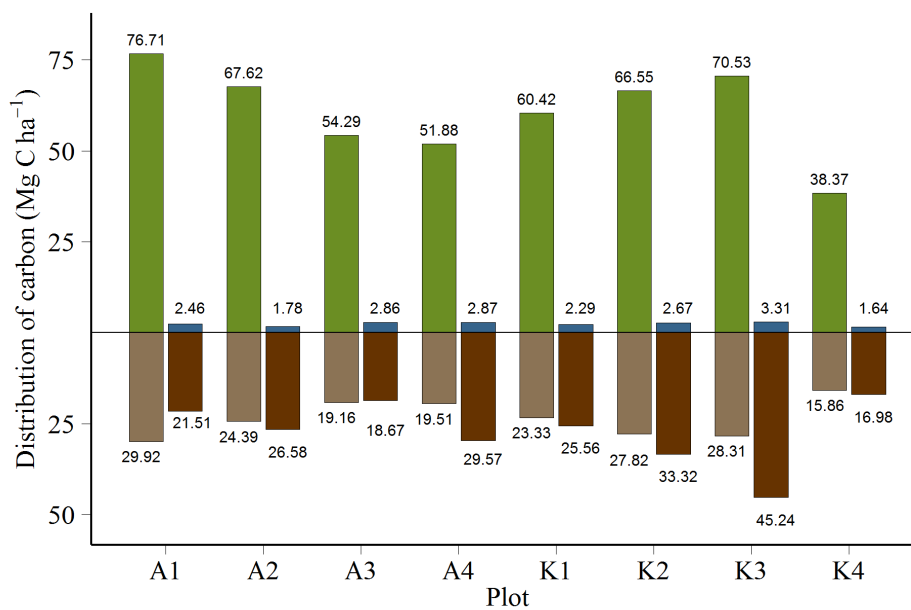
Figure 3. Distribution of C stocks (Mg C ha^{-1}) by compartment. Aboveground tree (upper left), belowground tree (bottom left), understory (upper right) and organic layer soil (bottom right). The understory compartment consists of field layer vegetation, mosses and saplings.

Tree carbon stocks

The number of trees per ha^{-1} varied from 270 to 688, containing a total tree C stock ranging from 54.23 to 106.63 Mg C ha^{-1} (Fig. 3). From 30 to 47% of the estimated tree C were found in the stems, while branches and needles accounted for 22 to 33% (data not shown). The fraction of root (> 2 mm) C in total tree C, 26 to 30%, reveals the importance of reporting the below ground tree compartment when presenting estimates of forest C. There was a negative correlation between mean plot dbh and stem density ($r_{(8)}$ = -0.96 (95% CI: -0.79, -0.99), $p < 0.001$), with lower stem densities in stands with higher mean stem circumference. We were unable to associate above- and below-ground tree C stock with stem density (C_a $r_{(8)}$ = -0.48 (-0.89, 0.34), $p = 0.23$, C_b $r_{(8)}$ = -0.57 (-0.90, 0.22), $p = 0.14$), and mean stand age (C_a $r_{(8)}$ = -0.47 (-0.89, 0.34), $p = 0.24$, C_b $r_{(8)}$ = -0.33 (-0.84, 0.49), $p = 0.43$). On an individual tree basis, tree age was positively correlated with both dbh ($r_{(805)}$ = 0.48 (0.42, 0.53), $p < 0.001$) and tree C ($r_{(805)}$ = 0.38 (0.32, 0.44) $p < 0.001$) (Fig. 4).

A conditional marked point pattern analysis revealed that stems with close neighbors (2.5 to 10 m) were inclined to have a lower dbh than the average within the plots, a pattern which were consistent across the different plots (results not shown). This dynamic was further seen in the marked (dbh) stem pattern analysis, which indicated suppression of larger stems on shorter distances (*Appendix Fig. A1*).
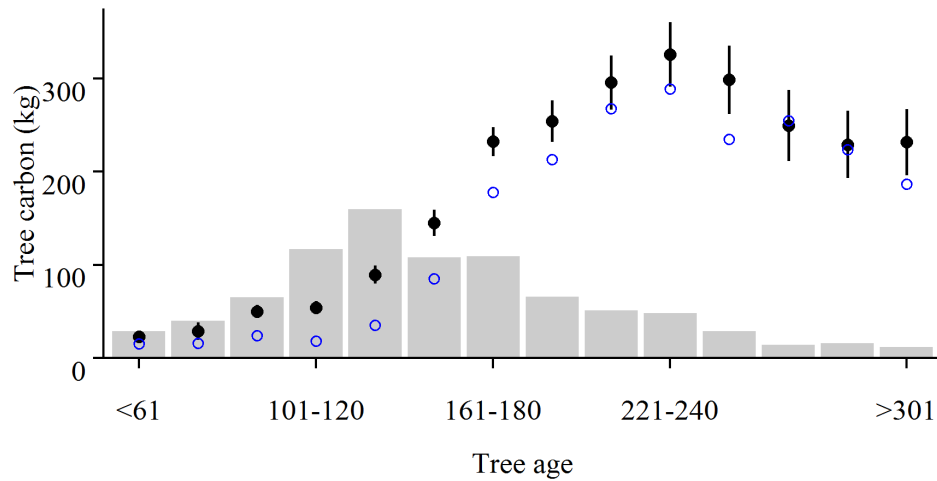
Figure 4. The relationship between mean tree C stocks (filled circles) and median (empty circles) for age groups (n = 805). Error bars indicate 95% confidence interval around mean. Bars show number of stems in each age bin.

Understory carbon stocks

The field layer, mosses and saplings, which comprise the understory compartment, were analyzed individually. Mean field layer C stocks varied from 0.41 to 0.88 Mg C ha^{-1} (Fig. 3), with coefficients of variation (CV = s/mean, %) within each plot ranging from 58 to 75%. The variances in the field layer C stocks between plots were heterogenic (Levene's test, $p < 0.001$), while differences were statistically significant, Welch's $F (7, 243) = 13.03$, $p < 0.001$. There was a negative correlation between plot basal area and field layer C stock ($r_{(8)} = -0.82$ (95% CI: -0.97, -0.27), $p = 0.012$).
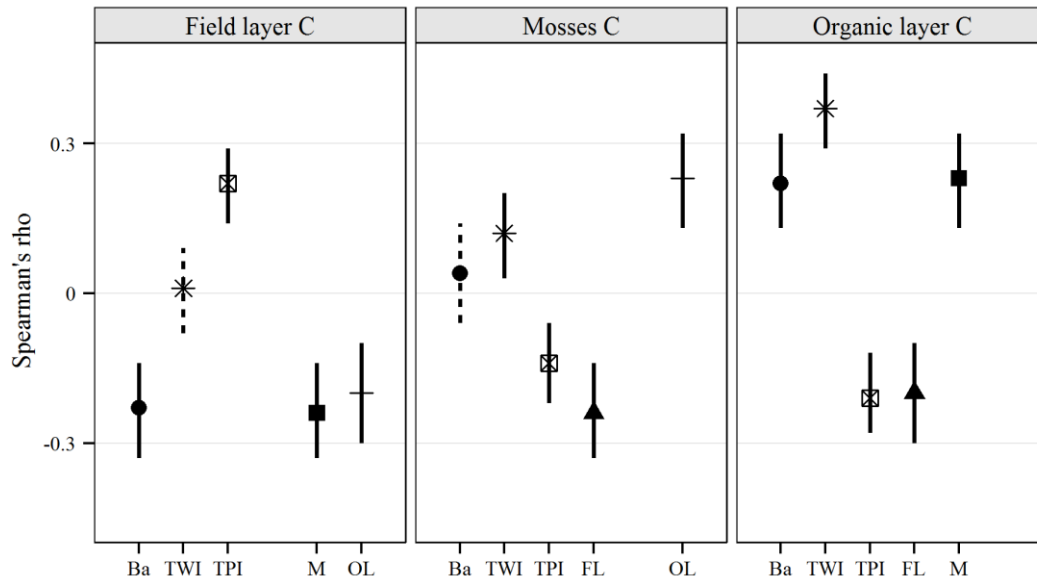
Figure 5. Spearman rank correlation (two tailed) between C compartments and attributes of individual sampling point. Full lines indicate significant correlations (p < 0.01), while dotted lines show non-significant correlation (p > 0.01). Basal area (Ba) is computed in a radius of 5 m around each of the sampling points (n = 379). Topographic position index (TPI) and topographic wetness index (TWI) are derived from an interpolation of lidar ground echoes on 1 m^2 grid cells (both n = 577). The figure also shows correlation between individual C compartments, where FL = Field layer C (n=580), M = Mosses C (n=583) and OL = Organic layer C (n=556). Correlations coefficients are displayed with 95% CI determined by bootstrapping 1000 random trials for each dataset.

The influence of trees on the field layer C stock was further investigated on a point scale using a nearest neighbor analysis and neighbor densities. We found that models of tree density performed better when including a measure of tree size, such as

basal area, rather than models with only stem density. Significant trends were then observed between basal area density (in a radius of 5 m around each sampling point) and the field layer C stock in the overall model Spearman's rho ($\rho_{(580)}$ = -0.23 (-0.33, -0.14), p < 0.001) (Fig. 5), and in six of the eight plots (results not shown). A pairwise t-test revealed significantly higher field layer C stock at sampling points situated at canopy-interspace locations than under canopy in six of the eight plots (Welch's $F_{(1, 509)}$ = 140.345, p < 0.001, Fig. 6).

The mosses C stocks ranged from 0.76 to 2.52 Mg C ha^{-1}, and were highly variable within each plot (CV 55 to 97%). Mosses C stock were statistically different between plots, Kruskal-Wallis $\chi2$ (7) = 109, p < 0.001. We could not associate the mosses C stock with any of the stand attributes. The relationship between mosses and field layer C stocks at a plot level was inconclusive ($r_{(8)}$ = -0.63 (-0.93, 0.13), p = 0.11), while the overall model indicated a significant negative correlation, Spearman's rho ($\rho_{(580)}$ = -0.17 (-0.22, -0.12), p < 0.001) (Fig. 5).

Saplings numbered from 21 to 163 per plot, and never contributed more than 0.1 Mg C ha^{-1} to the understory compartment. We could not associate sapling properties with any of the stand attributes.
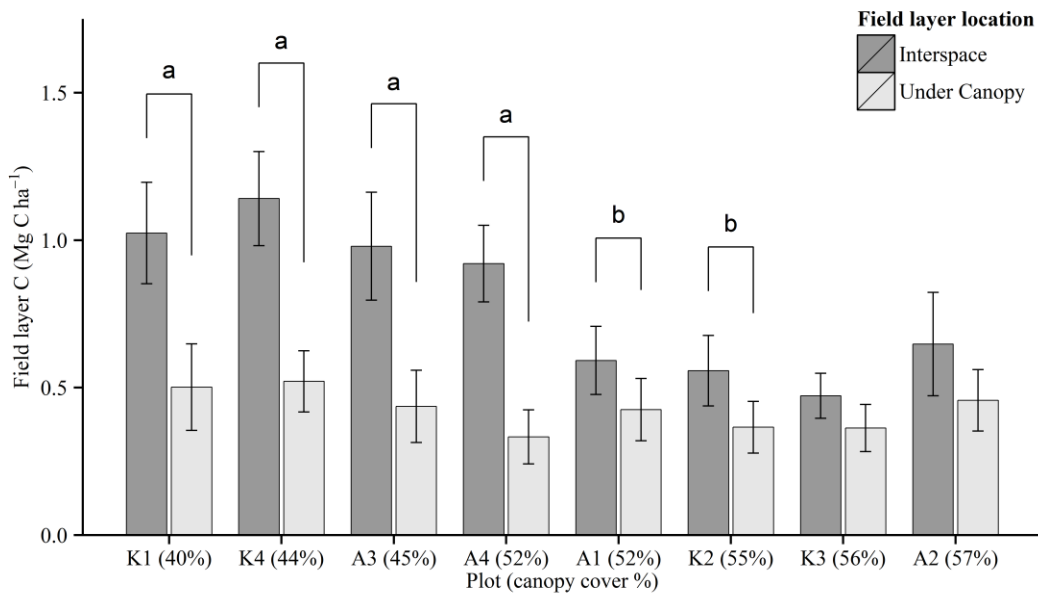
Figure 6. Bars show average plot values for the field layer C stock measurements at sampling points located under and in canopy interspace. Plots are ranked by relative canopy cover (% values) derived from lidar canopy density (cd_0). Whiskers indicate 95% CI for the mean. Differences in mean values are indicated by significance [a] ($p < 0.01$) and [b] ($p < 0.05$).

Soil organic layer carbon stocks

Mean values ranged from 16.98 to 45.24 Mg C ha^{-1} (Fig. 3) and were statistically different between plots, Kruskal-Wallis χ^2 (7) = 105, p < 0.001. There were large variations in the amount of organic layer C within each plot (CV 31 to 84%), all which exceeded the intra-plot variation (CV 22%). Differences between high and low values commonly ranged from 4 to 20 times the minimum value. At one location, plot K3, the

distribution was highly right-skewed, as the south-west corner of the plot was located in a transition zone between forest and peatland. Here we measured maximum values ~100 times larger than the minimum value.

The organic layer C stock was positively correlated with moss C stock at plot level ($r_{(8)}$ = 0.74 (0.07, 0.95), p = 0.03) and in an overall model, Spearman's rho ($\rho_{(556)}$ = 0.24 (0.16, 0.32), p < 0.001) (Fig. 5). When grouped by plot, the correlation was only significant in two plots (results not shown). Besides the association with mosses, we could not detect any significant relationship between the organic layer C stocks and plot attributes. However, an overall model indicated a positive relationship between individual measurements of organic layer C stock and basal area density, Spearman's rho ($\rho_{(379)}$ = 0.22 (0.12, 0.31), p < 0.001) (Fig. 5). Analyzed separately, the relationship was significant at only four of the study plots (results not shown).

2.3.2. Lidar data in forest carbon assessments

After assessing the field measured compartmental C stocks and their relationship, we then associated the data to lidar derived forest metrics. We investigated the use of lidar variables as predictors for the different forest C compartments, and analyzed the potential scale effects on the relationship of: (1) lidar metrics of above-ground stand characteristics and mean plot values of C components, (2) point specific topographical data derived from lidar and individual sampling points at individual plots and in one overall model.

Lidar correctly identified > 90% of the individual trees and their location in the plot. Because closely situated stems are a typical feature of unmanaged old growth forests, some stems were likely masked by dominating trees among the canopy point cloud. Horizontal canopy densities (cd_0), which corresponds to the proportions of lidar echoes > 1.5 m of the number of total echoes ranged from 44 to 58%.

The selected models for above- (C_a) and below-ground tree C (C_b) stock contained a variable relating to canopy density, and h_{90}, representing the 90th percentiles of the canopy heights. The model for C_a explained 94% of the variability, whereas the model for C_b explained 76% of the model variability (Table 2). The selected regression model for above-ground tree C stock revealed that both maximum height h_{max} and h_{90}, could be used to achieve similar explanatory power. Although the absolute difference was minimal (R^2 and standard deviation of residuals), h_{90} had a slightly smaller standard deviation of residuals and was thus selected for the final model. Canopy density did not add any significant value to the model for below-ground C. The partial R values for above-ground C were 0.81 (h_{90}) and 0.28 (cd_0). The RMSE was 3.38 and 2.47 for above- and below-ground tree C stock, respectively. The variance inflation factor (VIF) was < 1.5 in both models, so multicollinearity was not considered an issue.

Overall, the agreement between the models was good; above-ground tree C ($r_{(8)}$ = 0.97 (0.84, 0.99), $p < 0.001$); below-ground tree C ($r_{(8)}$ = 0.90 (0.57, 0.98), $p = 0.002$). When the selected models were cross-validated, we found no significant difference

36

between the observed and predicted values for neither C_a (t-test; $p > 0.05$, df = 7) nor C_b (t-test; $p > 0.05$, df = 7). The mean differences between the observed and modeled above-ground tree C ranged from -5.33 to 3.01 Mg C ha^{-1}, with a corresponding SD of the differences of 2.77 Mg C ha^{-1} (4.9%) for the above-ground tree C, and -3.79 to 2.83 Mg C ha^{-1} with SD of 2.00 Mg C ha^{-1} (8.5%) for below-ground tree C.

Lidar measurements and understory carbon compartments

The observed negative association between field layer C and basal area at a plot scale was also captured by a lidar data model using canopy density, explaining 83% of the variability (Table 2, Fig. 7). The RMSE was 0.08 Mg C ha^{-1}. Adding a buffer of 2 m for the computation window did not improve the model notably, while further expansion of the canopy computation window reduced the model fit (results not shown). Other lidar metrics such as canopy height measurements did not provide any significant correlation with the field layer C stock (Fig. 7). Overall, the agreement between the model and field data were good; field layer C ($r_{(8)}$ = 0.91 (0.61, 0.99), p = 0.001). When the selected models were validated, we found no significant difference between the observed and predicted values for field layer C (t-test; $p > 0.05$, df = 7). The mean differences between the observed and modeled field layer C ranged from -0.10 to 0.08 Mg C ha^{-1}, with a corresponding SD of the differences of 0.07 Mg C ha^{-1} (10.2%) for field layer C.

The proportion of understory echoes from non-canopy echoes (understory plus ground echoes) ranged from 0.19 to 0.28, with a U_i ranging from 0.7 to 1.7 echoes/m^2. Mean understory heights ranged from 0.31 to 0.39 m. A total of 56 variables representing understory echoes, such as height quantiles and densities (*Appendix Table A1*) were tested against the field layer C stock situated in canopy interspace, but no consistent association could be determined. Similarly, the variability in sapling numbers or C stock could not be explained by any of the above-ground or topographical lidar data at a plot level.

Table 2. Regression models for C stocks in trees, field layer and the soil organic layer using lidar echoes

Explanatory variable	Model (Mg C ha^{-1})			
	Tree C_a	Tree C_b	Field layer C	Organic layer C
Intercept	-30.68^b (11.15)	-11.48 (8.14)	1.97^a (0.25)	-207.99^a (54.99)
h_{90}	3.30^a (0.41)	1.12^a (0.30)		
cd_0	59.93^b (21.75)	31.01 (15.88)	-2.66^a (0.49)	
TWI				29.00^a (6.78)
R^2	0.95	0.82	0.83	0.75
Adj - R^2	0.94	0.76		
RMSE	3.38	2.47	0.08	4.88
VIF	1.1	1.1		

Note: ^{a} term is significant at the 0.01 level, ^{b} term is significant at the 0.05 level. Numbers in brackets represent the standard error of the coefficient.

The variability in moss C stock could not be explained by any of the above-ground or topographical lidar data at a plot level (Fig. 7). When individual sampling

points were used in an overall model, we detected a significant positive correlation between the moss C stock and TWI, Spearman's rho ($\rho_{(583)} = 0.15$ (0.07, 0.23), $p < 0.001$) and a negative correlation between moss C stock and TPI score, Spearman's rho ($\rho_{(583)} = -0.13$ (-0.05, -0.21), $p = 0.003$) (Fig. 5).

Lidar measurements and organic layer carbon

At a plot level, we discovered a positive relationship between mean stand values of TWI and organic layer C, explaining 75% of the model variation (Table 2), with larger C stocks in plots with higher TWI values (Fig. 5). The model RMSE was 4.88 Mg C ha^{-1}. None of the above-ground stand characteristics added any significant explanatory power to the model. Overall, the agreement between the model and field data for organic layer C was good ($r_{(8)} = 0.87$ (0.43, 0.98), $p = 0.005$). When the selected models were validated, we found no significant difference between the observed and predicted values for organic layer C (t-test; $p > 0.05$, df = 7). However, the mean differences in between the observed and modeled organic layer were still the largest in the study, ranging from -6.15 to 7.49 Mg C ha^{-1}, with a corresponding SD of the differences of 4.25 Mg C ha^{-1} (15.6%) for organic layer C. Similarly, there was a negative association between plot TPI and the organic layer C stock ($r_{(8)} = -0.78$ (-0.17, -0.96), $p = 0.023$), with larger organic layer C stocks in stands located in areas that are lower than the surrounding landscape. Modeling TWI and TPI with organic layer C stocks by individual points was significant in the

overall models (Fig. 5), but inconclusive when investigated plot by plot (results not shown).
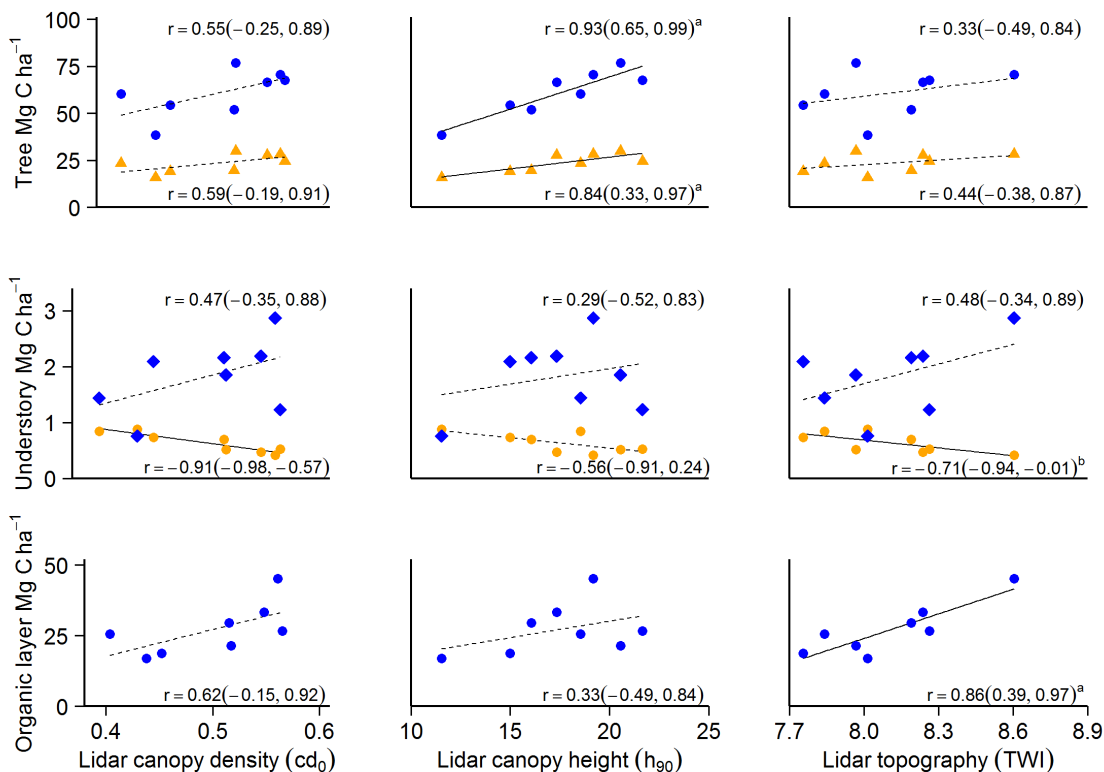
Figure 7. Pearson's correlation (two-tailed) of five forest C compartments and three lidar variables for the plots used in this study (n = 8). Top row show aboveground (filled circles) and belowground (filled triangles) C stocks, second row show mosses (filled triangles) and field layer (filled circles) C stocks, while bottom row represent organic layer C stocks (filled circles). Correlation coefficients are presented with (95% CI). Full line indicate that the correlation is significant (level of significance is indicated by subscript letter (a: $p < 0.01$, b: $p < 0.05$), while the dotted line show non-significant results.

We also conducted a Mann-Whitney U test to determine if there were differences in organic layer C stocks between the two canopy classes (under − interspace). Distributions were similar, as assessed by visual inspection. Overall, the organic layer C stock was higher in sampling points under canopy (Median = 2.44, n = 253) than in canopy interspace (Median = 2.29, n = 298), U = 32767, z = -2.65, p = 0.008. However, when individual points within each plot where investigated separately, the results were inconclusive.

2.4. Discussion

This study explored the use of lidar data beyond just quantifying tree C stocks, and found evidence that lidar canopy data can be extended to model field layer C stocks, while topographical variables from lidar ground returns provides valuable indicators of the mosses and soil organic layer C stock. However, attempts to increase the spatial resolution of these relationships from plot scales to 1 m^2 cells within plots were to a large extent unsuccessful.

2.4.1. Stand characteristics and carbon stock

On a local scale, the standing biomass and thus the tree C stock vary with site factors and stand properties such as tree age, stem density and species. The stands in this study have grown undisturbed from active forest management for at least 100 years (Lie et al., 2012), and the majority of trees in the canopy layer are more than 120 years old,

considerably higher ages as compared to a typical managed forest stands in Norway. Mean and median dbh was negatively correlated with the number of stems, likely a result of density dependent mortality leading to self-thinning (Luyssaert et al., 2008). Trees accounted for ~ 97% of C in living biomass, with the majority (68 to 72%) in above-ground tree compartments, which corresponds well with previous studies of mature boreal forest stands (Finer et al., 2003; Liu and Westman, 2009). By not including the C pool in fine roots (< 2 mm), a small portion (2 to 3%) of the tree C stock (Makkonen and Helmisaari, 2001) was left out of the assessment. However, because an estimated 10 to 40% of fine roots are located in the organic layer (Helmisaari and Hallbäcken, 1999; Makkonen and Helmisaari, 2001), a portion of this C compartment may have been included in the soil C data.

2.4.2. *Predicting tree carbon stocks using lidar*

In this study, we were able to explain 76 to 93% of the variability in the below and above-ground tree C stock using regression models relating lidar metrics of tree height and canopy density. Our findings support previous studies showing that tree and canopy height (Magnussen et al., 1999; Nilsson, 1996; Næsset, 2007; Næsset and Økland, 2002), stand basal area (Holmgren, 2004; Holmgren et al., 2003) and stand volume (Holmgren, 2004; Nilsson, 1996) and can be accurately estimated using lidar measurements, often with more accuracy than traditional assessments (Maltamo et al., 2009; Næsset, 2007).

Lidar measures of height were closely correlated to above- and below-ground tree C. Because bigger trees contribute a larger proportion of the C stock, indices reflecting height traits, should be most correlated (Lefsky et al., 1999). Models containing information about large trees, such as h_{90}, will weight these trees more than other measures, for example mean heights, resulting in better model fit. Much of the reported findings linking field measurements of above-ground biomass and tree C with lidar data have been conducted in deciduous temperate forests, with R^2 values ranging from 0.74 to 0.93 (Lefsky et al., 1999; Lefsky et al., 2005). In a comprehensive study on boreal conifer stands, conducted across a broad variety of characteristics, Næsset and Gobakken (2008) reported comparable overall R^2 values of 0.88 (RMSE = 2.1) in their estimates of above-ground biomass, which is less than the local model in this study (R^2 = 0.95, RMSE = 3.38). Because the aim of this study was to explore the use of lidar in mapping variations between plots with comparable ecological traits, all plots were located in the same geographic region. Næsset and Gobakken (2008) demonstrated the importance of geographical region (explaining 32 to 38% of the variability) when estimating above-ground biomass, and emphasized the importance of local sample plots for calibrating regression equations.

The estimated root compartment, which accounted for approximately a quarter of the measured tree C stock and one fifth of the measured C in these plots, highlights the importance of including roots in forest C assessments. To our knowledge, only two

previous studies have reported lidar models of below ground biomass and C stock from boreal forest stands. Our coefficient of determination $R^2 = 0.82$ (RMSE = 2.47) is comparable to Næsset (2004) who reported a R^2 value of 0.86 (RMSE = 1.4), and Næsset and Gobakken (2008) with $R^2 = 0.85$ (RMSE = 2.2).

The most reliable way of determining tree C stocks is through harvest and laboratory analysis, which is a destructive and labor intensive method. Thus, tree biomass and C stock is commonly estimated from regression models based upon sample trees. In this study the C estimates were based on allometric models for above-ground biomass derived from Marklund (1988), who developed the models from data across Sweden, covering a variety of stand properties like stand age, site index and basal area. The below-ground estimates of tree C are based upon work by Peterson and Ståhl (2006), which is an expansion of Marklund (1988). Peterson and Ståhl (2006) reported adjusted R^2 values of 0.95 or higher for all of their below-ground biomass models. Assuming the general validity of these equations, there is no reason to believe that our predictions of root C are less valid than the above-ground estimates, showing that also the root compartment can be accurately estimated using lidar data.

Although estimation of dead woody debris was outside of the scope of this study, it may contain a substantial amount of above-ground C in mature boreal forests (Laiho and Prescott, 2004; Siitonen et al., 2000), and is therefore an integral component in a full forest C inventory. Pregitzer and Euskrichen (2004) estimated this compartment at 7.9 ±

7.5 Mg C ha^{-1} across the boreal forest. Several studies have reported on relationships between the variability of dead woody material and stand structural properties (Bradford et al., 2009; Siitonen et al., 2000), which may be derived from remote sensing. In a study from boreal forests, Pesonen et al. (2008) reported that remote sensing estimates for downed dead wood (RMSE 51.6%) were more accurate than the estimates based on field-measured characteristics of living trees, while standing dead wood volume estimates were less accurate (RMSE 78.8%).

2.4.3. *Understory carbon pools and lidar*

While the majority of published work on the C dynamics and stock of the boreal forest have focused on the role of trees and soils, less is known about the role and magnitude of the understory vegetation. The amount of C bound in the understory vegetation (field layer and mosses combined) is low (2 to 5%) compared to the total above-ground C stock, a number which corresponds well with previous findings from studies in boreal forest locations (Finer et al., 2003; Havas and Kubin, 1983; Mäkipää, 1995). Regardless of its relatively small contribution to forest C stock at a given time, it can be an important source of fresh biomass C (and nutrients) to the soil (Havas and Kubin, 1983; Muukkonen and Mäkipää, 2006; Nilsson and Wardle, 2005). The productivity in the understory vegetation depends on a number of factors, such as e.g. light availability (Messier et al., 1998), nutrient availability (Nilsson and Wardle, 2005) and the activity of the soil microbial community (Wardle et al., 2004; Wardle et al.,

2012). Self-replacement through gap-fill dynamics, gives older unmanaged forests a more multi-layered characteristic than even-aged second-growth forests (Messier et al., 1998). The heterogeneous understory growth observed in our plots is likely a result of limited and patchy light availability. As the canopy closes throughout stand development, understory vegetation shifts from early successional species like herbs and grasses towards more species adapted to low light environments, like mosses growing on the forest floor (Lindholm and Vasander, 1987). Structural changes in older stands can cause a reduction in the leaf area index, resulting in a higher relative contribution of understory vegetation to the overall net productivity (Luyssaert et al., 2007). Thus, stand age has been found to be a reasonable predictor of understory C storage across landscapes (Muukkonen and Mäkipää, 2006). Although we could not reach a similar conclusion, the limited age span in our stand data (115 to 190 years) was likely inadequate for an analysis across stand development stages.

The amount of understory vegetation in boreal forests have been found to decline with increasing basal area (Hansson et al., 2011; Pase and Hurd, 1958), but neither the findings in this study, or Muukkonen and Mäkipää (2006) supports such conclusions when the understory is classified as a single layer. As the C stocks of field layer and mosses were negatively correlated, models improved by treating the two compartments separately instead of aggregated in a single (understory) compartment. While no conclusions could be drawn from the relationship between above-ground structures and

the mosses C stock, we observed a negative association in both absolute and relative amounts of field layer C (as a proportion to the understory C stock) under stands with higher basal area. Lower light conditions in denser canopies will likely limit growth of shade intolerant species such as *V. myrtillus* (Mäkipää, 1999), which were commonly observed on all plots in this study. Such findings are comparable to Muukkonen and Mäkipää (2006), who reported a negative correlation between stand basal area and field layer biomass in spruce, pine and broad-leaved forest stands in Finland. When the resolution of basal area was increased from a single value representing plots to the basal area density in a 5 m radius of individual sampling points, the relationship to field layer C stock became more diffuse. However, these models were slightly improved by fitting the density of above-ground biomass instead of basal area. While basal area is a function of dbh squared, biomass is a product of wood density and stem volume (basal area and height), and will therefore increase as a function of dbh to a power greater than 2 (Lefsky et al., 1999), and hence give a higher weight to larger trees. The improved model fit from shifting from basal area to above-ground biomass might therefore be explained by the effects of larger trees within each stand (Lutz et al., 2012).

The literature associating lidar data directly with understory characteristics are rather scarce. Structural parameters from lidar have successfully been used to identify site class (Vehmas et al., 2009), map distribution of mosses (Peckham et al., 2009) and lichen (Korpela, 2008) in boreal conifers, and understory species composition in temperate

47

deciduous woodlands (Hill and Broughton, 2009; Hill and Thomson, 2005) and subalpine conifer dominated forests (Nijland et al., 2014). Other studies have found lidar to provide accurate estimations of leaf area index (Korhonen et al., 2011; Solberg et al., 2009) and canopy gaps (Vepakomma et al., 2008), both which affects light transmittance to the ground. Because light availability is considered the main limiting growth factor for field layer vegetation (Barbier et al., 2008; Pelt and Franklin, 2000), canopy density measures from lidar have shown to be good proxies for understory light availability (Alexander et al., 2013). When the understory was investigated separately, our results indicate that on a plot scale, canopy density measures from lidar were better predictors of field layer C stock than any of the stand measurements collected in the field. Similarly, the effect of the canopy on field layer C stock was also observed at a point scale where samples were classified by their location in canopy gaps or under canopy. Martinuzzi et al. (2009) reported similar findings for shrub presence in both young and mature mixed conifer forests in Northern Idaho, USA. However, it is worth noticing that our field layer C stock is 2.5 to 5.6 times smaller than the standard deviation of predicted above-ground tree C. Although the limited number of observations in this study prevents development of regression models with a large generality, the possibility that a significant correlation could be found even among plots of comparable characteristics is encouraging, and suggests that further investigation across a range of ecological variables could yield valuable insight.

Even though the field layer C stock in canopy gaps was dissimilar between plots, we could not find evidence associating any lidar understory metrics to this variability. While the interspace field layer C stock varied from 0.47 to 1.14 Mg C ha^{-1} (140%), the mean understory height only ranged from 0.32 to 0.44 m (35%) and understory density from 0.19 to 0.28 (47%). Computation of understory lidar metrics were done by applying different filters and classifications, but only marginal differences in height indices were found. The poor fit between understory returns and the field layer might be a result of a low pulse density and the ability to differentiate among small height classes (Pfeifer et al., 2004). Thus, errors may occur where the ground vegetation is dense, making it difficult to separate ground hits from low vegetation (Hyyppä et al., 2008; Pfeifer et al., 2004).

It is clear from the point pattern analysis that the saplings displayed aggregation on small scales, likely in canopy gaps. The lack of association between any of the lidar plot variables with the sapling data may be a result of the limited dataset used in the study. It may also be a result of unsuitable plot area (~2000 m^2), as neighboring trees will have a greater influence on light conditions than more distant ones. In a study conducted in boreal forest stands, Bollandsås et al. (2008) found significant relationships between canopy structure derived from lidar and seedling numbers. However, the results were scale dependent, as they achieved better model fit on 225 m^2 plots, than 25 m^2 and 100 m^2 plots (Bollandsås et al., 2008). Although the results seen here are encouraging, more

data from varied forest structures and different plot sizes are needed to draw any conclusions.

2.4.4. *Organic layer carbon and lidar*

The organic layer in boreal forest commonly displays great spatial variability (Häkkinen et al., 2011; Muukkonen et al., 2009), with differences between minimum and maximum values up to 100 times over relatively short distances, making precise estimates of the organic layer C stock inherently challenging. The complex configuration of organic layer C is not a result of linear and additive set of causes, but is instead affected by a range of interrelated environmental variables, each with a number of potential effects, making precise mapping and monitoring soil C a formidable task.

Tree species have long been recognized as an important factor for organic layer dynamics (Simonson, 1959), affecting the properties by root activity, microclimate and chemical constituents in the litter (Högberg and Ekblad, 1996; Yarwood et al., 2009). Most plant litter (leaves and dead roots) is distributed near or at the surface (Liski and Westman, 1995) and contains different chemical constituents decomposing at different rates (Berg, 2000; Janzen, 2005; McTiernan et al., 2003). Although the relative contribution of different tree compartments (roots, leaves) to the soil organic C pool varies between species and local conditions (Liski et al., 2002), the link between above and below-ground processes are strong (Hogberg and Read, 2006; Wardle et al., 2004). Stand basal area, which can be derived from lidar data (Holmgren, 2004), have also been

associated with soil C storage (Hansson et al., 2011). In a study from boreal forest stands in Sweden, Hanson et al. (2011) found that organic layer C stocks in adjacent spruce and pine stands were positively correlated to basal area. We found comparable results between basal area densities and the organic layer C stock in only three out of the eight plots used in this study. However, when scaled from single sampling points up to mean plot densities, this association was no longer detectable. This might be a result of the relatively low number of plots in this study, or that such patterns might only be observable when compared across a wider range of age classes.

Due to quality differences in plant residue and mineralization rates among deciduous and conifer stands (Krankina et al., 1999; Polyakova and Billor, 2007), and even between spruce and pine (Hansson et al., 2011; Stendahl et al., 2010), observed differences in organic layer C stock have been linked to the local dominating tree species (Vesterdal et al., 2013). In particular, studies have found the organic soil layer under spruce stands to be both thicker and have a higher C stock than those of pine and birch (Hansson et al., 2011; Stendahl et al., 2010). Whether these observed differences are due to tree species effects is questionable, since trees themselves are not randomly distributed in natural forests, but follow gradients in climate, successional stage, soil type and other abiotic factors (Vesterdal et al., 2013). Because the forest stands used in this study were heavily dominated by Norway spruce, we were unable to test this hypothesis. Nevertheless, in boreal forests, which consist of relatively few tree species, lidar has

successfully been used to predict species of individual trees. The overall classification accuracy is high, ranging from 88 to 96% (Holmgren and Persson, 2004; Holmgren et al., 2008; Ørka et al., 2009).

Because soil attributes have been linked to the local topography (Mulder et al., 2011; Thompson and Kolka, 2005), another promising aspect of lidar for assisting in mapping soil organic C is the capacity to provide fine scale topographical information from interpolating ground echoes (Mulder et al., 2011; Van Leeuwen and Nieuwenhuis, 2010). The absolute accuracy of the DEM is a function of sampling density, scanning angle, canopy density and closure (Hyyppä et al., 2005; Hyyppä et al., 2008). Hyyppä et al (2005) presents results which can be used in optimizing lidar flights for the level of DEM quality needed. In the boreal zone, under the right conditions, terrain models with random errors less than 20 cm can be obtained (Hyyppä et al., 2008). Due to the internal consistency of lidar elevation data, topographical variables derived from DEM products, such as slope and aspect, usually have higher accuracies than the lidar elevation data (Gangodagamage et al., 2014). Slope, which is computed from the local differences among adjacent ground returns, is more sensitive to the relative vertical error of each individual point, than the absolute accuracy of the lidar elevation data. In a recent study, Gangodagamage et al. (2014) reported relative vertical errors in lidar elevation data to 0.0014 m, and maximum slope errors from 0.003 to 0.004 m/m. For the purpose of mapping soils, accuracy can be further enhanced by combining DEM and local soil data

using soil mapping methods (Mulder et al., 2011). Depending on the existing soil information, terrain attributes from lidar can be used as a soil covariate in an interpolation approach filling in gaps in the soil map (McBratney et al., 2003). Several studies have used topographic features derived from DEM to predict and map soil attributes (Gessler et al., 1995; Pei et al., 2010; Ziadat, 2005) and soil C pools (Mueller and Pierce, 2003; Seibert et al., 2007; Thompson and Kolka, 2005). For predictions of soil or mosses C stocks, topographical features which are particularly interesting are the local elevation, slope, and concavity, as these influences the local hydrological conditions and thus the C accumulation rate (Binkley and Fisher, 2012). Secondary indexes computed from elevation and slope, such as topographic wetness index (TWI) and topographic position index (TPI), which were associated to the organic layer C in our plots, have also been used in earlier studies to estimate soil attributes and C stocks. For example, Seibert et al (2007) reported increasing organic layer C content with higher TWI from study sites across Sweden. A similar pattern has also been observed by Laamani et al. (2013) who reported a greater mean organic layer thickness in gentle slopes (≤1.8%) compared to steeper slopes (> 3.2%) using topographic data derived from lidar.

Despite the ability to delineate high resolution data on topographical variables, there have been very limited attempts to directly associate boreal soil C stock with lidar data. At a plot scale, our results indicate that the variability in both organic layer and mosses C stocks can be partly explained by topographical variables, such as TWI and

53

TPI. However, when the resolution is enhanced from single plot averages to 1m grid cells within the plots, the correlation becomes increasingly diffuse. This could be a consequence of spatial inaccuracy in field measurements, or the ability to differentiate between ground returns and biomass in areas with dense understory vegetation, masking some of the fine-scale topographical features.

2.5. Conclusion

The high resolution sampling design employed in this study, combined with lidar data acquisition, provide a unique opportunity to examine the association between stand structure characteristics and C pools in different forest compartments across different scales. At a plot level ($\sim$2000 m^2), we find that canopy density and height metrics derived from lidar can be used to accurately estimate both above and belowground tree C, while canopy density measures alone are strong predictors of the field layer C stock. However, attempts to associate echoes directly from the field layer with the C stock in this compartment were unsuccessful. Increasing the laser density or incorporating airborne lidar with other remote sensing techniques may enable the use of such data. In addition, we also demonstrate that the organic layer C stock can be modeled with good accuracy using topographical characteristics derived from lidar ground echoes. Efforts to associate individual sampling points to local terrain characteristics by increasing the resolution from a plot level to 1 m^2 did not yield consistent results, possibly due to the low echo density in areas under canopy. In the search for an effective tool to measure and monitor

forest C pools, we find the capabilities of lidar to effectively map forest C encouraging. The methods employed in this study warrants further investigation across a wider range of ecological variables and scales.

Chapter 3: Spatial variability of organic layer thickness and carbon stocks in mature boreal forests stands – Implications and suggestions for sampling designs

Terje Kristensen[a], Mikael Ohlson[b], Paul Bolstad[a], Zoltan Nagy[c]

[a] Department of Forest Resources, University of Minnesota, 115 Green Hall, 1530 Cleveland Ave. N., St. Paul, MN 55108, USA

[b] Department of Ecology and Natural Management, Norwegian University of Life Sciences, P.O.Box 5003, 1432 Aas, Norway

[c] f+n: Design & Engineering Consulting, Zurich, Switzerland

Summary

Forest soils commonly exhibit large spatial variability, making any efforts to map soil carbon (C) storage challenging. Accurate field measurements from inventories across fine spatial scales are critical to improve sampling designs, and to increase the precision of forest C cycling modeling. By studying soils undisturbed from active forest management, we give a unique insight in the naturally occurring variability of organic layer C, and provide valuable references against which subsequent and future sampling schemes can be evaluated. We analyze the fine-scale heterogeneity of the soil organic

layer in seven 2000 m^2 unmanaged boreal forest stands, using a sampling scheme that incorporates samples separated from 0.15 m to 50 m. The organic layer C stocks ranged from 1.69 to 3.33 kg C m^{-2}, but were highly variable within each plot, as indicated by the coefficient of variation, 31 to 63%. A geostatistical analysis revealed spatial autocorrelation of the organic layer C stock at distances ranging from 0.86 to 2.85 m, emphasizing the importance of considering spatial dependencies when designing sampling strategies for soil C inventories. When spatial autocorrelations is known, we show that a minimum of 20 inventory samples is needed to determine the organic layer C stock with a precision of ±0.5 kg C m^{-2} in a 2000 m^2 plot. Our data also demonstrates a strong relationship between the organic layer C stock and horizon thickness (R^2 ranging from 0.58 to 0.82), which suggests that intensifying *in situ* measurements of horizon thickness can simplify and reduce the cost of future C inventories.

3.1. Introduction

Boreal forests store an estimated 22% of the global forest carbon (C) stock (Pan et al., 2011) and are believed to be a net sink of atmospheric C, sequestering approximately 0.5 ± 0.1 Pg C per year (Pan et al., 2011). The circumpolar boreal forest region is of particular interest because it is situated at latitudes expected to undergo substantial warming and climatic changes in the coming decade (Nabuurs et al., 2007), possibly altering forest C stocks and C sink strengths (Koven, 2013; Kurz et al., 2008; Ågren et al., 2007).

The majority of boreal forest C is found in the soils (Malhi et al., 1999), and several field and modeling studies have reported local and regional estimates of C stocks (see Baritz et. al 2010 for an overview). However, the soil organic carbon (SOC) pool is influenced by complex ecological processes (Jungqvist et al., 2014; Stockmann et al., 2013), and large uncertainties still exist as regard the size of the boreal forest SOC pool. A further factor that contributes to the uncertainty about the boreal forest SOC pool size is a lack of sampling protocol consistency among previous studies. The variability and patterns in organic soil C stock estimates have been associated with a series of physical, biological, and chemical processes, such as; climatic conditions (Callesen et al., 2003; Hilli et al., 2010), soil type (Baritz et al., 2010), tree species composition (Mueller et al., 2012; Schulp et al., 2008; Stendahl et al., 2010; Vesterdal et al., 2013), stand age (Häkkinen et al., 2011; Kolari, 2004), and topography (Seibert et al., 2007; Thompson and Kolka, 2005).

To avoid considerable uncertainty in C estimates it is essential to consider the spatial dependency of soil properties, meaning that proximal measurements tend to have more similarities than distant ones (Post et al., 2001). Many earlier soil C surveys, which form the basis of most meta-studies and modeling efforts, have been conducted under the assumption of random spatial variability, and consequently provide little information about spatial structures (Jandl et al., 2014; Lindner and Karjalainen, 2007). However, ignoring spatial dependence may introduce a systematic bias in regional and national

SOC stock estimates, if the spatial dependence component is not accounted for in the overall estimates of uncertainty (Ortiz et al., 2013).

When designing soil C inventories, prior knowledge of the scale in which spatial dependency occurs can ensure unbiased sampling and improve sampling efficiency. In most cases however, the spatial structure is unknown, and needs to be estimated by an early procedure in the overall sampling design. Accurate assessments of spatial distributions of soil C requires a large number of data points (Birdsey, 2004), making the cost and labor efforts associated with such measurements high (Mäkipää et al., 2008). Since methods for analysing C concentration (C_c) of a given sample are well established and can be carried out with high precision (Conant et al., 2011), the challenge is to develop effective sampling designs. These designs should account for the natural variation and identify the number of observations required to achieve the necessary accuracy, or as resources are typically limited, what accuracy is possible under the given resource constraints (Peltoniemi et al., 2004; Post et al., 2001; Ståhl, 2004). As most expenses in soil C stock assessments occur during sample collection and laboratory analysis (Mäkipää et al., 2008), advancing current sampling designs can improve the economic feasibility of inventories and verification protocols.

Several studies have quantified local spatial variability of soil C in temperate forests (Heim et al., 2009; Schöning et al., 2006) and tropical forests (Rossi et al., 2009), but data with high spatial resolution and precision from forests in the boreal region

remains scarce. In two studies conducted on managed young and middle aged forest stands in Finland, Muukkonen et al. (2009) and Häkkinen et al. (2011) found strong spatial dependencies for soil C in the organic layer, with autocorrelation distances ranging from 0.75 m to > 7m. However, spatial assessments of SOC pool sizes in soils from actively managed forests are problematic due to the mostly unknown, confounding effects different management practices have on soil attributes (Finer et al., 2003; Hedde et al., 2008; Schulp et al., 2008). Residual effects from management are inherently difficult to quantify because they will vary greatly with practices, soil types, across landscapes and harvest season (Block et al., 2002; Kolka et al., 2012). We would therefore emphasize that to achieve the best possible applicability across locations, investigating the spatial distribution of forest SOC in soils under natural conditions will yield greater insight to natural spatial scales.

The objective of this study is to assess the spatial structure of the soil organic layer C pool across fine spatial scales in unmanaged boreal forests, and to provide a reference against which subsequent and future sampling protocols can be evaluated. Using a sampling protocol with high spatial resolution that is replicated on multiple forest sites, we aim to (i) examine the spatial variation in organic layer C stocks within and between old growth boreal forest stands, (ii) provide explicit guidance on appropriate sample sizes for estimating mean C stock, and (iii) discuss the implications of this study for future soil C inventories.

3.2. Materials and methods

3.2.1. Study area

This study was conducted combining a systematic random sampling and a model-based approach, in seven random forest stands in the south boreal zone in SE Norway (Fig. 1). To enable comparison of the natural occurring variability in organic layer attributes within and among stands with similar characteristics, all forest stands were in late phases of succession. No active management has occurred within the forests over the last 100 years (Lie et al., 2012). The forests were classified as medium fertility mesic heath forests (Cajander, 1926; Cajander, 1949), heavily dominated by Norway spruce (*Picea abies* (L.) Karsten), with occurrences of Scots pine (*Pinus sylvestris* L.) and silver birch (*Betula pendula*). The stands had a multi-layered structure and were of uneven age. Some Norway spruce trees were >400 year old (Lie et al., 2009), and the forest stand mean ages ranged from 115 to 190 years, which are considerably higher ages as compared with a typical managed forest stand in Norway. Soils were mesic to mesic/moist podzols, the most dominant soil type in this region (Baritz et al., 2010). General properties of the study plots are shown in Table 1.
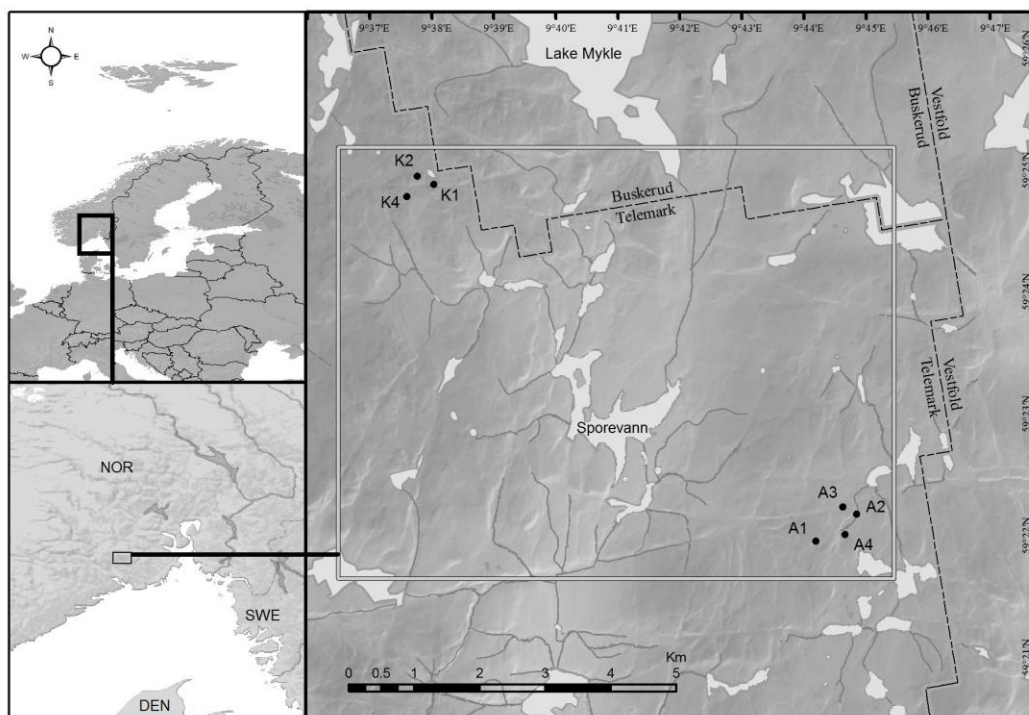
Figure 1. Location of sampling plots used in this study. Four plots were situated in the Årum area (A) and three plots were located near Lake Kapteinstjern (K).

Table 1. General properties of the seven boreal forest plots investigated this study.

	Plot						
	A1	A2	A3	A4	K1	K2	K4
Location N	59°21'15	59°21'58	59°21'57	59°21'02	59°24'57	59°25'00	59°24'51
Location E	9°44'05	9°44'39	9°44'27	9°44'33	9°38'00	9°37'45	9°37'33
Altitude	549	473	475	484	605	619	607
Stand age	115	121	146	143	190	183	188
Mean dbh (cm)	28	20	17	17	30	25	17
Stem density (ha^{-1})	351	611	688	652	270	484	565

3.2.2. *Sampling design*

In all seven forest stands we established a circular study plot ($\sim$2000 m^2). The plots were divided into a systematic grid containing 73 sampling points (grid nodes), with a distance between each point being 5 m in both north-south and east-west directions (Fig. 2). To capture the small scale spatial variation we randomly selected 14 sampling points in each of the grids, where 5 subsamples were collected in lag distances ranging from 0.15 m and up to 2.5 m, measured between core centers (Fig. 2). Using a cylindrical steel corer (56 mm diameter) we sampled the soil organic layer consisting of the F (O_e) and H (O_a) horizon down to the mineral soil boundary. Because of the low faunal mixing of decomposing litter in these forests there were visually clear horizon boundaries between the organic layer and the mineral soil. The organic horizon and the mineral soil are likely to differ substantially in both bulk density (BD) and C concentration (C_c) (Baritz et al., 2010; Lundström et al., 2000; Muir, 1961), thus using a genetic horizon sampling protocol, instead of a fixed depth sampling can significantly reduce the variability of mean SOC stock (VandenBygaart et al., 2007). The sampled F and H horizon consists of both partially decomposed matter and well-decomposed organic matter. Undecomposed surface litter (L (O_i) horizon) was excluded from the sample and further analysis to minimize any seasonal effects. The thickness of the soil core was measured to the nearest cm.
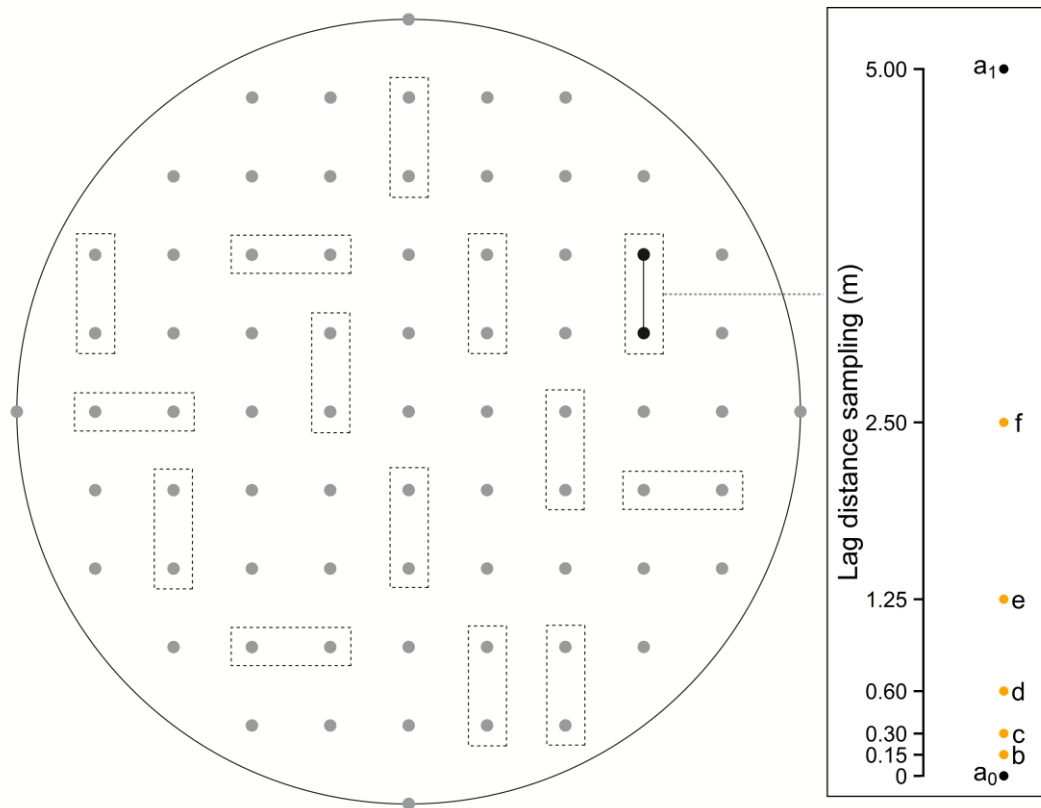
Figure 2. On all seven plots, soil samples were systemically collected from a grid with 5 m intervals (samples marked a). To assess the small scale variability, we randomly selected 14 grid locations where 5 new additional samples were collected at 0.15 (b) – 0.30 (c) – 0.60 (d) – 1.25 (e) and 2.50 (f) meters apart from the grid sample (a_0).

3.2.3. Soil analysis

Samples were oven dried at 65 °C (Thermax Series TS8000) until no further weight loss occurred, then weighted, before they were sieved down to < 2 mm. Samples were then weighed again to determine the stone mass. Bulk densities was calculated from the dry mass and the core volume after being corrected for coarse fragments (> 2mm) (Throop et al., 2012). To determine C_c, samples were grounded to a size of <100 µm using a ball mill, before the homogenized mixture was analysed using a VarioMax (Elementar Analysensyterne GmbH, Hanau, Germany). The analysis was done at the Skogforsk commercial laboratory and complied with ISO 9000 certified methods. We refer to total sample C as organic carbon, since the amount of inorganic C is considered low in these acidic soils (Huntington et al., 1989; Nielsen et al., 2007). To avoid inclusion of mineral soil in the organic layer samples, all concentrations are expressed on an organic matter basis. The sample C stock was estimated by multiplying the sample weight of the organic material (per unit area) with the C_c derived from the sample material. Carbon stocks are presented in kg m^{-2}, since extrapolation over large scales (using Mg ha^{-1}) can be problematical due to a range of unknown correction factors, such as spatial variation, large roots and stumps.

3.2.4. Data analysis

Standard statistical methods were used to describe central trends and spread, without considering the spatial nature of the data. One-way analysis of variance (ANOVA) was used to determine if there were any statistically significant differences between means or distributions. Statistical significance was accepted at $\alpha = 0.05$ level for omnibus tests. Pairwise comparisons were done post hoc using either Games-Howell (Games and Howell, 1976) or Dunn's procedure with Holm-Bonferroni correction (Dunn, 1964; Holm, 1979; Rice, 1989). Associations between soil parameters were described using Pearson's correlation coefficient or least squares regression. Effect estimates are given as: r (Pearson's corr.), η^2 (ANOVA), and adjusted R^2 for linear regressions. All coefficients and effect estimates are presented with 95% confidence intervals.

To investigate how standing trees influence the spatial structures of organic layer C, a nearest neighbor analysis was conducted to determine the separation distances between every sample location and its closest stem. As samples collected near the plot border can have their nearest neighboring tree outside the sampling window, all observations situated closer to the plot border than the nearest tree was excluded. A linear regression was used to establish the association between stem proximity and organic layer C.

Standard geostatistical methods were used to examine the spatial variation in the measured soil properties across the study plots (Webster and Oliver, 2001). First we

computed experimental variograms, which describes the structure and nature of the spatial variation using both raw and transformed data (Eq. 1 to 5). Second, after spatial dependency was established, the parameters of the variogram models were used for ordinary kriging, which interpolates values based on local weighed averages (Eq. 7).

Because of variogram sensitivity to distribution skewness and outliers (Webster and Oliver, 2001), data were controlled for normality with Shapiro-Wilk test statistics (Shapiro and Wilk, 1965), and outliers identified with Grubbs test (Grubbs, 1969). A total of 11 samples were removed from the dataset. A lag distance equal to the minimum separation distance of sample points (0.15 cm) was used in the variogram computations. We did a preliminary examination of anisotropy, which assesses whether the plots exhibits differences in the spatial structure in any direction. Anisotropy can be detected by computing the autocorrelation among points oriented to each other in specific directions and comparing whether there are structural differences (Legendre and Fortin, 1989). No anisotropy was detected, and the plots were therefore considered isotropic. Thus, all variograms were calculated on an omnidirectional basis.

The structure of the spatial autocorrelation is evaluated by means of the semivariance γ, calculated for each variable at a given separation vector, h (Eq. 1). Most commonly, $\gamma(h)$ increases with distance between the observations until it levels off, approaching a constant value called the sill (C). The range (a) is found at the distance where the sill reaches maximum variance, meaning the distance where samples no longer

are considered spatially autocorrelated. The nugget variance (C_0) is found where the lag distance approaches zero and intercepts with the y-axis. Theoretically this should be zero, but because of the spatial heterogeneity of scales less than the minimum sampling distance or sampling errors, this number is usually positive. Nugget, sill and effective range parameters were estimated using a weighted least squares criterion, where weights are given by the number of pairs within the interval with lag h (Webster and Oliver, 2001).

$$\gamma(h) = \frac{1}{2n(h)} \sum_{\alpha=1}^{n(h)} \{z(x_\alpha) - z(x_\alpha + h)\}^2 \tag{1}$$

where, $\gamma(h)$ denotes the experimental variance of data pairs $z(x_\alpha)$ and $z(x_\alpha + h)$ at spatial point x_i and $x_i + h$. $N(h)$ is the number of pairs in each bin, separated by a separation vector (h). Spherical (Eq. 2) and exponential models with a variable nugget component were fitted to the experimental variograms (Webster and Oliver, 2001). Models were then selected based on the lowest weighted sum of squares differences between experimental and model variogram values (Cressie, 1985). Since there were no marked differences between raw or transformed data, predicted values are therefore presented on the original scale of measurement. Values from the best fit model were used to describe patterns of spatial dependencies, as well as provide input parameters for the kriging interpolation.

$$\gamma(h) = \begin{cases} 0, & |h| = 0 \\ c_0 + c_1 \left[\frac{3|h|}{2a} - \frac{1}{2}\left(\frac{|h|}{a}\right)^3 \right], & 0 < |h| \leq a \\ c_0 + c_1, & |h| \geq a \end{cases} \tag{2}$$

where c_0, c_1 and $a \geq 0$.

The exponential model is defined as (Eq. 3):

$$\gamma(h) = \begin{cases} 0, & |h| = 0 \\ c_0 + c_S \left[1 - e^{-3|h|/a} \right], & |h| > 0 \end{cases} \tag{3}$$

where c_0, c_S and a are similar to the spherical model; ≥ 0.

To enable comparison of the relative size of the nugget effect across soil properties, a spatial correlation index (SCI) was quantified using spatial class ratios (nugget/sill ratio) to define distinctive classes of spatial dependence within the data (Eq. 4) (Cambardella et al., 1994). The SCI denotes the degree of spatial dependence and is considered having strong dependency if the nugget/sill ratio is $< 25\%$; between 25 and 75% as moderate, while $> 75\%$ as weak.

$$SCI = \frac{c_0}{c_0 + \sigma_0^2} \times 100 \tag{4}$$

where c_0 represents the nugget variance and σ_0 the partial sill.

The correlation between two variables is usually expressed using a product-moment correlation coefficient, which simply summarizes the relation between i and j without considering the spatial location of the observations.

To assess the scales of spatial correlation between attributes we first computed omnidirectional cross-correlations at 1 m distance intervals (Goovaerts, 1998). For each distance class, a Mantel test is performed and a Mantel r statistic with a corrected

70

Bonferroni p-value is computed. The coefficients of spatial association at given lag distance (h) are indicated by the Mantel correlogram (Cliff and Ord, 1981). Second, cross-variograms modeled by linear model of coregionalization (LMCR) were used to examine how two soil properties jointly vary over a vector (h) (Eq. 5) (McBratney and Webster, 1983).

$$\hat{\gamma}_{ij}\left(h\right) = \frac{1}{2n\left(h\right)} \sum_{\alpha=1}^{n(h)} \left[z_i(x_\alpha) - z_i(x_\alpha + h) \right] \times \left[z_j(x_\alpha) - z_j(x_\alpha + h) \right] \quad (5)$$

where $z_i(\chi_\alpha)$ and $z_j(\chi_\alpha)$ are the values of variable z_i and z_j at location χ_α, while $z_i(\chi_\alpha+h)$ and $z_j(\chi_\alpha+h)$ denote values of z_i and z_j at the location $\chi_\alpha+h$. If both variables are positively related, an increase in z_i from χ_α to $\chi_\alpha + h$ will be associated with an increase in z_j over the same distance, h.

The cross variogram (Eq. 5) was then normalized into the codispersion coefficient, ρ, (Eq. 6). This coefficient can be interpreted as a linear correlation coefficient between vector increments of selected variables, and is based on the construction of ranks associated to given coordinates (Goovaerts, 1998).

$$\rho_{ij} = \frac{\hat{\gamma}_{ij}(h)}{\sqrt{\gamma_{ii}(h)\gamma_{jj}(h)}} \in \left[-1, +1\right] \quad (6)$$

where γ_{ij} (h), γ_{ii} (h) and γ_{jj} (h) are the semi-variance of variable X, the semivariance of variable Y and the cross-semivariance between X and Y and lag distance h, respectively. If the relation between both variables does not change with spatial scale, then $\rho_{ij}(h)$ will

be constant for all h and the variables can be considered intrinsically correlated. Under the condition of second-order stationarity, ρ_{ij} (0) equals the ordinary product-moment correlation coefficient (Goovaerts, 1998) .

Mean C stocks for each plot were also estimated using an ordinary kriging approach. The kriging approach gives a more realistic estimate than calculations of averages from samples which might be spatially autocorrelated. While spatial autocorrelation enlarges the variance of the mean in single plots, it may decrease the estimated variance in a kriging approach. By including the parameters from the fitted variogram models, the kriging method predicts the value of an unobserved location by interpolating measurements at nearby points (Webster and Oliver, 2001). The kriging estimate Z at the point X_0 is defined as (Eq. 7):

$$\hat{Z}(x_0) = \sum_{i=1}^{N} \lambda_i z(x_i) \tag{7}$$

where $Z(\chi_0)$ is the value to be estimated at location of χ, $z(\chi_i)$ is the measured data at location neighboring the interpolation point χ_i, e_i is a weight factor which depends on the variogram model and n is the number of neighboring measure data points used for interpolation. The weights sum to 1, which decrease the estimation variance, σ_k^2, and assures a lack of bias (Webster and Oliver, 2001).

To further improve time- and cost-effective sampling designs for C under similar conditions, we need more knowledge on how sample size influences the reliability of the

mean value. A satisfactory number of samples are reached when additional sampling no longer significantly reduces the variability of the mean estimate. Using a bootstrap method with a random seed we did 1000 simulation runs on the sample mean and its confidence interval (95%). The resampling process was conducted without replacement on samples sizes ranging from two to the maximum number of samples on each plot.

Data processing and analysis was performed off-line using a commercial software package (MATLAB 2011b, MathWorks Inc., Natick, MA, USA 2012) and R 3.0.2. (R Core Team, 2013).

3.3. Results

3.3.1. Descriptive statistics
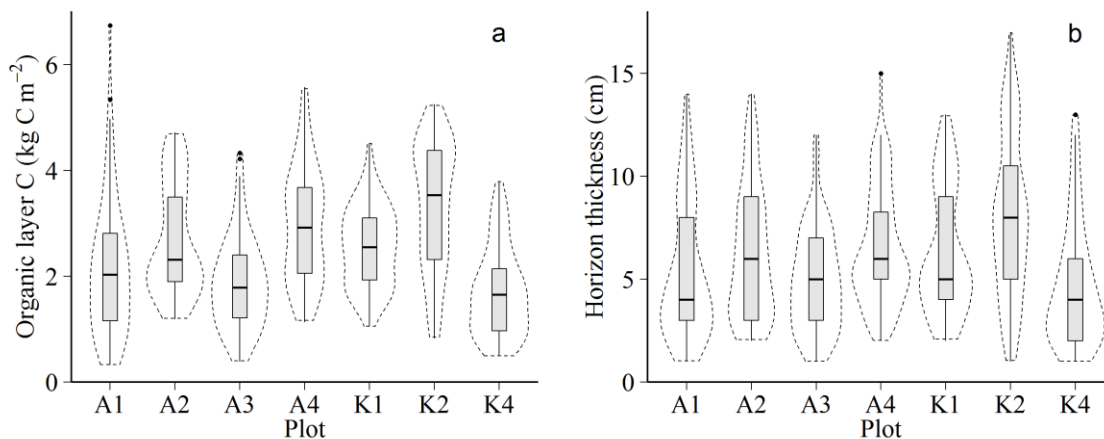
Figure 3. Tukey's box plots of (a) organic horizon C and (b) thickness showing 10, 25, 75, and 90th percentiles, medians and outliers for the different plots. Violin plot (dotted line) denotes sample distribution. Soil samples were separated by 5 m and can therefore be considered independent according to the spatial analysis (Table 3).

Mean thickness of the organic soil layer (i.e. the thickness of the F and H horizons) ranged from 4.7 to 8.1 cm (Table 2, Fig. 3), with coefficients of variation (CV = s/mean, %) among grid samples ranging from 44 to 64%. Differences in horizon thickness between plots was significant ($\chi2 = 46.6$, df = 6, p < 0.05; Kruskal-Wallis rank sum test).

Increasing horizon thickness was associated with increasing bulk density (Welsh $F_{(1,483)} = 298.24$, p < 0.001, RMSE = 0.079). Horizon thickness accounted for 38.2% of the observed variability in BD (Fig. 4). In contrast, the relative variation bulk density decreased as the horizon thickness increased ($r_{(15)} = -0.81$ (-0.51, -0.93), p < 0.001).
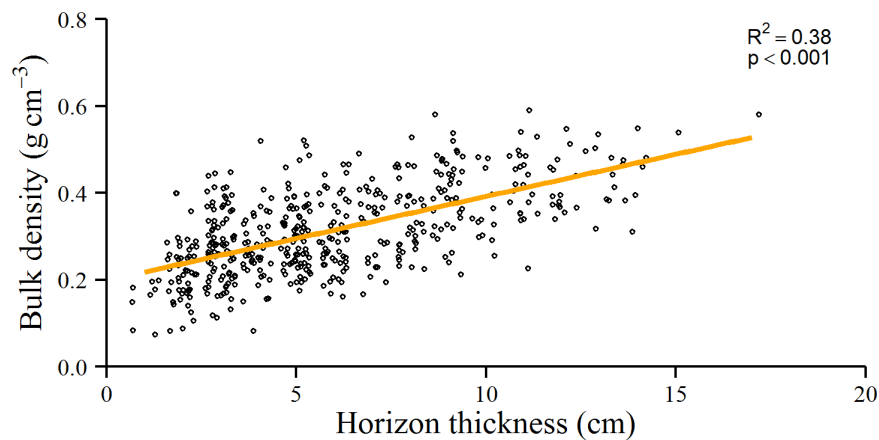
Figure 4. Scatter plot showing the relation between bulk density and horizon thickness (n = 484).

The elementary C concentration in the SOC ranged from 37 to 45%, and was less variable (CV 10% to 17%) than other measured SOC properties. Plots were significantly different, Welch's $F_{(6, 208)} = 16.664$, $p < 0.001$, and a Games-Howell post-hoc analysis revealed that 11 out of 21 plot pairs were statistically different. Negative coefficients indicated an inverse relationship between C concentration and horizon thickness (Welch's $F_{(1, 483)} = 207$, $p < 0.001$), with horizon thickness explaining 30% of the variation. In addition to lower C concentrations in thicker layers, the C_c variability also increased. Horizon thickness explained 68% of the model deviation ($r_{(15)} = 0.884$ (0.679, 0.961), $p < 0.001$).

There were large variations in the amount of organic layer C within each location (CV 31 to 63%), all which exceeded the intra-plot variation (CV 22%). The variances in the organic layer C between plots were heterogenic (Levene's test, $p = 0.002$). Mean values ranged from 1.87 to 3.33 kg m^{-2} (Table 2, Fig. 3), and were statistically different between plots (Welch's $F_{(6, 212)} = 24.252$, $p < 0.001$). Pairwise comparisons using Games-Howell post-hoc analysis revealed that out of 21 location pairs, 14 were found to significantly differ. In contrast to the C concentration, we observed a negative correlation between horizon thickness and the variation of C stock ($r_{(15)} = -0.77$ (-0.92, -0.42), $p = 0.011$). A correlation test between mean C values and CV was non-conclusive ($r_{(7)} = -0.64$ (-0.94, 0.21), $p = 0.12$).

Table 2. Descriptive statistics of the organic layer. Organic layer consisting of: OF (O_e) horizon (fragmented and/or altered), partly decomposed (i.e. fragmented, bleached, spotted) organic matter, and OH (O_a) horizon (humus, humidification, humic layer): well-decomposed amorphous organic matter.

							Organic layer properties					
	Carbon stock						Thickness		Bulk density		Carbon conc.	
Plot	Mean	SD	Min	Max	OK	OKSD	Mean	±1SD	Mean	SD	Mean	SD
A1	2.15	1.31	0.32	6.74	2.32	1.08	5.35	3.23	0.29	0.12	40.7	4.2
A2	2.67	1.04	1.19	4.71	2.75	0.88	6.21	3.15	0.34	0.08	41.9	5.4
A3	1.87	0.87	0.38	4.33	1.90	0.70	4.96	2.43	0.26	0.08	44.7	5.0
A4	3.01	1.22	1.13	5.57	2.96	0.99	6.49	2.83	0.37	0.12	42.1	6.4
K1	2.54	0.72	1.05	4.52	2.61	0.60	6.37	3.06	0.32	0.06	42.5	5.1
K2	3.33	1.20	0.83	5.25	3.34	0.92	8.09	3.80	0.39	0.10	37.3	6.2
K4	1.69	0.87	0.49	3.79	1.75	0.71	4.65	2.96	0.25	0.07	43.3	4.8

Note: OK denote values computed from ordinary kriging. Carbon concentration is expressed as % of organic matter, C stock in kg m^{-2}, horizon thickness (cm) and bulk density in (gr cm^{-3}). SD = ±1 Standard deviation.

Using least squares regression, we found significant associations between horizon thickness and organic layer C on all plots (Table 3). The effects of location on regression slopes was not significant, (p = 0.187, η^2=0.005 (0.00, 0.035)), thus we assume homogeneity of slopes. An overall linear regression with horizon thickness explained 68% of the variation in the organic layer C stock (Welch's $F_{(1, 483)}$ = 977, p < 0.001). The regression equation was: organic layer C = 0.71 (95% CI: 0.58, 0.83) + 0.29 (0.27, 0.31) x (horizon thickness) + ε_i.

Table 3. Regression coefficients of organic layer thickness and C stock.

Plot	Regression coefficients					
	Intercept	SE	Slope	SE	R^2	RMSE
A1	0.36	0.18	0.33	0.03	0.68	0.74
A2	0.88	0.14	0.29	0.02	0.74	0.54
A3	0.40	0.12	0.29	0.02	0.71	0.44
A4	0.99	0.22	0.31	0.03	0.58	0.71
K1	1.34	0.14	0.19	0.02	0.60	0.49
K2	1.30	0.21	0.25	0.02	0.62	0.75
K4	0.44	0.08	0.27	0.01	0.82	0.34
Overall	0.67	0.06	0.30	0.01	0.68	0.66

Note: SE = ±1 Standard Error

3.3.2. *Effects of tree proximity on organic layer carbon*

A nearest neighbor distance analysis revealed that ~13% of the samples were closer to the plot border than the nearest tree, and were thus excluded from further analysis to avoid any edge effects. There was a negative association between the distance to the nearest stem and organic layer C stock, (Welch's $F_{(1, 422)} = 17$, $p < 0.001$), explaining only 4% of the variation (Fig. 5). On a plot level, this relationship was observed for two of the plots. Although significant, the regression models never explained more than 10% of the variability in the data (results not shown).
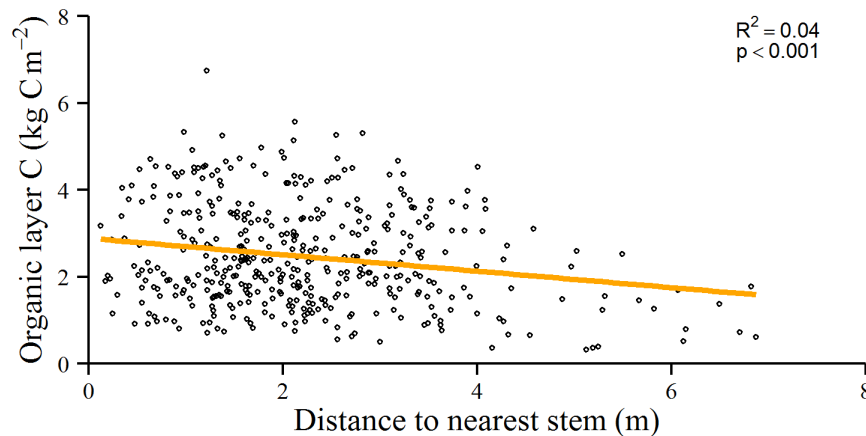
Figure 5. Relationship between observed values of soil organic layer C and the proximity to nearest stem (n = 422).

3.3.3. *Spatial variability of soil organic layer attributes*

Spherical models (Eq. 2) gave the best fit with bin variances at the given lag distances, indicated by lower values of the summed square of residuals. We therefore assume that parameters from the spherical model best describe the spatial structure of the measured soil property. All variograms for organic layer C (Fig. 6) and horizon thickness (not shown) were transitive, reaching a finite semivariance (sill) close to the sample variance. The difference between the sample variance and the sill was relatively small, which suggests that experimental model is valid. Organic layer C was autocorrelated at distances ranging from 0.86 to 2.85 m (Table 4).

Table 4. Parameters from spherical models fitted in experimental variograms for organic layer C

Plot	Variogram model coefficients				
	Range (a)	Nugget (C_0)	Sill (C_0+C)	SCI	SSE
A1	2.85	0.01	1.68	Strong	3.87
A2	1.11	0.11	0.73	Strong	1.58
A3	1.90	0.17	0.56	Medium	0.54
A4	0.86	0.14	0.97	Strong	7.95
K1	1.64	0.11	0.46	Strong	0.16
K2	1.51	0.15	1.01	Strong	2.60
K4	1.07	0.07	0.86	Strong	0.23

Note: SCI = Spatial correlation index
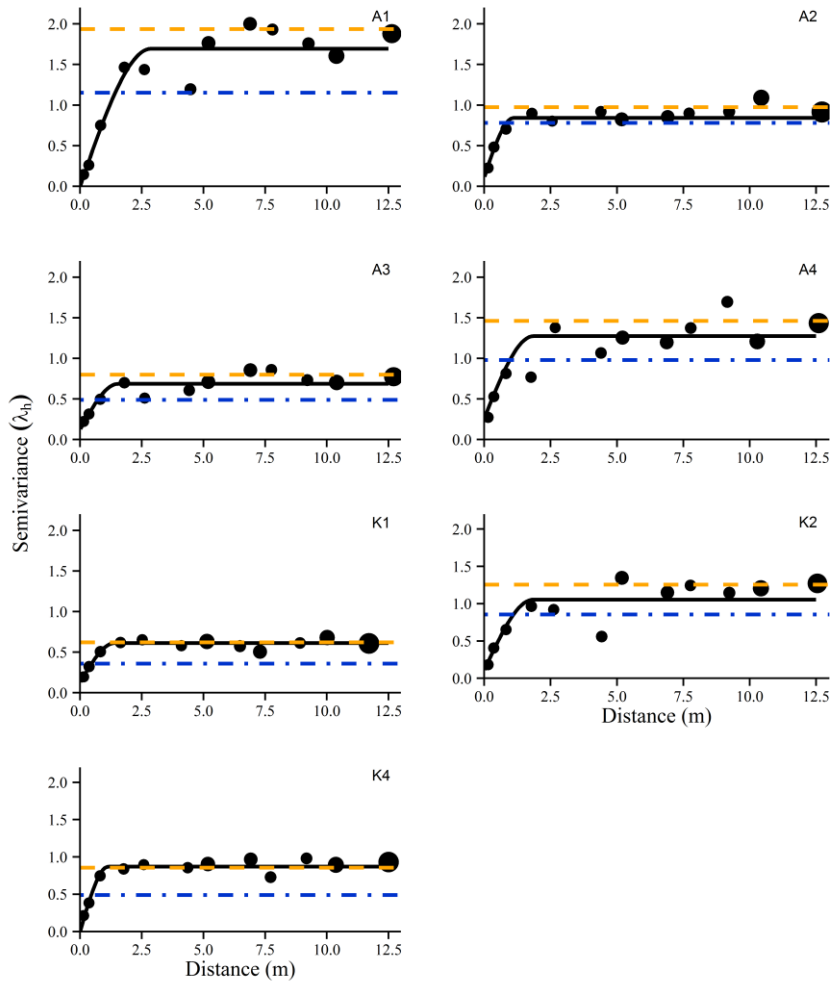
Figure 6. Experimental omnidirectional variograms of organic layer C for each of the study plots. The semivariance of sample pair bins (filled circles) plotted against pair distance (in meter). Sizes of filled circles indicate the number of pairs in each bin, categorized in five, ranging from 25 to 1200. Bins with less than 25 pairs were excluded from the analysis. Range, nugget and sill were derived from fitted spherical models (solid lines).The plot variance (grid and spatial samples combined) is represented by the horizontal dotted lines (orange), while the double-dotted lines (blue) show kriging variances.

This suggests that C samples collected from the grid (5 m separation) can be considered spatially independent. Low nugget values indicate that sample pairs with the shortest lag distance (0.15 m) were collected with a separation distance sufficient to explain the local variation at a very fine scale. The relative size of the nugget compared to the sill was small (2% to 31%), indicating that the majority of variability is associated with space, primarily the lag distance between samples.

The low nugget/sill ratios indicate a strong spatial structure, which improves the accuracy of geostatistical techniques such as kriging. Although the plot mean C stock values derived from the grid sampling did not differ significantly from the kriging estimates (mean = 0.05 (-0.01, 0.11), p = 0.085) (Table 1), the kriged predictions had a 28 to 41 % lower variance compared to the absolute values, which corresponds to a reduction of 17 to 23 % in the proportion of the standard deviation to the observed mean.

Cross-correlations (Fig. 7) and the codispersion coefficient (Fig. 8) were used to assess the presence of spatial correlation between horizon thickness and the organic layer C stock. The cross-correlations, quantified by the Mantel r, decreased more or less linearly to a distance of 4 m where the correlation was close to zero or non-significant. On all seven plots the correlations were significant at distances up to 2 meter, indicating that the associations between the samples at the shortest distance classes were higher than one could expect by chance alone. From the codispersion function it can be observed how the correlation between the horizon thickness and organic layer C approached the

ordinary product-moment correlation coefficient with increasing separation distances (Fig. 8). For increments between nearby data points, up to approximately 4 m, the spatial relationships were weaker, while their strength remained in most cases more or less constant for increments of sample points separated by >4 m.
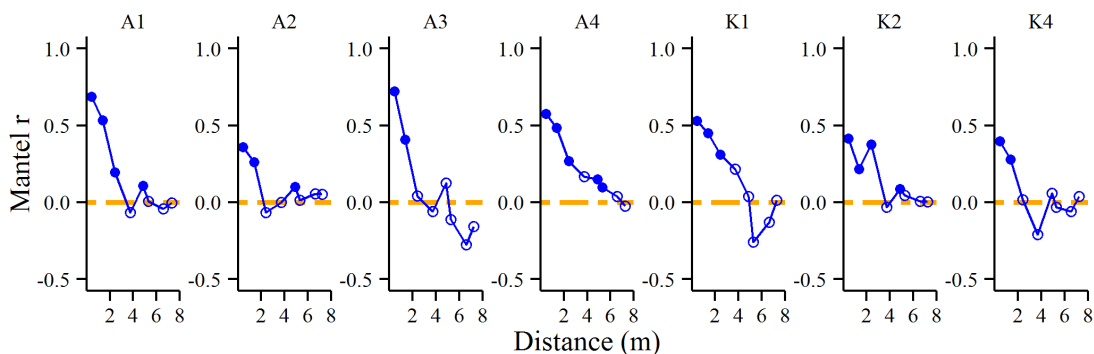
Figure 7. Omnidirectional Mantel correlogram showing the strength of the spatial correlation between organic layer C and horizon thickness for soil cores within different distance classes (at 1000 permutations). Points are plotted at the midpoint of each distance class. Bins with less than 25 pairs were excluded from the analysis. Solid circles represent significant correlations, while open circles show correlations that are not significantly different from zero. At the distance where the plotted lines approach the x-intercept (red dotted line) objects are no more similar than that expected by-chance-alone across the plot.
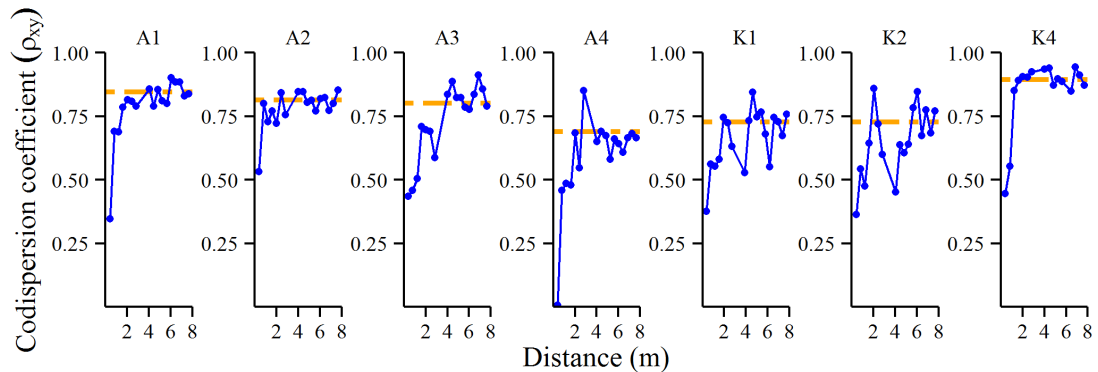
Figure 8. Codispersion coefficients (ρ_{XY}) of organic layer thickness and C stock. The horizontal line (blue dotted) denotes Pearson's correlation coefficient. This coefficient is a normalized version of the cross-variogram between two the organic layer C and horizon thickness, and can interpreted as a linear correlation coefficient between spatial increments of both attributes.

3.3.4. Estimate precision and sample size

Using the bootstrapping method we analysed how different sample sizes of soil C influenced the variability of the mean and its 95% confidence interval. The spatial variability analysis indicated that samples which were collected on 5 m intervals can be considered spatially independent. Thus, only observations from the main grid (Fig. 2) were included in the model. As expected, the variability around the estimated plot means decrease with increasing sample sizes.
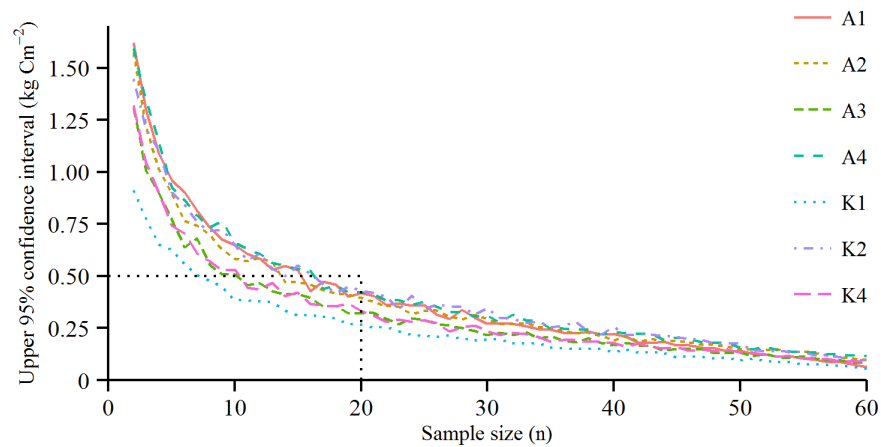
Figure 9. Upper half of 95% confidence intervals of the organic layer C stock according to sample size (n). Samples used in the bootstrapping approach have separation distances greater (5 m) than the spatial autocorrelation range (max 2.8 m), and can therefore be considered independent. Each plot is represented by an individual line.

With a high initial marginal value of additional observations, the gain diminishes when 25 to 40 samples have been collected (Fig. 9). After 20 samples, all 95% confidence intervals were $< \pm 0.5$ kg C m^{-2} from the sample mean. The confidence widths are in the range of 10 to 20% of the respective site means. After 40 samples the uncertainty was further reduced to 5 to 11% of the plot mean. The widths of confidence intervals were correlated to plot variance of C stocks ($r_{(7)}$= 0.50 (0.35, 0.65), p = 0.003), but we could not detect any relation to stock size ($r_{(7)}$ = 0.12 (-0.25, 0.37), p = 0.21).

84

3.4. Discussion

Results from this study demonstrate the inherently heterogeneous nature of organic layer C in boreal forest soils. Until now little has been known about the spatial variability of podzols in mature boreal forests, as nearly all previous studies have been conducted in young and middle aged stands. Our data indicate that observations of organic layer C are autocorrelated at only short distances, ranging from as little as 0.86 to 2.85 m. Interestingly, the results shown here are comparable to findings from younger stands, where reported autocorrelation range rarely exceeds 7 m (Häkkinen et al., 2011; Muukkonen et al., 2009). Based on our data we propose that when conducting similar surveys on boreal podzols, a minimum of 20 samples separated by ~5 m will obtain estimates with a precision of better than ± 0.5 kg C m^{-2}. Moreover, we establish a strong spatial coupling between the organic layer C stock and layer thickness. This suggests that relatively inexpensive measurements of horizon thickness can supplement the physical collection of soil C samples, to reduce sample size needed, or to increase the spatial resolution of organic layer C mapping.

3.4.1. Organic layer carbon

There was considerable heterogeneity in organic layer C stocks within each plot, where the corresponding coefficient of variation ranged from 29 to 61%. On all plots we found a strong and corresponding spatial pattern for organic layer C, with autocorrelation distances ranging from 0.86 to 2.85 m. The variation and spatial patterns are comparable

85

to results from young and middle aged boreal forest stands across Finland where the autocorrelation range rarely exceeded 7 m (Häkkinen et al., 2011; Liski, 1995; Muukkonen et al., 2009). Although the previous studies don't refer to what harvesting methods were used in the stands, it is interesting to note that the degree of heterogeneity does not appear to change fundamentally between the natural variation revealed in this study and those conducted in actively managed stands. However, the current knowledge is based on results from a very limited number of plots, and the collection of empirical data across a range of ecological variables should be a priority. Further, more information on how different harvesting techniques influence the spatial and temporal variability of soil C is also needed. The assumption of an unchanged spatial variation over time should be tested with empirical data. Nevertheless, similar autocorrelation ranges between studies suggest that the spatial information given here could be used as a proxy for sampling dependencies in later inventories conducted in boreal coniferous forests. It should be noted however, that the range itself is no absolute estimate of the spatial structure, thus the predictability among individual sampling points within the range can still be low. If the sample design is out of phase with the local variability it will fail to detect local fluctuations, and the resulting nugget/sill ratios will be high, an indication of weak spatial structures. For example, the high nugget/sill ratio (>60%) and autocorrelations ranges of >55 m reported by Worsham et al. (2010) in a study of forest soil C is likely a consequence of a sample design inadequate to assess small scale

fluctuations. Similarly, efficient sampling designs aiming to determine spatial dependence must have sufficient sampling intensity and be conducted in a sampling window exceeding the local autocorrelation range. If any of these are aspect are insufficient, it might lead to the use of improper models. This can result in unrealistic spatial interpretations, such as some the plots presented in Häkkinen et al. (2011), where the autocorrelation distance for organic layer C in middle-aged boreal forest soils was estimated at 950 m.

Many earlier soil C assessments that form the basis of current larger inventories, present quantified soil information without considering the spatial dependency of the observations, and consequently contain little information of spatial structures (Jandl et al., 2014; Lindner and Karjalainen, 2007). By not accounting for the spatial coordinates of the observations, these surveys have assumed a flat variogram where the sill equals the population variance. This may have resulted in major systematic bias in many meta-studies and modeling efforts, where the unreliability of such surveys is not captured in the overall estimates of uncertainty (Ortiz et al., 2013). Precise estimates of variance are also important for future inventories and verification protocols, as the number of samples required to achieve acceptable levels of precision is determined by the variance. We demonstrate how a quantification of the spatial structure can lower the variance (Table 2), which improves the statistical power to detect a change. Mäkipää et al. (2008) reported that the main cost of soil C analysis occurs during the sample preparation and laboratory

87

analysis. Thus, lowering the number of samples required for laboratory analysis could substantially reduce the cost of future inventories and improve the economic feasibility of verification protocols (VandenBygaart et al., 2007).

3.4.2. *Horizon thickness as a predictor of organic layer carbon*

Despite measurable biological differences in the plot stands, we found horizon thickness to be a strong predictor of organic layer C stocks, explaining 68% of the overall model variation. This correlation was also significant when analysed spatially, as indicated by Mantel's r (Fig. 8) and codispersion coefficient (Fig. 9). On all plots two distributions converged around the correlation coefficient, which suggests that the correlation structure is maintained across the different stands. Our findings support results from Schulp et al. (2009), who established a strong association ($R^2 = 0.59$) between horizon thickness and C stock across different tree species (incl. conifers) in the Netherlands. Grüneberg et al. (2010) also reported similar correlations in a study on Cambisols, Luvisols and Stagnosols from Germany. Surprisingly, this pattern has not yet been reported by earlier studies of boreal podzols, as most studies concerning soil C have used fixed depth increments instead of sampling by horizon (Don et al., 2007; Schöning et al., 2006). Carbon estimates from fixed depth sampling are problematic in podzols because confounding effects of spatial and temporal variation cause a large dissimilarity in soil properties between horizons (Hilli et al., 2008; Kulmatiski and Beard, 2004). For example, mineral soils usually contains C concentrations less than ~2%, but have bulk

densities which exceeds the organic layer by several magnitudes (Olsson et al., 2009). Thus, mixing horizons will in most cases amplify the variance, which in turn will increase the sample requirement for both inventories and future resampling if the maximum sample error is pre-determined.

3.4.3. *Stem proximity*

As much as 70 to 80% of the annual input to the organic layer C stock (Liski et al., 2002) comes from plant litter distributed near or at the surface (Liski and Westman, 1995). Since a large portion of this is residue from nearby trees one can anticipate that the organic layer within the tree influence zone will display different attributes than soils situated in canopy openings. With higher litter input, the expected accumulation of organic layer C have shown to be greater at locations closer to tree stems (Bens et al., 2006; Liski, 1995; Penne et al., 2010). Hanson et al. (2011) found a positive association between the organic layer C stock and neighboring basal area in younger spruce and pine stands. In a study conducted on a single 6 x 8 m plot in Finland, Liski (1995) reported higher C densities and larger organic horizon variability in the vicinity of Scots Pine stems. However, the local accumulation depends not only on the proximity, but also on the litter quality, which have shown to differ between species (Hansson et al., 2011; Palviainen et al., 2004; Stendahl et al., 2010). Using stands with comparable biophysical characteristics allowed us to qualitatively assess the influence of tree proximity on the spatial structure of organic layer C. Although inconsistent, significant associations

between organic layer C stock and tree proximity were detected at two of the plots. Interestingly, the stands which showed a positive correlation between the organic layer C stock and stem proximity were dominated by fewer and larger trees. Thus, the relative influence of larger trees to its surroundings is therefore expected to be higher at these locations. Overall, the plots in this study were situated in relatively dense forests stands, and the differences in distribution of plant residues might therefore have been small, which might explain why we did not detect this relationship in five of the seven plots. However, the current spatial structure of the organic layer is influenced, not only by present stem location, but will to some extent also reflect past vegetation patterns. Unmanaged mature stands are characterized by gap-filling dynamics which gives the multi-layered structure seen in these stands. Self-replacement in canopy gaps by younger trees can therefore have contributed to mask this relationship at some of the plots. Nevertheless, these positive results indicate that the correlation between stem and organic layer C might be ecological relevant, and warrants further investigation across a wider range of variables. The variances of spatial autocorrelation distances in these mature forests were relatively small, and did not appear to associate with the current configuration of stems. This suggests that other environmental gradients, such as the local terrain attributes are essential to explaining the structural heterogeneity of soils. Topographic features such as slope is known to influence hydrological conditions (Beven and Kirkby, 1979), and several studies have found variable degrees of associations

90

between the terrain characteristics and SOC (Binkley and Fisher, 2012; Mueller and Pierce, 2003; Seibert et al., 2007; Thompson and Kolka, 2005).

3.4.4. *Optimizing future sampling*

While short sample separation distances are required to reveal the local spatial structure, an optimized inventory design has sample points which exceed the variogram range, meaning there are no autocorrelation between the samples. When required distance for sample independence is determined, we illustrate in the bootstrapping analysis (Fig. 7) how the number of independent samples influences the confidence intervals of seven C inventories. We find that 10 to 20 measurements in an area of 2000 m^2 are necessary to provide a reliable estimate ($\pm$ 0.5 kg C m^{-2}). Muukkonen et al. (2010) proposed similar requirements in a study on young forests stands in Finland, which suggests that these results might have a general application in boreal forests. The CI widths of the bootstrapped values are positively correlated with the local variation of organic layer C, meaning that the sampling effort needed to achieve the critical precision will increase in plots with higher variability.

If no prior knowledge about the spatial structure is available, a stepwise sampling procedure is recommended: where the investigator first considers the spatial dependency by a reconnaissance sampling before deciding on the final sampling strategy. Similar suggestions have also been given by Webster and Oliver (2001). If the assumption of a strong correlation between organic layer C stock and horizon thickness is constant across

the landscape, horizon thickness should be considered in an adaptive inventory strategy (Marchant and Lark, 2006). Compared to C_c, which is highly seasonally dependent (Hogberg et al., 2001) and has to be estimated in laboratory analysis, horizon thickness has the benefit of *in situ* measurements. High resolution data on horizon thickness can be obtained quickly and at a relatively low cost, making it optimal as a reconnaissance element in a stepwise sampling design. After initial observations of horizon thickness, variograms can be computed to find the most efficient sample separation distance for a grid sampling design that will achieve a target error variance, or even propose optimal sampling placement of individual sampling points.

Although the plots in our study were isotropic, we propose that variogram parameters of horizon thickness can be particularly beneficial when they reveal anisotropic patterns, as this implies that an equilateral sampling grid might not be the optimal design for the selected area. To detect anisotropy from variograms, observations should be collected from three or more directions (McBratney et al., 1981). Under such circumstances, where the variation of horizon thickness is geometrically anisotropic, placement of individual sampling points should be denser in the direction of higher variability (van Groenigen, 2000). If conditions are isotropic, a sample separation distance equaling twice the range has been found to maximize the area spatially correlated (van Groenigen et al., 1999).

Measurements of horizon thickness could also be used as a secondary variable in an ordinary cokriging approach. Cokriging is a multivariate extension of ordinary kriging, which uses the cross-correlation between the variables in addition to the autocorrelation of the primary variable. This method is commonly used in studies where the primary variable is sampled less densely because of cost or practical difficulties and cannot be used as an exhaustive variable in a detailed mapping practice, whereas the secondary variable can be obtained more effectively (Goovaerts, 1999; Webster and Oliver, 2001). When variables are correlated, the use of cokriging can yield more precise estimates than using ordinary kriging of the lesser sampled variable alone (Atkinson et al., 1992). A number of studies in the soil literature have successfully demonstrated that uncertainties can be substantially reduced with the aid of the secondary data (Kunkel et al., 2011; Simbahan et al., 2006). For example, Odeh et al. (1995) combined kriging and linear regression with a digital elevation model to determine landform attributes for prediction of C_c in topsoil. The strong correlation between horizon thickness and C stock shown here, therefore suggests that the resolution of soil C mapping can be improved by using a denser sampling scheme of horizon thickness measurements as a covariate for organic layer C stocks.

3.5. Conclusion

Information about spatial structures is not only interesting for basic and applied ecological purposes, but could also be very valuable for reducing costs of measuring and

monitoring C in any future market with incentives for C sequestration. The ecological complexity and heterogeneity of soils makes estimations of C stock for inventories or monitoring challenging, thus to improve the precision of large scale modeling more evidence from accurate small scale inventories are critical. New data and information on different scales and environmental gradients, in conjunction with technologies such as remote sensing is desired to improve our knowledge about the size and dynamics of this large C pool.

This study shows that the organic layer C stock is spatially autocorrelated on distances between 0.86 to 2.85 m. When conducting similar surveys on boreal podzols, we found that 10 to 20 samples in an area of 2000 m^2, separated by ~5 m are sufficient to obtain unbiased estimates with an accuracy of ±0.5 kg C m^{-2}. Despite significant differences among soil properties within and between plots, it is evident that horizon thickness and organic layer carbon C were closely correlated. We therefore suggests that measurements of horizon thickness can be valuable component in an adaptive design aiming to measure C stock, as a proxy for the local spatial structure of C and as a predictor or covariate a in C estimations. This can lower the number of samples needed for treatment and C analysis, which in turn would simplify and reduce the cost of future soil C surveys.

Chapter 4: Relocation of paired samples: Implications for soil C monitoring

Terje Kristensen[1], Paul V. Bolstad[1], Mikael Ohlson[2], Charles H. Perry[3], Randall Kolka[4]

[1] Department of Forest Resources, University of Minnesota, 115 Green Hall, 1530 Cleveland Ave. N., St. Paul, MN 55108, USA

[2] Department of Ecology and Natural Management, Norwegian University of Life Sciences, P.O.Box 5003, 1432 Aas, Norway

[3] USDA Forest Service, Northern Research Station, 1992 Folwell Avenue, St. Paul, MN 55108, USA

[4] USDA Forest Service, Northern Research Station, 1831 Hwy 169 East, Grand Rapids, MN 55744, USA

Summary

Assessing changes in organic layer C stocks is complicated by the inherent short-range variability of soils. Due to the destructive nature of soil sampling, where primary samples are physically removed, a true paired sampling cannot be implemented. Instead samples must be relocated, meaning that the paired sample is only an approximation of the baseline sample. Thus, some of the estimated difference between the observations

95

from baseline and revisit may therefore not be a result of a change, but instead reflect the spatial variability already present at time of baseline sampling. In this study we analyzed how the short-range variability in organic layer C affects sample size requirements when paired samples are relocated. We contemporaneously collected organic layer C sample pairs separated by 15, 30, 60 and 125 cm from seven different plots scattered across a forest. All plots were situated on podzols in a multilayered boreal forest in south east Norway. Because samples were collected contemporaneously at each plot, the difference in sample pairs reflects the spatial variability rather than a change over time. The results shows that sample repeatability rapidly declines with sample separation distance, and the *a priori* sample sizes needed to detect a change in the organic layer C stock vary by a factor of ~4 over 15 to 125 cm separation distance. By simulating changes in the organic layer C stock over 25 years, we show that longer time intervals between baseline sampling and revisit may compensate for lacking spatial sampling precision. Our results indicate that time between sampling, sample relocation distance, and coefficient of variation at the time of baseline sampling all provided explanatory value to the regression model of sample requirements. The information provided by this study can be considered indicative of the magnitude and variability of one can expect when monitoring soil organic layer C stocks in boreal forests. Our results clearly demonstrate the importance of spatial sampling precision on the sample size requirements to detect changes in the organic layer C stock.

4.1. Introduction

Policymakers and regulatory authorities have recognized the need to evaluate soil organic carbon (SOC) stocks, and monitor their changes over time (Morvan et al., 2008). The large amount of carbon (C) stored relative to the yearly change is a major obstacle to detecting temporal changes in SOC (Post et al., 2001). For example, modeling efforts in boreal forest regions have predicted sequestration rates 1.4 to 56.0 g C m^{-2} yr^{-1} (de Wit et al., 2006; Liski et al., 2002; Wirth et al., 2009; Ågren et al., 2007), which represents only a fraction (0.1 to 2.5 %) of the full SOC stock. Consequently, changes in SOC must be large or persistent over longer periods of time for change detection to be feasible (Yanai et al., 2003).

Although some of these changes will occur in mineral soil horizons, we expect the most rapid change to occur in the surface organic layer (Gaudinski et al., 2000), also known as the forest floor. However, detecting any changes in the organic layer C stock is challenging due to the considerable short-range variability caused by local topography and organic inputs which may vary greatly over time and space (Simonson, 1959). The efficiency, accuracy, and cost of monitoring organic layer C can be optimized considerably by appropriate sampling designs, guided by statistical, operational and site-specific conditions. To optimize sampling strategies balanced between acceptable margins of error and operational constraints, one must recognize that establishing baseline stock size and detecting changes in the stock are two different objectives with

97

unequal variability (Lark, 2009). Ultimately, a sampling design suitable for estimating C storage at a given time might not suffice for monitoring stock changes with the same level of confidence at the same location.

When the goal is to detect fluctuations in soil C stocks with a high level of statistical confidence, a paired re-sampling is almost always preferable to independent random sampling (de Gruijter, 2006; Yanai et al., 2003). In a paired sampling protocol, the surveyor gathers data from the same sampling point twice, separated by time. This maximizes the covariance between samples, which in turn reduces the sample requirement needed to detect any changes that might have occurred over time. However, due to the destructive nature of soil sampling, where primary samples are physically removed, a true paired sampling cannot be implemented (de Gruijter, 2006). Instead an *approximation* of the primary sampling location will have to suffice. Despite the similarity of proximate samples, conducting a paired secondary sampling within centimeters from the baseline sample is unlikely to eliminate all residual small scale-variability (Häkkinen et al., 2011; Liski, 1995; Muukkonen et al., 2009; Schöning et al., 2006).

When sample locations are revisited over time to determine if there has been any change, it is not the resampled observations *per se* that we are interested in, but the difference (Y) between these and the baseline observations. The difference is distributed as (Eq. 1) (Lark, 2009):

$$Y \sim \mu_Y, \sigma_Y^2 + 2\sigma_\varepsilon^2 + \sigma_L^2 \qquad\qquad (1)$$

where μ_Y is the mean difference, and the total variance of Y is given by $\sigma_Y^2 + 2\sigma_\varepsilon^2 + \sigma_L^2$.

The variance component σ_Y^2 represents the sample variance of Y, σ_ε^2 can be classified as measurement uncertainty and is composed of the variance from sampling and analytical errors from both baseline and resampling observations. The magnitude of σ_ε^2 depends on the sample procedure, whether the same procedure was used for all samples, and will decline with increasing number samples. This variance is multiplied by 2 because the samples taken are independent in time and space. The last variance component, σ_L^2, which this paper will examine in detail, denotes the relocation variance. The relocation variance is due to the shift in sample placement over heterogenic soils, and must therefore be taken into consideration when planning to perform a paired sampling. Unfortunately, this component has largely been ignored in studies aiming to provide guidance on sampling to monitor organic layer C stocks. To improve protocols for C monitoring, the lack of information about the magnitude of relocating samples has been highlighted by earlier studies (Allen, 2010; Lark, 2009; Yanai et al., 2003).

This paper's objective is to demonstrate how change detection of organic layer C stocks is affected by spatial separation in a paired sampling. We collected paired samples over four different sampling distances from seven boreal forest plots. Because all samples are collected contemporaneously, any differences between samples will be a reflection of

the local variability and not change through time. We use these data to explore the magnitude and variability of sample relocation: (1) across four different separation distances, (2) across the landscape, and (3) in a time-space continuum. Finally, we discuss the implications of spatial accuracy in sample protocols for detecting changes in the organic layer C stock, and aim to present practical advice for future surveys. To ensure that the observed effect is a result of the naturally occurring heterogeneity in forest soils, all study plots are located in forests not impacted by any form of forest practices over the past century.

4.2. Methods

4.2.1. Study area

Eight circular study plots with a 50 m diameter ($\sim$2000 m^2) were positioned in mature and multilayered spruce forests in the Årum – Kapteinstjern area, located approximately 35 km north of Skien in Telemark County, South East Norway. A detailed description of the plot characteristics, such as topography and vegetation structure is presented in Kristensen et al., *in review*. The area is situated in the border of the south – middle boreal vegetation zone, with oceanic climate (Moen, 1999). The forests belong to the *Picea - Vaccinum myrtillus* type, the most abundant forest type in NW Europe (Cajander, 1949; Kielland-Lund, 1981). The multi-layered structure was dominated by Norway spruce (*Picea abies* (L.) Karsten), with occurrences of Scots pine (*Pinus sylvestris* L.) and birch (*Betula pendula*). Ground vegetation in the area is dominated by

100

European blueberry (*Vaccinium myrtillus*), Feather moss (*Pleurozium schreberi*), Green peat moss (*Sphagnum girgensohnii*), Common haircap moss (*Polytrichum commune*), *and* Stair-step moss (*Hylocomium splendens*). To ensure that the observed effects of sample relocation is a result of a natural occurring variability in organic layer attributes, the study was conducted on plots with no active forest management since logging occurred in 1903 – 1910 (Lie et al., 2012). Soils were mesic to mesic/moist podzols, nutrient poor with a low pH (Nielsen et al., 2007).

4.2.2. Field sampling

Plots were divided into a systematic grid with 5 m spacing between grid nodes in both north-south and east-west directions (Fig. 1). Each grid contained 73 baseline samples (B). From these grid nodes we randomly selected 14 sampling points where four additional soil samples were collected in lag distances ranging from 15 cm and up to 125 cm, measured between core centers. Using a cylindrical steel corer (56 mm diameter) samples were extracted from the F (O_e) and H (O_a) horizon, consisting of partially decomposed matter and well-decomposed organic matter, down to the mineral soil boundary. The boundary between the organic horizons and mineral soil could be clearly determined visually due to the low faunal mixing of decomposing litter in these forests. Coarse wood fragments >2 mm in diameter, such as living roots, were excluded from the sample. Samples were collected contemporaneously and fresh surface litter (L (O_i) horizon) was omitted to minimize any seasonal effects.

101

Figure 1 – Sample design
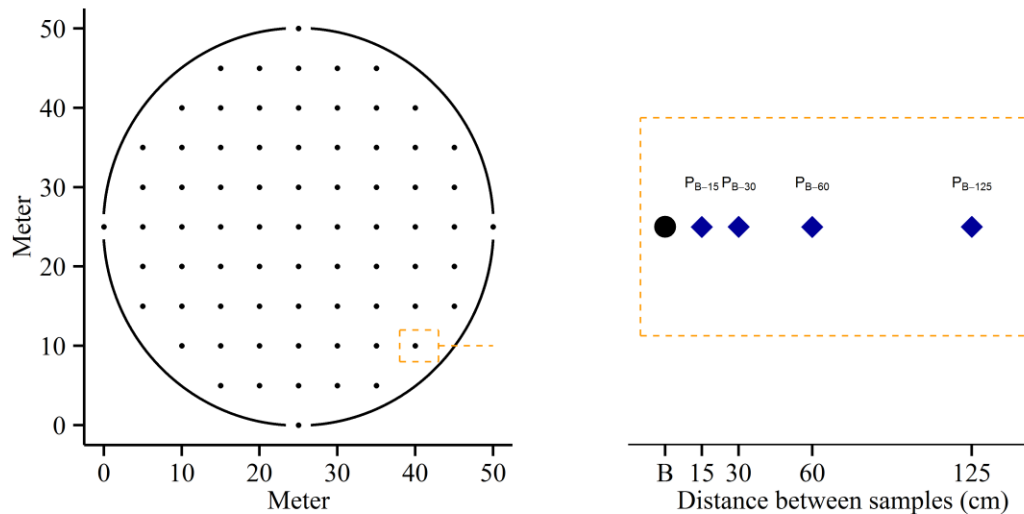
Figure 1. Organic layer C sampling strategy. The effects of relocation were computed from baseline measurements (B) and a second sample (P), relocated at four different lag vectors (h) from B. Subscript numbers indicate the distance between baseline and paired sample (e.g. P_{B-15} for sample pair separated by 15 cm, then P_{B-30}, P_{B-60}, P_{B-125}).

Sample error from the use of different surveyors was controlled for by using only one surveyor and identical sampling procedure across the plots (Goidts et al., 2009; Kulmatiski and Beard, 2004). Any systematic errors such as a consistent bias in measurements will not have any effect, as they will disappear when differences between samples are computed. After collection, all samples were stored in separate paper bags and dried at room temperature (15 to 20°C).

4.2.3. *Laboratory analysis*

Soil samples were dried at 65°C in a drying oven (Thermax Series TS8000) to a constant mass. Samples were then sieved down to <2 mm to find stone content and dry weight. To determine C concentration (C_c) samples were ground to a size of <100 μm using a ball mill, and the homogenized mixture was analyzed using a VarioMax EL CHN analyzer with TCD detector (Elementar Analysensyterne GmbH, Hanau, Germany). The analysis was conducted according to ISO 9000 certified methods at the Skogforsk (Ås, Norway) commercial laboratory. Because the amount of inorganic C in these acidic soils are low, sample C was considered organic (Huntington et al., 1989). The C content in the organic layer (C_{OL}) was calculated using (Eq. 2):

$$C_{OL} = C_c \times \sum (SW_{OD} / A) \tag{2}$$

where C_c is the organic C content of the sample, as determined by the CHN analyzer (g C g^{-1}, dry soil), SW_{OD} is the oven dry weight of the sample (g), A is the cross-sectional area of the core.

4.2.4. *Statistical analysis*

Standard statistical methods were used to describe central trends and spread. Outliers were identified with Grubbs test (Grubbs, 1969). The coefficient of variation (CV), defined as the sample standard deviation expressed as percentage of the sample mean, was used as a measure to describe the variability of soil organic C in each plot. A one-way analysis of variance (ANOVA) was used to determine if there were any

statistically significant differences between means or distributions. Statistical significance is accepted at $\alpha = 0.05$ level for omnibus tests. Associations between sample pairs were described using Pearson's correlation coefficient. Coefficients and effect estimates are presented with 95% confidence intervals. Data analysis was carried out in R 3.0.2 (R Core Team, 2013).

4.2.5. *Quantification of sample relocation variance*

To assess the sample relocation variance in repeated soil organic layer C measurements, we quantified the effects of the spatial precision in sampling protocols as a function of relocation distance. During the baseline sampling the surveyor collected a sample (B) at location i at time 1. To monitor the status of soil C, a paired sampling protocol is commonly recommended (de Gruijter, 2006), where a paired sample (P) is collected at time 2. Due to the physical removal of sample B_i, the second sample will only be an approximation of the baseline sample, collected at $i + h$, where h is the relocation vector. The magnitude of the sample relocation error (B_i - P_h), which is a result of the short-range variability in soils, depends on the precision of the sampling protocol used, whether the sample locations was physically marked or relocated by other means. Even if precise identification of the baseline sample location is possible, it is likely that the surveyor wants to move P to avoid sampling in disturbed soil. To investigate how sample spatial precision influences the reliability of results we compute the aggregated effects of sample relocation at four different separation distances on each plot, 15, 30, 60

and 125 cm (Fig. 1). Because all samples at each plot are collected contemporaneously, the offset is a reflection of the spatial heterogeneity and not any temporal changes. For our models, the effects of relocation is considered isotropic; meaning it only depends on the distance between samples, and does not reflect the relative orientation between samples. The magnitude of sample relocation error can therefore be considered a normal random variate D, with probability density function f(D) and distribution (Lark, 2012):

$$D \sim N (0, \sigma^2) \hspace{4cm} (3)$$

where the distribution is a realization of a random variable drawn from a normal distribution with an expected mean of zero. Model bias was minimized by bootstrapping 1000 new datasets by drawing random samples with replacement from the empirical distribution of paired differences. This procedure was repeated for each of the four lag vectors. The short-range variance was compared to the plot variance, across different vectors (P_{B-15} vs. P_{B-30}) and between similar classes from different plots ($P_{B-15(A1)}$ vs. $P_{B-15(A2)}$).

4.2.6. Carbon accumulation models

Constructing a sampling design aiming to monitor changes in soil C is an optimization problem, where the surveyor has to consider the trade-off between available resources and reliability of results. To assess the implications of a shift in sampling location between the baseline sampling and revisit, we evaluate the sampling efforts

required to detect a change in the soil organic layer C stock in our plots. Because the variance of change is not known beforehand, we modeled 25 years of C accumulation for each of the baseline sampling points. The first model, hereafter referred to as the independent additive C model, assumes that the change is independent of baseline measurements. In these circumstances (Lark, 2009):

$$Cov[B,Y] = 0 \qquad\qquad (4)$$

where the covariance between the baseline (B) samples and change (Y) is random.

Second, we modeled a correlated additive change, where the C accumulation is spatially dependent. This model will be referred to throughout as the correlated additive model. The data was generated from a randomization of plausible C accumulation rates for Fennoscandian boreal forests soils, ranging from 0.1% to 2.5% (de Wit et al., 2006; Liski et al., 2006; Peltoniemi et al., 2004; Ågren et al., 2007). The rates were randomly drawn with replacement in increments of 1/100 of a percent. Although annual accumulation *rates* for each sampling point were random, the C *input* for each sampling point will depend on the baseline measurements (Lark, 2009):

$$Cov\,[B,\,Y] = C \neq 0 \qquad\qquad (5)$$

where the covariance between the baseline (B) samples and change (Y) is non-random. Here, organic layer C stock change will have a consistent positive correlation to the spatial C stock pattern observed at each sampling point. The accumulation will depend on the baseline value and will thus not be identical across the area.

106

At each location we obtain an estimate of the change in organic layer C stock. Because we anticipate that a relocation of the sample point occurs during the revisit, we must consider the additional variance for the mean difference between paired samples (Lark, 2009):

$$Y \sim (\mu_Y, \sigma_Y^2 + 2\sigma_\varepsilon^2 + \sigma_L^2) \tag{6}$$

where the mean difference between baseline and paired samples (Y) has mean μ_Y with distribution $\sigma_Y^2 + 2\sigma_\varepsilon^2 + \sigma_L^2$, where the variance of relocation is a measure of the short-range variability of soil organic layer C.

4.2.7. Effects of sample relocation in paired sampling

After establishing how spatial variability affects the estimate of paired differences, we computed the minimum detectable difference (MDD) at each plot as a function of lag distance between samples (Zar, 2010):

$$MDD_{paired} \geq \sqrt{\frac{\sigma_d^2}{n}(t_{\alpha(2),v}) + (t_{\beta(1),v})^2} \tag{7}$$

where the variance of paired differences, σ_d^2 encompasses the effects of sample relocation, n is the sample size, v is degree of freedom, and t is the t-statistic at given significance level ($\alpha = 0.05$, two-sided). The probability of type II error (β) is set at 0.2, giving a statistical power of 0.8. Although this study exclusively models a net accumulation of soil C, and could thus have enhanced the statistical power by selecting a one-tailed test, it

is unlikely that the surveyor will know the direction of the change beforehand. It is therefore recommended that a two-tailed test is used (Allen, 2010). To avoid overestimation in sample requirements, the MDD tests used in this study should only be conducted on parametric data (Poussart et al., 2004). If the assumptions for parametric tests are not met, non-parametric alternatives based on ranked data is recommended (van der Hoeven, 2008). To enable comparisons across the seven plots, the minimum detectable difference was calculated as a percentage of the plot mean organic layer C stock (μ_B), established from the grid samples: $\delta_{rel} = MDD/\mu_B \times 100\%$.

4.2.8. *Predicting sample requirements*

Stepwise multiple regression (Eq. 8) was used to examine what influences the sample requirements to detect a change at a plot level. Explanatory variables of interest were in particular temporal and spatial distance from baseline measurements. In addition, the regression included baseline quantities of the organic layer C stock, such as plot mean and measures of variability. Assumptions of linearity, independence of errors, homoscedasticity, and normality of residuals were controlled for using standard statistical methods. The goodness of fit was evaluated by root mean square error (RMSE), adjusted R^2 and residual studies.

$$y = b_0 + b_1 x_1 + ... b_n x_n + \varepsilon \qquad (8)$$

where y represents the required sample size, b_0 is the constant; $b_1 ... b_n$ represents the regression coefficients of the best fit model; $x_1 ... x_n$ are explanatory variables

representing time since baseline sampling (yr^{-1}), spatial sampling accuracy (cm) and baseline measurements, such as plot mean (kg C m^{-2}) or a measures of plot variability, while ε is a normally distributed error term. The relative importance of predictors was assessed from bootstrapping (n =1000) the model explained variance into non-negative contributions (Grömping, 2006).

4.3.   Results

The Grubbs test recognized a total of four outliers which were removed from further analysis. None of the identified outliers were paired with additional lag samples. The mean soil organic layer C stock ranged from 1.87 to 3.33 kg m^{-2} (Table 1), and were statistically different between plots (Welch's $F_{(6, 212)} = 24.252$, $p < 0.001$). There was considerable heterogeneity in organic layer C stocks within each plot (CV 31 to 63%); exceeding the variability between plots (CV 22%). Variances in the organic layer C between plots were heterogenic (Levene's test, $p = 0.002$). A correlation test between mean C values and CV was non-conclusive ($r_{(7)}$ = -0.64 (95% CI: -0.94, 0.21), $p = 0.12$).

Table 1. General properties study plots located in Årum (A) and Kapteinstjern (K).

	Plot						
	A1	A2	A3	A4	K1	K2	K4
Latitude N	59°21'15	59°21'58	59°21'57	59°21'02	59°24'57	59°25'00	59°24'51
Longitude E	9°44'05	9°44'39	9°44'27	9°44'33	9°38'00	9°37'45	9°37'33
Altitude (m.o.s.l.)	549	473	475	484	605	619	607
Stem density (ha^{-1})	351	611	688	652	270	484	565
Organic Layer C (kg C m^{-2})	2.15	2.67	1.87	3.01	2.54	3.33	1.69
Organic Layer C (SD)	1.31	1.04	0.87	1.22	0.72	1.20	0.87
Organic Layer C range (m)[†]	2.85	1.11	1.90	0.86	1.64	1.51	1.07

Note: Organic layer consisting of: OF (O$_e$) horizon (fragmented and/or altered), partly decomposed (i.e. fragmented, bleached, spotted) organic matter, and OH (O$_a$) horizon (humus, humidification, humic layer): well-decomposed amorphous organic matter.
[†]The geostatistical range is derived from Kristensen et al., *in review* (Chapter 3).

4.3.1. Sample repeatability

We observed declining repeatability of organic layer C measurements with increasing lag distance between baseline and replicate sample (Fig. 2). Correlation between sample pairs declined from r = 0.88 (P_{B-15}) to r = 0.46 (P_{B-125}). Simultaneously, the mean absolute difference (± 1 SD) between sample pairs increased from P_{B-15} (0.49 $\pm$ 0.33), to P_{B-30} (0.58 $\pm$ 0.40), to P_{B-60} (0.94 $\pm$ 0.57) to P_{B-125} (1.17 $\pm$ 0.88). Distributions of absolute differences were similar for all sample pair populations, as assessed by visual inspection of a boxplot. A Kruskal-Wallis H test revealed that the median absolute differences were unequal between groups, $H_{(3)} = 81.213$, $p < 0.001$.
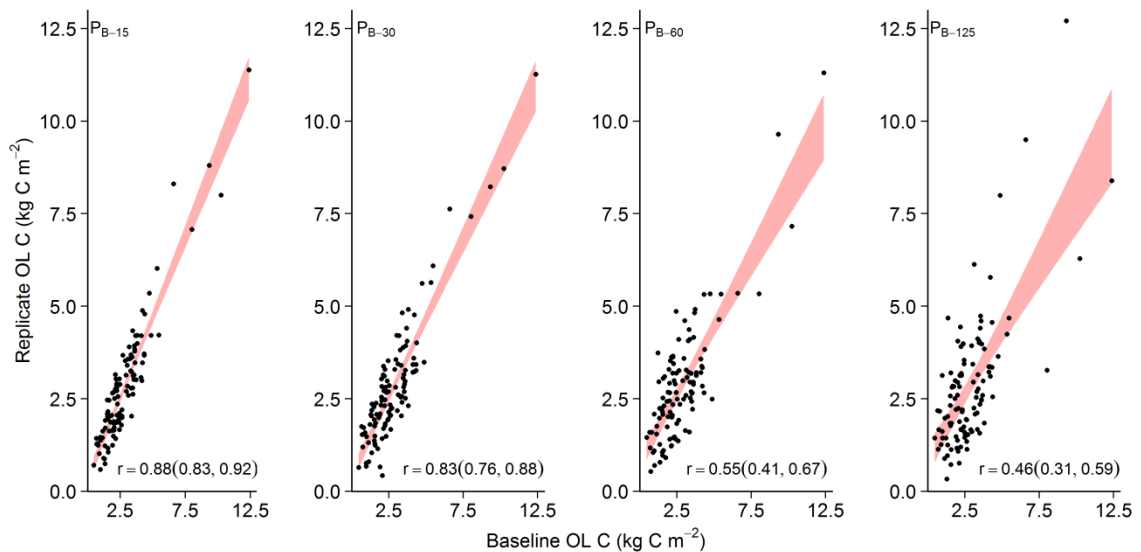
Figure 2. Spearman rank correlation of soil organic C measurements in baseline and replicate sample (n = 112 for each group). Distance between observations is displayed in each figure (P_{B-15} to P_{B-125}). Correlation coefficients are presented with a 95% CI (shaded area). All correlations are significant at a 0.01 level (2-tailed).

4.3.2. *Quantification of sample relocation effects*

Mean differences in sample pairs did not significantly differ between plots $(P_{B-15(X)} vs. P_{B-15(Y)})$. Samples were normally distributed (Shapiro-Wilk test, $p > 0.05$), but variances were heterogeneous (Levene's test, $p < 0.001$). Thus, a one-way Welch ANOVA was used to determine if the difference of sample pairs was unequal between plots. No significant differences were found between the sample pair observations across the different plots ($p < 0.001$).

Mean pair differences following sampling relocation were also investigated over different lag distances $(P_{B-15} vs. P_{B-30})$. The calculated mean pair differences were normally distributed (Shapiro-Wilk test, $p > 0.05$). Variances were not homogenous (Levene's test, $p < 0.001$), and a one-way Welch ANOVA was therefore used to determine if the error distribution from relocating the sample during a revisit was unequal. Mean pair differences from different separation distances were statistically significant (Welch's F (3, 234.70) = 29.45, $p < 0.001$).

The variance (around the biased corrected mean, $\mu_{B-R} \sim 0$) was dependent on the sample separation relocation distance, *h*, and sample size (Fig. 3). After ~20 samples, the marginal value of additional samples for determining the effects of sample relocation becomes small. The standard deviation depends on *h*, and increased more than two-fold over the distance range sampled: P_{B-15} (± 0.15), to P_{B-30} (± 0.19), to P_{B-60} (± 0.31) to P_{B-125} (± 0.40). For the surveyor this means that (1) a sufficient number of samples (here: > 20)

is required to determine the magnitude of spatial variability, and (2) we expect greater variance around the mean pair differences when the sample separation distance increases.
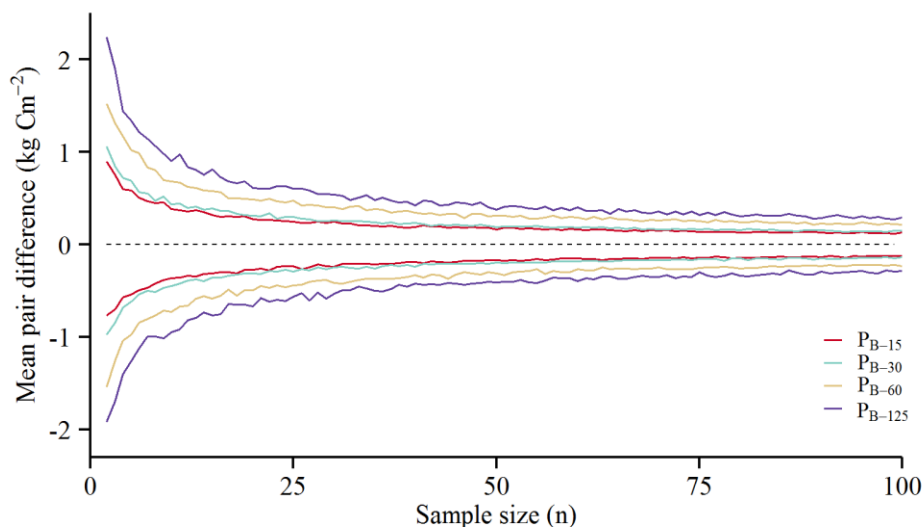
Figure 3. The distribution of differences in sample pairs, μ_{B-R}, converges around ~ 0 with a distribution σ^2. Because both samples are collected contemporaneously, the differences are a reflection of the short-range spatial variability. This indicates the additional uncertainty the surveyor must take into consideration when samples are relocated. The variability around the mean differences depends on both sample size and distance between the paired samples.

4.3.3. *Effects of sampling relocation under an independent additive model*

First we computed the sample size needed to verify a fixed change, using the assumption of no sample relocation. This was done to enable a comparison of the relative importance of considering spatial variability when deciding on a sampling protocol to

113

monitor organic layer C stocks. In our plots we would need between 8 to 17 samples to detect a change of ± 0.5 kg C m^{-2} (Fig. 4a). The sample requirements decreases with increasing detection threshold, and at ± 1 kg C m^{-2} the sample requirements are between 5 and 11 (Fig 4a).

However, because the surveyor must relocate samples during the revisit, additional uncertainty should be taken into consideration when estimating sample size for verifying a change. The magnitude of the uncertainty depends on the relocation distance (Fig. 3). To detect a change, fewer samples are needed when they are located near past samples (Fig. 4a). We calculate that between 9 and 19 samples are sufficient to detect a ± 0.5 kg C m^{-2} change in organic layer C stock (blue region in Fig. 4), while 5 and 8 samples for a ± 1 kg C m^{-2} change when re-samples are taken with 15 cm of the original samples (green region in Fig. 4). For sample pairs located 30 cm apart, we would need sample sizes of 13 to 26 and 6 to 11 to detect a change of ± 0.5 and ± 1kg C m^{-2}, respectfully. While the difference in required sampling effort between samples relocated with 15 or 30 cm or less is small, a 125 cm shift requires between 3 and 4 times as many samples to detect the same degree of change (Fig 4a). The increase in sample size requirements is expected to increase until the observations no longer are spatially dependent, e.g. the sampling can be considered random.

114
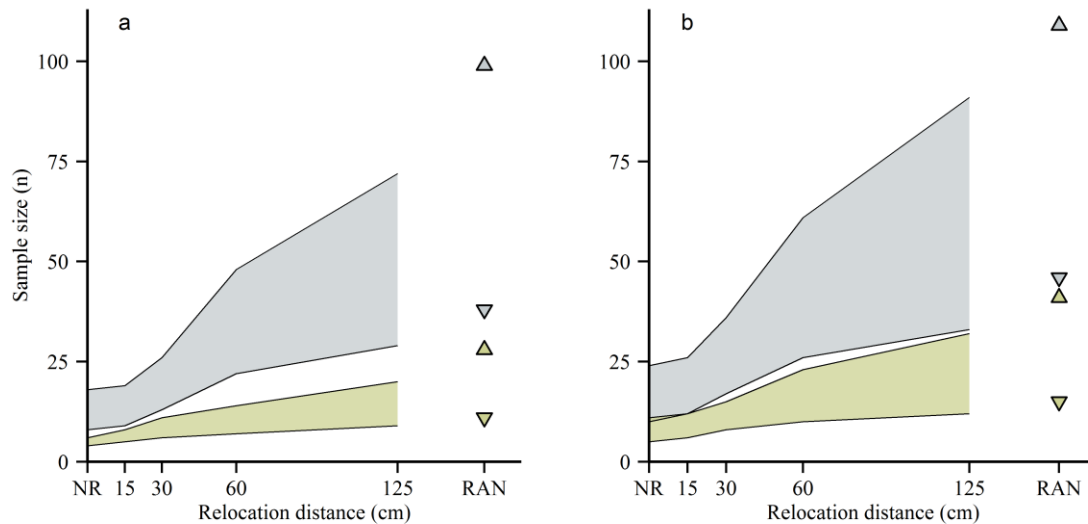
Figure 4. Effects of relocation distance on the sample size required to detect a change of 1 kg C m^{-2} (bottom segment) and 0.5 kg C m^{-2} (top segment) when there is (a) independence between baseline measurements and the change at any given sampling location, or (b) accumulation is spatially correlated. Segments show the range of sample sizes from the seven plots (maximum – minimum) for each relocation distance. NR indicates the sample size if effects of relocation is ignored, while RAN (triangles) shows the estimated sample size for a random sampling.

4.3.4. *Effects of sampling relocation under a correlated additive model*

The correlated additive model of C increase results in both higher C content means and higher C variability through time. The model, which assumes a C accumulation of 0.1 to 2.5% yr^{-1} of the baseline values, predicts an increase of 11 to 14% in C content after 10 years. This corresponds to an increase of 0.28 to 0.53 kg C m^{-2}.

115

After 25 years the predicted organic layer C stocks have increased with 38 to 42% compared to baseline measurements of the soil organic C stock. Accumulation of organic layer C follows an approximately linear trend in all plots over the 25 year period (Fig. 5).

The correlated additive model increases the plot variance over a 25 year period (Fig. 5). This means that areas with higher C stock during baseline sampling have a higher likelihood of a greater C accumulation than areas with low C stocks. Compared to the variance of paired differences at the time of baseline sampling, the paired variances increase from 3 to 6% to 22 to 30%, after 10 and 25 years, respectfully. Because a shift in sampling location between baseline and revisit is necessary, the sample pair differences measured by the surveyor will be a result of both the 'true change' which occurred over time and the short-range variability already in place during the baseline sampling (Eq. 5).
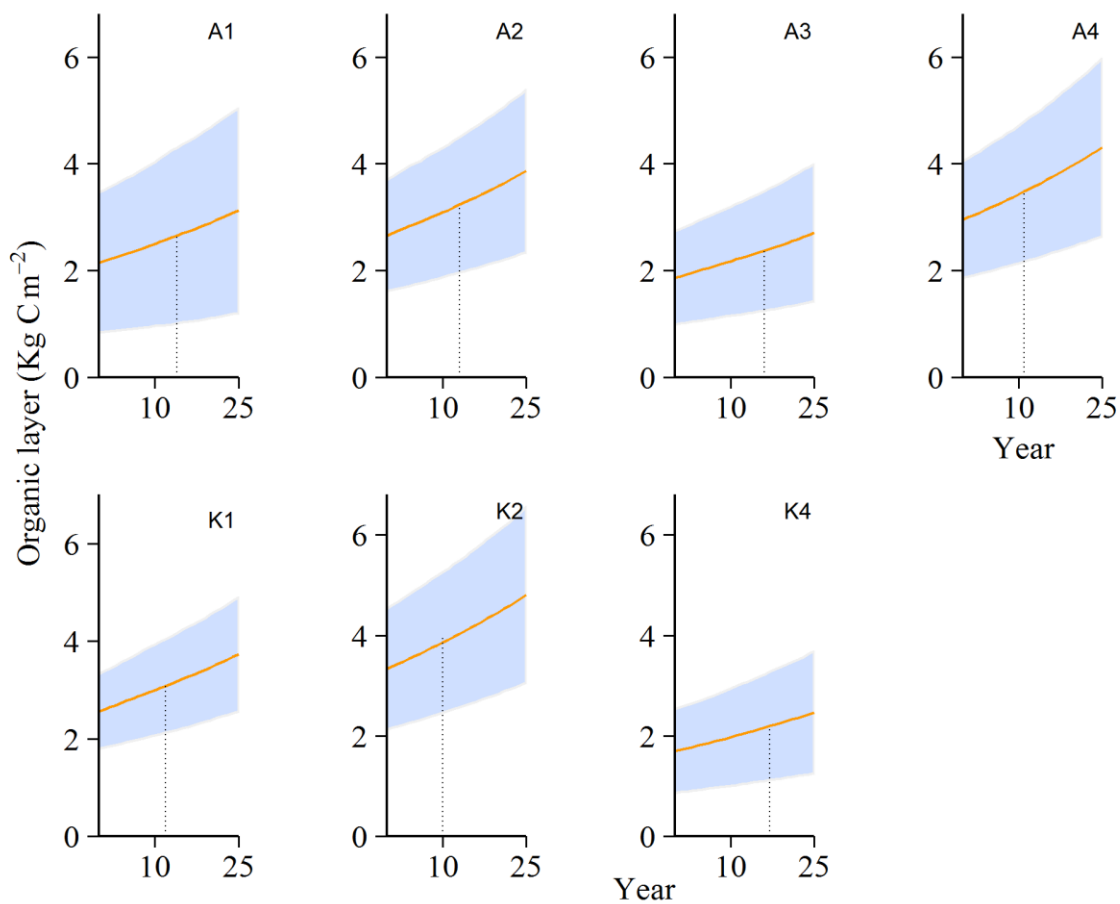
Figure 5. Modeled increase in soil organic layer C over 25 years for four boreal forest plots located in the Årum area, SE Norway. Shaded area indicates ± 1SD of the estimated organic layer C stock. The dotted line indicates an accumulation of 0.5 kg C m^{-2}. Due to the spatially depend input rates plots would reach a mean increase of 0.5 kg C m^{-2} at different times. Over the span of this model, the organic layer accumulate 34 to 59 gr C m^{-2} yr^{-1}, equivalent to 1.13 to 2.17 t CO_2 ha^{-1} yr^{-1}.

The relative contribution of spatial variability to the total variance of paired differences exceeds the projected variance (Fig. 6). In other words, the short-range spatial variability exceeds the temporal variability. However, after 20 to 25 years the variance of paired differences at the shortest relocation distances (P_{B-15} and P_{B-30}) is equally a result of the 'true' difference in C stock and the spatial difference, which existed at the time of baseline sampling.
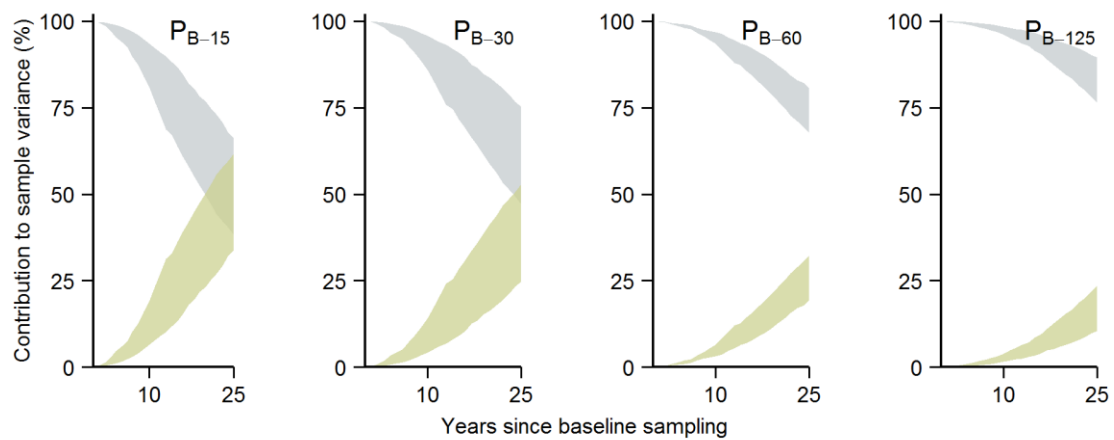
Figure 6. The relative contribution of spatial variance (top segment) and temporal variance (bottom segment) to the variance of paired differences modeled over 25 years. Each segment represents maximum - minimum contribution. At time zero all variance of the paired differences is a result of short range heterogeneity.

For the correlated additive model, we therefore have two components influencing the sample size requirements – in *opposite* directions. First, the spatially dependent accumulation increased variances around the paired differences, while the predicted

118

increase in mean differences between two sampling times reduces the sample size required to detect a change.

4.3.5. *Sample size requirements for correlated additive change*

The number of samples required to detect a change in the organic layer C stock increases under a correlated additive C accumulation model. This does not occur in under an independent additive change model, where any temporal variance of the paired differences is negligible (data not shown). For the correlated additive change model, we calculate that between 12 and 26 samples are sufficient to detect a ±0.5 kg C m^{-2} change, and 6 and 12 samples for a ±1 kg C m^{-2} change, when re-samples are taken with 15 cm of the original samples. In the correlated additive model, the estimated sample requirements are ~20% higher (Fig. 4b) than in the independent model (Fig 4a) and reflects the additional uncertainty following an unequal C accumulation across the plots. However, the magnitude of this additional uncertainty on the required sample size depend the model parameters.

Sample size requirements can also be assessed with a fixed time between baseline and revisit, rather than a fixed magnitude of change. The time needed to reach a desired magnitude of change may vary widely between plots. For example, under the correlated additive change model, the plots in this study will have accumulated 0.5 kg C m^{-2} after some 10 to 17 years, depending on the baseline C stock. Thus, for observations relocated with only 15 cm, we estimate that 14 to 41 samples are needed to detect the modeled

change after 10 years, while only 5 to 11 samples are needed after 25 years (Fig. 7a). For

samples collected 125 cm apart, we would need 46 to 106 and 11 to 36 samples after 10

and 25 years, respectfully (Fig. 7a). This decline in sample size corresponds to a ~4%

decrease in sample requirements per year. Our data suggests that the sample requirements

may be underestimated by 10 to 22% if sample relocation is ignored (Fig. 7a).
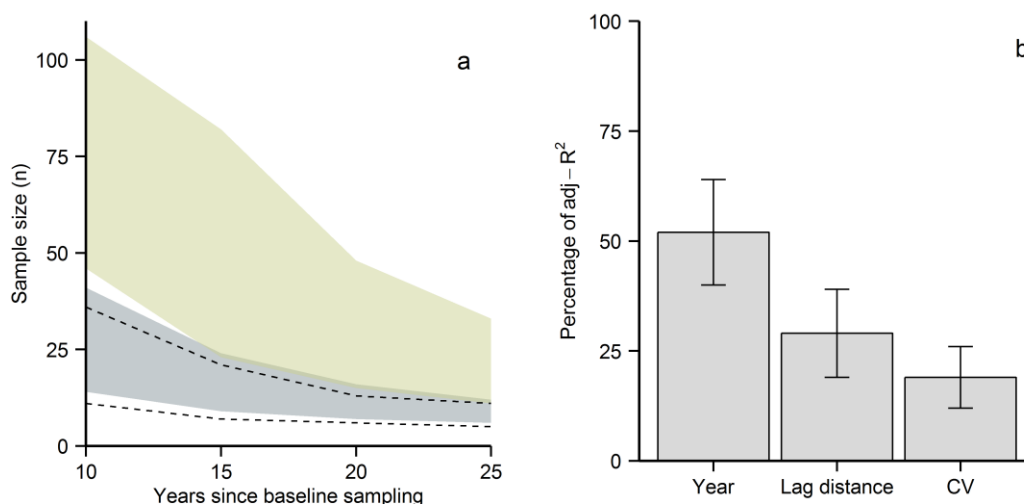
Figure 7. (a) Maximum and minimum sample size required to detect the modeled
organic layer C accumulation (Eq. 5) plotted against years since baseline sampling.
Segments indicate sample size requirements when samples are relocated 125 cm (top
segment) and 15 cm (bottom segment) from the baseline sample. Dotted line indicates
maximum and minimum sample size requirements when the effects of sample relocation
are ignored. **(b)** Relative importance of the explanatory variables in the linear model
(normalized to sum 100%) to the adjusted-R^2 = 79%. The variables represent time
interval between baseline sampling and revisit (year), lag distance (relocation effects),
and coefficient of variation (CV) measured from the baseline sampling. Error bars
indicate bootstrapped 95% CI.

4.3.6. *Determining sample size requirements*

A linear regression determined that sample size requirements could be obtained from model inputs of temporal and spatial variability. Significant predictors of sample size were years since baseline sampling (yr^{-1}), coefficient of variation of baseline inventory (CV), and spatial precision of sampling protocol (cm) ($p = 0.001$) (Table 2). Plot mean organic layer C stock did not add any explanatory value to the model ($p = 0.23$), and were excluded from the final model. Assumptions of linearity, independence of errors, homoscedasticity, unusual points and normality of residuals were met (Shapiro-Wilk, $p < 0.001$). All remaining variables added statistically significantly to the prediction, $F (3, 55) = 71.86$, $p < 0.001$, adj-$R^2 = 0.79$. Years since baseline sampling had the highest explanatory power in the model, explaining over 50% of the variability (Fig. 7b).

Table 2. Summary of multiple regression

Variable	B	SE$_B$	β
Intercept	20.25	9.25	
Year since baseline sampling	-2.70	0.23	-0.71
Sample relocation	0.29	0.04	0.43
Baseline coefficient of variation (CV)	1.03	0.18	0.35

Note: B = unstandardized regression coefficient; SE$_B$ = Standard error of the coefficient; β = standardized coefficient. All coefficient are significant at $p < 0.001$.

4.4. Discussion

This paper studies paired sampling of soil organic layer C stocks. Our analyses demonstrate that purposeful re-sampling near original locations will increase sampling accuracies, or can be used to reduce sample size to achieve target accuracy. For *a priori* sample size estimates, the relative importance of sample relocation depends on the degree of displacement, rate of change, and the time interval between sampling. The surveyor must therefore carefully evaluate the tradeoffs between timing, obtainable level of accuracy and the efforts required to detect a change.

4.4.1. Plot mean and variability

The attributes of the organic layer observed in the studied plots are comparable to other reports from boreal-temperate podzols, where organic layer C stock commonly range between 1 and 4 kg C m^{-2} (Baritz et al., 2010; Callesen et al., 2003; Marty et al., 2015; Olsson et al., 2009). The heterogeneity in the surface layer of boreal forest soils is usually large (Marty et al., 2015; Muukkonen et al., 2009), with coefficients of variations >30%. Although few studies have reported on spatial characteristics of organic layer C in boreal forests, the spatial dependencies of <3 m observed in the studied plots (Kristensen et al., 2015b) are comparable to results from boreal forest stands in Finland (Häkkinen et al., 2011; Muukkonen et al., 2009). The range of spatial independence has implications for the statistical assumptions of this study, as the baseline sampling was purposively established on a grid to maximize the spatial coverage of the plots, and does therefore not

meet the classical statistical assumptions of randomization. This may have led to an overestimation of the plot variance.

4.4.2. *Effects of sample relocation*

The advantages of a paired sampling over a random sampling can be large in terms of sampling efforts required to detect a change (Fig 4). However, the gain in sample size (compared to the required SRS size) is sensitive to the spatial accuracy of the sampling protocol. At short separation distances between baseline and repeated sampling, the covariance of soil samples is maximized, which in turn lowers the number of samples required to detect a change. In our study plots, the magnitude of sample relocation errors did not vary significantly among similar lag distances from different plots, but showed considerable variation across different separation distances. As the correlation between samples increases with sample proximity (Fig. 2), it is likely that relocation variance can be further reduced by decreasing the separation distance to less than the minimum 15 cm used in this study. However, little is known about how removal of soil cores influences the surrounding micro-environment, and at what distance one can consider soils unaffected by the intrusion. On the other hand, increasing the separation distance between paired samples inflates the effects of relocation, and thus enhances a priori estimates of adequate sample size. The increased uncertainty around the estimated mean of paired differences is due to the short-range spatial variability which is expected to increase with separation distance. Theoretically, this error should eventually reach an asymptote, at

which distance new samples can be considered independent from baseline samples (Fig 4). Previous work at these plots has shown organic layer C samples were no longer dependent at distances ranging from 0.9 to 2.9 m (Kristensen et al., 2015b). Although the short-range variability of soil C may differ markedly between soils types and areas with different histories of land-use (Häkkinen et al., 2011; Worsham et al., 2012), comparable variability has been found in other studies conducted on soil organic layer C stocks in boreal forests (Häkkinen et al., 2011; Liski, 1995; Muukkonen et al., 2009). Thus, geostatistical approaches have been suggested to assess the effects of sample relocation within experimental units directly. Lark (2009) presents a theoretical model for estimating the relocation variance on single points using a variogram model. However, the variogram is rarely known beforehand, and precise geostatistical modeling of forest soils usually requires substantial sampling efforts (Webster and Oliver, 1992). Similarly, most of the existing plots included in national inventories on soil C do not have a suitable sampling design nor sufficient density to obtain reliable information on spatial dependencies (Ortiz et al., 2013). Although attaining spatial information is recommended to avoid biased estimates, the cost of implementation is a limiting factor for many surveyors. These costs are dropping as reliable, centimeter level, GNSS field positioning becomes more widely supported.

We recommend that the surveyor collect paired samples during baseline sampling, where the observations are separated by a distance equal to the spatial accuracy

124

expected for later resampling. This can serve as an approximation of the sample relocation variance, which we have demonstrated here, is an essential component in later sample estimates. However, advice on sampling strategies based on observed statistics must be considered as general insights rather than explicit recommendations.

Nonetheless, it is clear that there are great advantages in sampling size requirements by devoting efforts on minimizing sampling relocation in a paired sampling when monitoring organic layer C stock through paired sampling. Figure 3 and 4 show that the difference in sample correlation can be large even when the relocation deviation is small. It is notable that the a priori sample sizes needed to detect a fixed change in the organic layer C stock vary by a factor of ~4 over 15 to 125 cm separation distance. Simultaneously, our data show considerable benefits of a precisely executed sampling protocol in contrast to a random sampling. This is a significant consideration with obvious practical implications, as coordinates derived from inexpensive handheld global navigation satellite system (GNSS) are unlikely to have the precision required for a paired sampling. Unless stationary GNSS with higher precision is used or precise positioning with real time kinematic (RTK), or other dual channel positioning capable of real-time decimeter accuracies, sample points should be physically marked for later identification. Experienced surveyors know that relying on physical ground marks for later revisits of individual sampling points may be challenging, given the time between visits and local disruptions from both abiotic processes (such as snow, rain, and erosion)

and the inherent curiosity of the living fauna. If only considering sample requirements, benefits of a static paired sampling over a random sampling may still be large, even when additional uncertainty from a shift in sample location is considered. However, it is likely that the additional cost of a precise spatial sampling protocol within each sampling plot will be less than that of collecting several times as many samples, with the analytical costs that each additional sample entails.

Alternatively, the surveyor may reduce the effects of short-range variability by compositing samples (Brus and Noij, 2008; Rawlins et al., 2009). However, this is not recommended for monitoring individual entities, as composite samples contains little information on the within-plot variability, and may therefore prohibit detection of change between the two rounds of sampling. Nevertheless, on a larger scale, such as regional or national soil C protocols, compositing samples may be a cost-efficient approach. For example, Mäkipää et al. (2008) concluded that using composite samples can reduce the cost of national soil C monitoring program in Finland by one-third.

Commonly we are interested in changes across landscapes rather than individual plots. An alteration of the C stock in one single plot cannot easily be extrapolated with statistical confidence across a forest or watershed (Yanai et al., 2003). However, extrapolations can be made by subjective inference from a combination of plots. As such, comparable results from plots across landscapes, such as those used presented this study, suggest that stratification of sample plots will reduce the monitoring cost for larger

126

scales. In stratified sampling, the plots are grouped into different stratum according to relevant plot traits, such as predicted accumulation rate, soil type or C content or variability. By optimally allocating samples to the different stratums, it has been estimated that the number of plots needed to detect a change without a loss in precision may be reduced with 25% (Peltoniemi et al., 2007). Alternatively, one could identify areas where the fine-scale variation of the soil is likely to be largest, and sample that region to get information on sample covariance when planning the sampling protocol (Lark, 2012). This would ensure that the sample size in the most variable areas was sufficient to detect the desired magnitude of change.

4.4.3. *Time as a substitute for spatial accuracy*

Although the rate of soil C change is not known, modeling studies of boreal forests have estimated an annual increase ranging from 0.014 to 0.56 Mg C ha^{-1} (de Wit et al., 2006; Liski et al., 2006; Pregitzer and Euskirchen, 2004), with most rapid and profound changes possibly occurring in the top organic layer (Gaudinski et al., 2000; Seedre et al., 2011). Nevertheless, if these expectations are correct and accumulation occurred *exclusively* in the organic layer, the relatively small annual C inputs makes detecting any change a challenging task for surveyors.

Under the modeled accumulation rates, time between sampling provided the strongest explanatory value for the regression model of sample requirements (Fig. 7b). Because the spatial variability (both plot and short-range) derived from the baseline

127

sampling is static, the variability around the predicted change is the only dynamic model variable. However, without consideration of the spatial variability, a single predictor model for sample requirements using only time performs poorly. For the plots in this study, time between sampling contributes ~50% of the explanatory power of the model. Thus, sample estimates are a function of both the projected accumulation and the observed spatial variability. First, under different rates of accumulation the sample requirements will also shift. In the models presented here, change is represent by time, and under different accumulation rates the same models can be used to derive on the correct sample number by simply shifting time scale corresponding to the projected change. Second, depending on whether the expected change is independent or correlated to the spatial patterns at the time of baseline sampling, the variance of pair differences will also change. Our second model (Eq. 5) therefore uses the most conservative method, assuming that the variances of sample differences also increase with time – meaning that the change is not independent of existing spatial patterns. Alternatively, one could model organic layer C stocks by the assumption that baseline measurements tells us nothing about the change likely to occur at that sampling location (Eq. 4). Because the expected rates of change are small (0.1 to 2.5%) compared to the organic layer C stock (Akselsson et al., 2005; de Wit et al., 2006; Liski et al., 2002), the change in variance of paired differences under a random yearly accumulation will likely be negligible for plots with comparable characteristics as those used in this study. With no inflation in the variance of

128

differences between sample pairs over time, the efforts required to detect a change in the organic layer C stock depends on the mean difference between paired samples and the variance resulting from a relocation of sample position. Most studies advising on sample size requirements for soil C monitoring only estimates the efforts required using the baseline variance and expected change (e.g. independent additive change). Besides the implications of sample relocation demonstrated in this study, we don't know beforehand how the magnitude and spatial variability of the change process will affect the sampling requirements. However, several studies have shown how the link between above and below-ground processes are strong (Hogberg and Read, 2006; Wardle et al., 2004), and that C accumulation in the organic layer is not entirely random, but can be associated adjacent tree species (Stendahl et al., 2010; Vesterdal et al., 2013), or other stand attributes, such as basal area (Hansson et al., 2011). Assuming no covariance between baseline measurement and change would therefore underestimate sample requirements, where the reduced statistical power may lead to rejections of true changes in the C stock (type II error). If the changes are correlated to already existing spatial patterns, the magnitude of this estimation error will increase with time interval between sampling. For a paired sampling to be an efficient approach when monitoring organic C it must be designed on the basis of estimates of the variance of the change variable (Lark, 2009). We therefore recommend that surveyors use the most conservative prediction of sample size.

Our results demonstrate how time intervals can compensate for spatial sampling accuracy in these plots. The tradeoff between time and spatial precision becomes clear by comparing the projected sample size of P_{B-15} and P_{B-125} after 10 and 25 years. Under similar statistically constraints, the surveyor have to wait 25 years to detect the same change at a 125 cm spatial relocation than what can be detect in 10 years with a 15 cm spatial relocation. However, temporal changes are not linear, and care must be taken to avoid any systematic variations, such as seasonal differences between sampling times. In this study, any seasonal effects were controlled for by collecting all samples contemporaneously and without the L layer, but in the case of different seasonal sampling times, additional non-random variance may be introduced. We emphasize that the type of change, whether it is linear or non-linear, correlated or independent from the baseline status will influence the sampling scheme and requirements, and should therefore be considered when deciding on sample protocol.

4.5. Conclusions

This study investigates how the short-range variability in typical boreal forest soils influence the efforts required to monitor the organic layer C stock. We draw the following conclusions regarding the effects of relocation in paired sampling: (1) Sample repeatability declines with sample separation distance, (2) By not considering the effects of sample relocation, sample requirements increase by a factor of 4, and (3) Longer time intervals between baseline sampling and revisit may compensate for lacking spatial

sampling precision. The information provided by this study can be considered indicative of the magnitude and variability of one can expect when monitoring soil organic layer C stocks in boreal forests, and provide motivation to further study the problem. Due to the close coupling between spatial accuracy and sample requirements, and the challenge of maintaining individual sample points (within cm) over decades, we hope to encourage surveyors to consider the practicality of conducting paired resampling for monitoring forest soil C.

Chapter 5: Optimum sampling allocation: Reducing the costs of organic layer C stock inventories in boreal forests using a double sampling approach

Terje Kristensen[a]

[a] Department of Forest Resources, University of Minnesota, 115 Green Hall, 1530 Cleveland Ave. N., St. Paul, MN 55108, USA

Summary

The soil organic layer C stock in boreal forests exhibit great spatial heterogeneity over short distances, and substantial sampling efforts are therefore required to determine the current status of the C stock with acceptable margins of uncertainty. Because precise estimates are costly it is of great interest to surveyors to develop cost-efficient sampling protocols aiming to maximize the spatial coverage, while minimizing the estimate variance. In this paper we utilize a nested sampling procedure with three levels, forest (25 km^2), plots (2000 m^2) and subplots (100 m^2) to investigate the mean and variability of organic layer C stocks and provide a case study for developing a cost-optimal sampling

approach. The study was on conducted on podzols across a multilayered boreal forest in SE Norway.

Our results show that approximately 70% of the estimated variance across the forest was confined within subplots emphasizing the importance of considering the short-range variability when conducting a large scale inventories. This article demonstrates how an optimal distribution of sampling units (plot, subplot and sample) is not only a function of the variance component within that dimension, but also changes with the sampling unit costs. Further, we find that the costs of conducting an organic layer C inventory can be reduced by more than 60% by increasing the inventory uncertainty from $\pm$ 0.25 Mg C ha^{-1} to $\pm$ 0.5 Mg C ha^{-1}. Finally, we demonstrate that sampling costs can be reduced by as much 80%, by conducting a double sampling procedure that utilizes the strong correlation between organic layer C stock (r = 0.79 to 0.85) and inexpensive measurements of layer thickness.

5.1. Introduction

Information about the variability in soil organic layer C stocks is essential for programs aiming to measure, monitor and manage soil carbon (C) stocks. Among many factors influencing the organic layer variability is the issue of scale. Several studies have investigated organic layer C variability at a single scale (Häkkinen et al., 2011; Muukkonen et al., 2009; Schöning et al., 2006), but less is known about the spatial heterogeneity across multiple scales (Lin et al., 2005). Quantification of heterogeneity

133

across scales is desirable for modeling and prediction (de Gruijter, 2006), which provides a foundation for developing an understanding regarding the scales of influence on variability and forms a framework upon which scaling of data may be possible (Lin et al., 2005).

According to Upchurch and Edmonds (1991), there are three main issues which need to be considered when planning a spatial assessment of soils: (1) location of sample points, (2) size of sample, and (3) total number of samples to be collected. To address issues (1) and (3), the surveyor selects either a design-based or model-based method (de Gruijter, 2006). Design- and model-based methods differ in the scale of appropriate application, resource requirements, and accuracy of data. If the study is concerned with unbiased estimates for the area as a whole, or for a restricted number of subareas, a design-based approach is considered the best choice. A model based approach is likely a better choice if the motivation is mapping the variable over the study area and predicting these values as precise as possible. Brus and De Gruijter (1997) present an extensive comparison of these two methods.

Nested (or multi-stage hierarchical) sampling enables the surveyor to investigate the magnitude of the mean and variability across spatial scales. The analysis derives from the model of nested variation, which is based on the notion that a population can be divided into different levels in a hierarchy or stratums (Price et al., 2009). Once the area of interest is stratified into classes, the sampling within each nested level of sampling can

be random, systematic, or along transects. Each level in the hierarchy represents a distance between sampling points, and plotting the accumulated components of variance for each sampling interval against increasing separating distance may provide an approximation to the geostatistical variogram. The results of a hierarchical analysis of variance from a nested sampling are therefore considered a hybrid between a model and design based method (Webster and Oliver, 2001). The benefit of a nested sampling method is that a wide range of spatial scales can be covered in a single analysis, which is particularly valuable where variation occurs in spatial scales that differ by several orders of magnitude simultaneously (Lin et al., 2005). Since first employed in soil variability assessments by Youden and Mehlich (1937), the nested sampling approach has been used to explore the variability of soil C across different scales (Conant and Paustian, 2002; Hoffmann et al., 2014; Homann et al., 2001).

Due to the sampling time and costs for a full sampling coverage, estimates of organic layer C for a forest or a region involve prediction of the response variable at many unsampled locations. Data are therefore often sparse in comparison to the extent of the scaled area, and as a result, the estimates are often highly uncertain across scales. Even though the area of interest has previously been stratified into more homogenous stratums, organic layer C stocks may still display considerable variation across different scales. These problems may be counteracted by using dense sampling protocols. Soil C

programs therefore face a critical dilemma when implemented: maximizing the precision and spatial coverage of the C inventory while minimizing the sampling effort.

The soil organic layer C stock in boreal forests exhibit great spatial heterogeneity over short distances, and substantial sampling efforts are therefore required to determine the current status of the C stock with acceptable levels of precision (Häkkinen et al., 2011; Muukkonen et al., 2009). For monitoring efforts this problem is confounded by the complex interactions between the factors driving changes in the organic layer C stock across different scales (Callesen et al., 2003), where the annual variability is small relative to the full C stock (Peltoniemi et al., 2004). Prior knowledge about and magnitude and scales of variability in organic layer C can assist in determining the most efficient sampling strategy. For example, to decide on the number of primary units (plots) to sample in comparison to the number of measurements to collect within each unit, the surveyor needs to know the relative variances of the two levels. The allocation of sampling efforts must be balanced with the constraints of the sampling protocols, as most surveys have limited resources or target a minimum level of precision.

For estimates of organic layer C stocks, one of the main costs is the collection and treatment of soil cores (Mooney et al., 2004; Mäkipää et al., 2008). Tenenbein (1970) demonstrated that when the association and cost difference between the principal variable of interest and an auxiliary variable is high, substantial gains can be achieved by using a double sampling approach. Thus, if the number of physically sampled cores could be

lowered without any loss in the estimate precision, for example with the use of a correlated and more cost-efficient auxiliary variable, the cost of sampling may be reduced. One measurement which has been found to correlate with organic layer C stock in forests is horizon thickness (Hunt et al., 2010; Schöning et al., 2006). In soils types where horizon boundaries may be determined visually, such as boreal podzols, measurements of organic layer thickness can be determined effortlessly, and may therefore be of great value as an auxiliary variable in a C inventory. However, its application as a substitute for full sample extraction and analysis to reduce inventory costs has not yet been assessed.

The main purpose of this study is to assess the scales of variability in the soil organic layer C stock within a multilayered boreal forest stand in SE Norway, and to identify the optimal allocation of sampling resources in order to achieve the most precise estimate of the organic layer C stock. More specifically, we (1) assess the variability of organic layer C across three scales, subplot (100 m^2), plot (2000 m^2) and forest (25 km^2), (2) determine the optimal sampling allocation between the different scales, (3) simulate how sampling costs influences the optimal sampling protocol, and (4) explore the use of organic layer thickness as an auxiliary variable for situations with unknown spatial means in cost-reduction efforts for organic layer C sampling.

5.2. Methods

5.2.1. *Study area and sampling design*

This study was conducted on organic layer soils in a mature and multilayered spruce forest in the Årum–Kapteinstjern area, located approximately 35 km north of Skien in Telemark County, South East Norway (59°21N, 9°45 E). The area is considered situated in the border of the south – middle boreal vegetation zone (Moen, 1999). The study plots are located between 470 and 600 m above sea-level. The forests belong to the *Picea - Vaccinum myrtillus* type (Cajander, 1949; Kielland-Lund, 1981), which is the most abundant forest type in North West Europe. The forests are dominated by Norway spruce (*Picea abies* (L.) Karsten), but scattered occurrences of Scots pine (*Pinus sylvestris* L.) and birch (*Betula pendula* Roth and *B.pubescens* Ehrh.) are common. To enable a quality assessment of the natural variability in soil organic layer C stock, the forest have not been impacted by any form of forest practices in the last century (Lie et al., 2012). Kristensen et al., *in review,* presents detailed information on the stand characteristics.

We used a two-level nested sampling to examine variance in soil organic layer C across the study forest. The nested sampling allows for the estimation of spatial variability of organic layer C across spatial scales, and enables us to evaluate the impact of small-scale variability on the larger scale. At the largest scale we analyze a forest stand (~25 km^2), where we randomly selected seven sampling plots (~2000 m^2), four located in

138

Årum, and three situated in the Kapteinstjern area. In each of these plots, we have selected four subplots (100 m^2), represented by nine organic layer C measurements (Fig. 1).
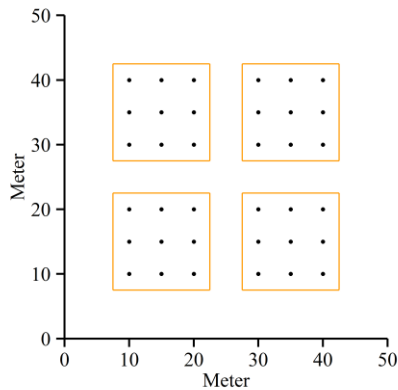
Figure 1. Variability of soil organic layer C was assessed across three hierarchal levels; stand scale (25 km^2), plot scale (2000 m^2) and between four subplots (100 m^2). Seven plots had four subplots nested in each. From each of the subplots, nine organic layer soil cores were extracted together with measurements of the layer thickness.

Using a cylindrical steel corer (56 mm diameter) we sampled the soil organic layer consisting of the F (O$_e$) and H (O$_a$) horizon down to the mineral soil boundary. Because of the low faunal mixing of decomposing litter in these forests there were visually clear horizon boundaries between the organic layer and the mineral soil. The organic horizon and the mineral soil will differ substantially in both bulk density (BD) and C concentration (C$_c$) (Baritz et al., 2010; Lundström et al., 2000; Muir, 1961), thus using a genetic horizon sampling protocol, instead of a fixed depth sampling can significantly reduce the variability of mean SOC stock (VandenBygaart et al., 2007). The

139

sampled F and H horizon consists of both partially decomposed matter and well-decomposed organic matter. Undecomposed surface litter (L (O_i) horizon) was excluded from the sample and further analysis to minimize any seasonal effects. The thickness of the soil core was measured to the nearest cm.

Samples were oven dried at 65 °C (Thermax Series TS8000) until no further weight loss occurred, then weighted, before they were sieved down to < 2 mm. Samples were then weighed again to determine the coarse fragment mass. Bulk densities was calculated from the dry mass and the core volume after being corrected for coarse fragments (> 2mm) (Throop et al., 2012). To determine C_c, samples were grounded to a size of <100 μm using a ball mill, before the homogenized mixture was analysed using a VarioMax (Elementar Analysensyterne GmbH, Hanau, Germany). The analysis was done at the Skogforsk commercial laboratory and complied with ISO 9000 certified methods. To avoid inclusion of mineral soil in the organic layer samples, all concentrations are expressed on an organic matter basis. Because the amount of inorganic C in these acidic soils are low, sample C was considered organic (Huntington et al., 1989).

The C content in the organic layer was calculated using (Eq. 1):

$$C_{OL} = C_c \times \sum (SW_{OD} / A) \qquad (1)$$

where C_c is the organic C content of the sample, as determined by the CHN analyzer (g C g^{-1}, dry soil), SW_{OD} is the oven dry weight of the sample (g), A is the cross-sectional area of the core.

5.2.2. Organic layer carbon variability across scales

Statistical models considered the hierarchical data structure with two levels: The forest stand being represented by seven plots with four subplots nested within each plot. Each subplot was represented by nine soil organic layer sampling points with paired measurements of organic layer thickness and C stock (Fig. 1). Standard statistical procedures were used to examine distribution, normality and homogeneity of variance. The organic layer C variability for each level was measured by the coefficient of variance (CV). The CV was either calculated based on individual samples within subplots, at the scale of subplots within plots, or based on the means within plots at forest scale.

Organic layer C stock was assumed to be explained by the nested linear model (Webster and Oliver, 2001):

$$Y_{ijk} = \mu + P_i + S_{ij} + \varepsilon_{ijk} \tag{2}$$

where μ represents the overall organic layer mean C stock in the study forest, P_i represents the effect of a given plot, S_{ij} represents the effects of a given subplot, while the error term, ε_{ijk}, represents the residual or unexplained variance (within-subplot variance).

Using the general linear model procedure, the nested ANOVA enables us to make inference about the variability of organic layer C stock across three different scales: (1) Among plots across the forests ($25 \ km^2$), (2) among subplots at a plot scale ($2000 \ m^2$) and (3) among sampling points in each subplot ($100 \ m^2$). Two hypotheses will be tested:

H_{01}: The variance between plots differ

141

H_{02}: The variance between subplots within each plot is different

Significant differences (α=0.05) in mean organic layer C stock values were determined from the ANOVA output for each level of analysis. The mean square (MS) values calculated by the ANOVA were used in order to partition the amount of variability attributed to each level in the sampling design. The variance at each level of the sampling design was estimated as:

$$s^2_{plot} = \frac{MS_{plot} - MS_{sub}}{n_{plot}n_{sub}} \qquad (3)$$

$$s^2_{sub} = \frac{MS_{sub} - MS_{samp}}{n_{sub}} \qquad (4)$$

$$s^2 = s^2_{plot} + s^2_{sub} + s^2_{samp(\varepsilon)} \qquad (5)$$

where Eq. (3) is the calculation for the variance at the plot level, s^2_{plot}, Eq. (4) computes the variance of subplots within a plot, s^2_{sub}, and Eq. (5) is the calculation for the total variance. Here, $s^2_{samp(\varepsilon)}$ represents the residual or unexplained variance (within-subplot variance). The values n_{plot} and n_{sub}, represent the number of plots and the number of subplots per plot, respectfully. The percent of the total variance attributed to each level in the sampling design was calculated by taking the variance at a particular level divided by the total variance.

5.2.3. *Optimal allocation of sampling units*

The optimal allocation of sampling units per level (plot, subplot, samples) can be expressed as a function of the variance of the sample mean and the efforts (costs) necessary to obtain the measurements. In the nested design, optimal allocation can be assessed by the ratio of each variance component to their respective residual variance (Cochran, 1977). To determine optimal sample allocation, statistical procedures commonly take one of two approaches. In the first, we are bound by a fixed limit, such as cost or sample size. When cost is fixed the optimal allocation is computed as the combination of sampling units which minimizes the variance estimator. In the second approach, we are bound by a set level of precision, and the optimal allocation is computed as the combination of sampling units which minimize the cost. In a random sampling approach, the most efficient sampling allocation for a fixed level of precision, $s_{\bar{Y}}^2$, can be estimated from (Cochran, 1977):

$$s_{\bar{Y}}^2 = \frac{s_{samp}^2}{n_{samp}n_{sub}n_{plot}} + \frac{s_{sub}^2}{n_{sub}n_{plot}} + \frac{s_{plot}^2}{n_{plot}} \tag{6}$$

where s_{plot}^2, s_{sub}^2 are the variance function for plot and subplot. The sample variance, s_{samp}^2 is computed from the nested ANOVA error term (Eq. 2), and represents the within subplot variance.

The relative efficiency of one strategy over another will only be meaningful if a measure of effort (time, cost) is taken into consideration. In this study we assume that the

143

expenses at each level are known and unequal. Thus, the total cost of sampling is a function of n sampling units for each level, with the coefficients representing the known costs per sampling unit. The costs of several potential sampling protocols and methodologies were determined. Rather than provide explicit cost estimations, these expenditures are meant to introduce the reader of tradeoffs between sampling precision and costs, and the potential benefits of considering auxiliary variables when designing a sampling protocol. Overhead costs, such as administrative expenses and equipment purchases, vary among sampling protocols, but have been ignored in this study as they do not enter into the optimization problems.

The cost of establishing one plot was computed as:

$$C_{plot} = C_{trav} + C_{fld} + C_{eq} \tag{7}$$

while the cost of establishing a subplot is:

$$C_{sub} = C_{fld} + C_{eq} \tag{8}$$

where C_{trav} is the costs of traveling to plot, C_{fld} is costs of fieldwork, while C_{eq} is costs related to necessary equipment required to establish the plot and subplot. The costs of traveling and fieldwork are proportional to t, the time in hours (h) needed to conduct the survey. We assume that the survey will be conducted by two field technicians at a labor costs at \$100/hour. Travel time between plots will highly depend on the area of interest. In this study we set the traveling time between plots at 2 hours, which is an approximation of the travel time used in this survey. Initial travel time to the study area is

144

not considered here, as we consider this part of the overhead costs. Fieldwork includes the establishment of plots and subplots with global positioning (GPS) units and preparation for sampling, and is set at 3 hours per plot, and 30 minutes per subplot. The costs of GPS units are considered negligible. Hence, the cost of establishing a plot comes out at $1000, while the costs of one subplot at $100.

The costs of actual sampling is the sum of the time taken to select the location of the random samples, extracting, packing, and marking samples for later laboratory analysis:

$$C_{samp} = C_{fld} + C_{lab} \qquad (9)$$

where C_{fld} is based on the hourly rate of field crew and C_{lab} represents the costs of storage, laboratory treatment and carbon concentration analysis. Sampling time can be difficult to predict since it depends on local conditions (Singh et al., 2013). Similarly, laboratory costs may vary greatly depending on methods used for analysis. Note that the laboratorial methods used also influences the precision of the estimate (Chatterjee et al., 2009). Goidts et al. (2009a) presents a detailed study of the magnitudes and sources of uncertainty in soil organic stock assessments at various scales.

To determine the optimal allocation and number of measurements per level which minimizes both variance and cost (Sokal and Rohlf, 1995):

$$n_{sub} = \sqrt{\frac{c_{plot} s_{sub}^2}{c_{sub} s_{plot}^2}} \quad , \qquad n_{samp} = \sqrt{\frac{c_{sub} s_{samp}^2}{c_{samp} s_{sub}^2}} \qquad (10)$$

145

where n_{sub} and n_{samp} indicates the optimal number of replicates at each level.

Finally, the total costs of three sampling levels, and without consideration of any overhead expenses, the cost can be expressed as (Sokal and Rohlf, 1995):

$$C = n_{plot}c_{plot} + n_{sub}n_{plot}c_{sub} + n_{samp}n_{sub}n_{plot}c_{samp} \qquad (11)$$

where *n* are the number of plots, subplots and samples, and c_{plot}, c_{sub}, c_{samp} are the cost at each level. As an example, the total cost of establishing three plots, containing two subplots with nine soil samples is estimated at (Eq. 11): \$1000 x 3 plots + \$100 x 2 subplots (x 3 plots) + \$25 x 9 samples (x 2 subplots x 3 plots) = \$5950.

5.2.4. *Double sampling design*

Double sampling is a form of multiphase sampling, where an estimate of a principal variable is obtained by utilizing its relationship to an auxiliary variable. The method can be cost-efficient if the variable of interest is difficult or costly to obtain, whereas the supplementary variable can be measured with less effort (Husch et al., 2002). Thus, the aim of the double sampling method is to reduce the number of observations from the principal variable of interest without sacrificing precision of the estimate (Husch et al., 2002). The double sampling method consists of two elements: (1) measurements of auxiliary variable and (2) measurement of main variable plus measurements of the auxiliary variable.

One promising measurement associated with the organic layer C stock in boreal forests is horizon thickness, as thickness measurements may be rapidly and inexpensively

146

be collected across a plot or landscape. To examine the relationship between organic layer C stock and organic layer thickness we computed linear correlation coefficients individually for each plot and in one overall by pooling all samples together. The sensitivity of the correlation coefficient to sample size was investigated from bootstrapping 1000 rounds with increasing sample sizes.

The optimal allocation of y to x in the double sampling procedure depends on the strength of the relationship between the variables and the relative costs of observing them. In contrast to simple regression estimators, the double sampling method incorporates the additional source of variability associated with the auxiliary sample in its estimate. Brus and Te Riele (2001) describe in detail the main differences between a simple regression estimator and a double sampling regression estimator. To simulate the potential benefits of using organic layer thickness measurements in a random sampling procedure within each subplot we incorporate the auxiliary data in a double sampling regression estimator. The regression estimator of the spatial mean for a double sampling is (Brus and Te Riele, 2001):

$$\hat{\bar{y}}_{Dr} = \hat{\bar{y}}_{D\pi^*} + \sum_{j=1}^{J} \hat{B}_{js} (\hat{\bar{z}}_{jD\pi} - \hat{\bar{z}}_{jD\pi^*}) \qquad (12)$$

where $\hat{\bar{y}}_{D}$ is the value of the spatial mean, $\hat{\bar{z}}_{jD\pi}$ and $\hat{\bar{z}}_{jD\pi^*}$ are the π estimator and the π^* estimator, respectively, of the spatial mean of the jth auxiliary variable $\hat{\bar{z}}_{jD}$ and $\hat{B}_{js}$ is the

147

regression coefficient (slope) B_{js} for auxiliary variable z_j. The double sampling regression variance estimator of a population, y, for a design based approach is (Cochran, 1977):

$$s_{\bar{y}}^2 = n_{samp}^{-1} s_y^2 (1 - \rho^2) + n_{aux}^{-1} \rho s_y^2 - N^{-1} s_y^2 \qquad (13)$$

where $s_y^2 = \sum_N (y - \bar{y})^2 / (N-1)$ is the population variance of y, and $\rho^2 = s_{xy}^2 / (s_x^2 s_y^2)$ is the coefficient of determination with the correlation coefficient, ρ.

To find the optimum allocation of soil organic layer C samples and thickness measurements that minimizes costs within fixed margins of error, a Lagrange multiplier is used to obtain the general formula for n_{samp} and n_{aux} (Thompson, 2012). The variance shown is minimized and subject to a fixed cost when:

$$n_{samp} = \frac{C f_0}{c_{samp} f_0 + c_{aux}} \qquad (14)$$

and

$$n_{aux} = \frac{C - c_{samp} n_{samp}}{c_{aux}} \qquad (15)$$

where

$$f_0 = \sqrt{\frac{1 - \rho^2}{\rho^2 R}} \qquad (16)$$

where f_0 is set equal to 1 if Eq. 9 gives $f_0 > 1$ and R equals c_{samp}/c_{aux}.

148

The optimal allocation ratio for a double sampling with unequal cost is estimated from (Thompson, 2012):

$$\frac{n_{samp}}{n_{aux}} = \sqrt{\frac{c_{samp}}{c_{aux}} \left(\frac{s_{aux}^2}{s_{samp}^2 - s_{aux}^2} \right)} \qquad (17)$$

where the sample ratio n_{samp}/n_{aux} is a function of the costs ratio.

For a fixed cost, the variance is minimized by (Chang and Yeh, 2007; Thompson, 2012):

$$s_{\bar{y}}^2 = s_y^2 \frac{\sqrt{c_{samp}(1-\rho^2) + c_{aux}\rho^2}}{C} - \frac{s_y^2}{N} \qquad (18)$$

The cost of collecting one measurement of organic layer thickness is set at \$1. To cover a range of potential expenses for sampling times and laboratorial methods, we include three different estimates of organic layer sample costs, set at \$25, \$50 and \$100 per sample. These costs are within the range of sample costs provided by earlier studies (Mäkipää et al., 2008; Singh et al., 2013). Thus, the influence of cost and correlation on the optimal allocation observations was assessed using three different cost ratios of organic layer samples (which include thickness measurements) vs. thickness measurements (25:1, 50:1 and 100:1). All statistical tests were performed with the R software, version 3.0.2 (R Core Team, 2013).

5.3. Results

5.3.1. Variability across scales

The mean organic layer C stock among plots varied at most by a factor of ~2. Plot K4 had the lowest plot mean (17.0 Mg C ha^{-1}), while the highest mean C stock was measured in plot K2 (34.5 Mg C ha^{-1}) (Fig. 2). Significant differences in soil organic layer C stock were observed among the seven plots ($F = 10.33$, $p < 0.001$), and as a result H_{01} was accepted.
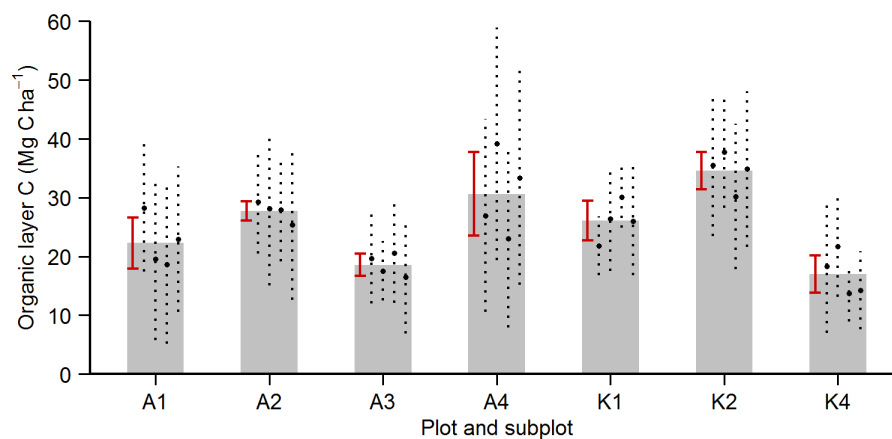
Figure 2. Organic layer C stock in plots and subplots. Plot means (bars) are computed from averaging subplot means, while subplot means (dot) are computed from 9 organic layer C samples in each. Means are presented with ±1SD for plots (error bars) and for subplots (dotted lines).

The contribution of plot variance to the overall estimation variance was 26% (1SD, ±6.1 Mg C ha^{-1}), which indicates that approximately a quarter of the overall

150

variance in the modeled organic layer C stocks from these plots can be attributed to differences across the forest stand.

Differences between the nested subplot means varied by a maximum factor of 1.8. With the exception of one plot (A4, F = 4.26, p = 0.012), the subplots did not significantly differ within plots. In the nested ANOVA, the contribution of variance between subplots was not significant (p = 0.112), and H_{02} was therefore be rejected. Variance at a subplot scale contributed 3% ($\pm$2.1 Mg C ha^{-1}) to the total variance.

Table 1. Summary of nested ANOVA

Component	Scale	df	MS	F	p	SS	V%	CV
Between plots	25 km^2	6	1462	10.33	<0.000	8771	26	25
Between subplots	2000 m^2	21	142	1.42	0.112	2971	3	15
Within subplots (Err)	<100 m^2	224	100			22369	71	45
Total						34111	100	

Note: df = degrees of freedom, MS = mean squares, F = ANOVA statistic, SS = Sum of squares, V% = Contribution to the overall variance. CV = Coefficient of variation.

The residual error term represents the variation within the subplots (Table 1), and is comparable to the nugget variance found in geostatistical analysis (Miesch, 1975). The variation within individual subplots (CV = 45%) was considerable higher than the variation between subplots (CV = 15%), and between plots (CV = 24%). In all seven plots, the variation within subplots exceeded the variance between subplots. The nested

ANOVA revealed that the majority of the variance, 71% ($\pm$10.1 Mg C ha^{-1}), across the investigated forest plots are confined *within* subplots <100 m^2.

5.3.2. *Optimal allocation of sampling units*

The optimal sample allocation is a function of the variance component for each of the levels in the nested analysis. Based on the distribution of variance across the scales, and ignoring any costs differences the sampling units may have, our model suggests that for each plot, one sub-plot containing 5 samples would be optimal. To provide an estimate of the mean organic layer C stock with a standard deviation of maximum $\pm$0.25 Mg C ha^{-1} we would need 10 plots randomly distributed in the forest.

However, the optimal allocation of sampling units changes when costs incorporated in the model (Fig. 3A). If the costs of establishing one plot is $1000, and one subplot is $100, while the price per organic layer sample is $25, we find that the most cost-efficient sampling distribution to estimate the mean organic layer C stock across the forest with a precision of $\pm$0.25 Mg C ha^{-1} are 9 plots with 1 subplots each where 9 samples are collected in each sub-plot. With higher sampling costs the total inventory cost increases (Fig. 3B), and the optimal distribution of sampling shifts towards more plots with fewer samples in each (Fig. 3A). The proportion of soil sampling cost to the overall costs increases from 17 to 27%, despite collecting fewer samples per subplot (Fig. 3C). The number of subplots remains unchanged (at only one per plot) at different cost levels, due to the low contribution of subplots to the overall estimate variance (Table 1).

152

Similarly, the total costs can be substantially lowered by accepting a higher margin of error. For example, in our study we find that the inventory costs can be reduced by >60% if we can tolerate an uncertainty of ±0.5 Mg C ha^{-1} instead of ±0.25 Mg C ha^{-1} (Fig. 6).
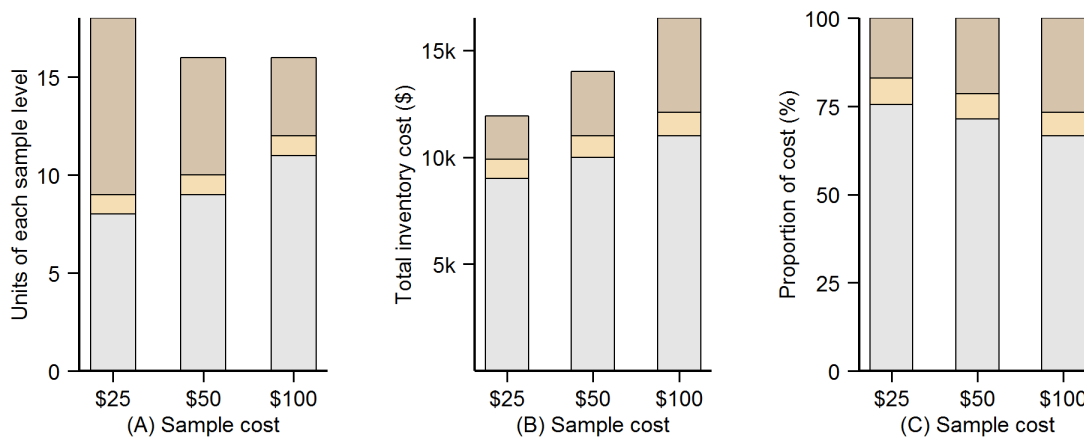
Figure 3. Optimal allocation of sampling units for plots (bottom segment), subplots per plot (middle) and soil organic layer samples per subplot (top) to estimate the mean soil organic layer C stock with a precision of ±0.25 Mg C ha^{-1}. With increasing sample costs, the sampling protocol changes from fewer plots and more samples to more plots and less samples in each. The total costs increases with the cost per organic layer sample (B), and the relative contribution of soil samples to the total costs gets bigger (C).

5.3.3. Double sampling

The association between organic layer C stock and layer thickness was significant for all plots (p < 0.001). The correlation between organic layer C stock and layer

153

thickness stabilizes for sample sizes above ~40 (Fig. 4). Here, plausible values of the true

correlation ρ, as expressed by a 95% confidence interval, range from 0.79 to 0.85 (Fig. 4).
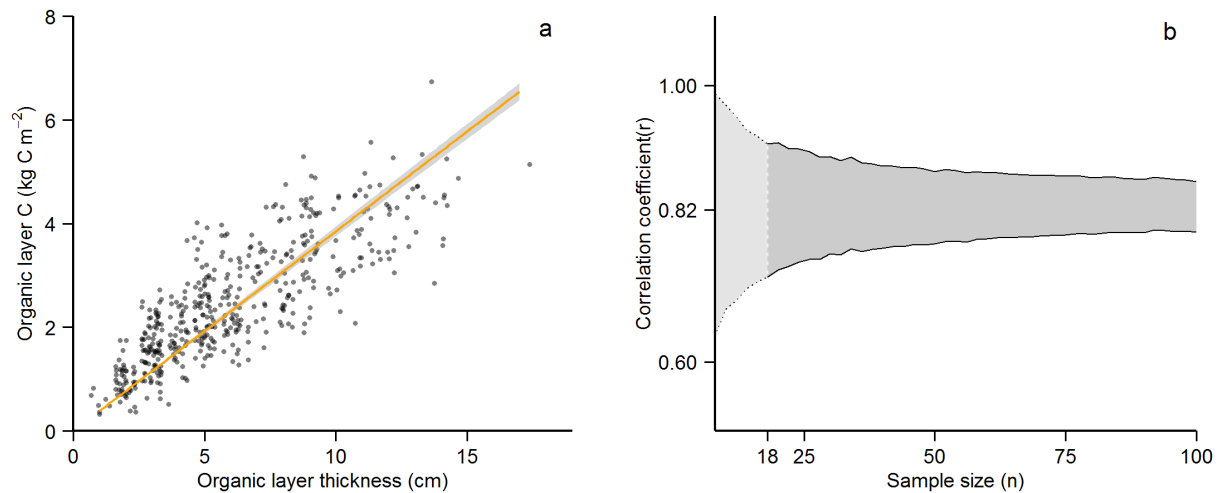
Figure 4. (a) Association between organic layer C stock and layer thickness. **(b)** 95% Confidence interval for the correlation between soil organic layer C stock and layer thickness. The confidence interval is bootstrapped with 1000 rounds for each sample size. At sample sizes < 18, correlation p-values become unstable (data not shown). The mean correlation is r = 0.82, n = 487.

The optimal allocation of organic layer C stock samples and thickness measurements depend on (1) the correlation between variables, and (2) their cost ratio. The allocation which minimizes the variance estimator in our data is 1:7, 1:9 and 1:14 (soil sample:thickness measurement), when one organic layer sample cost $25, $50 or $100 and measuring thickness costs $1 (Fig. 5). This means that when expenditures are fixed, and the costs of collecting soil samples are higher, the uncertainty around the

estimate is kept at a minimum by collecting more thickness measurements per soil core. In contrast, if the correlation is lower than observed from our data (Fig. 4), the surveyor should take fewer thickness measurements per soil core. The exact number and distribution of measurements is contingent on the required level of precision, or whether the survey is limited by a maximum cost.
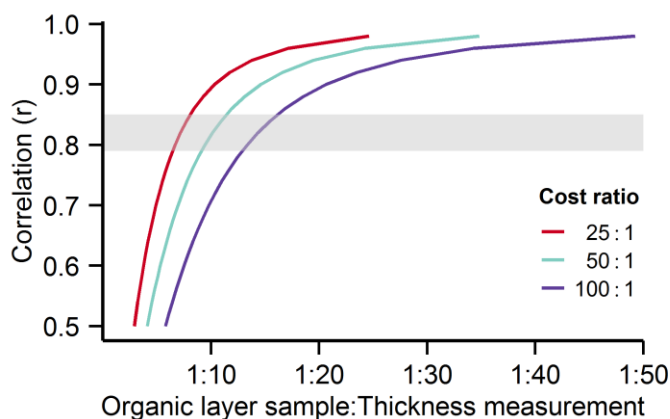
Figure 5. Optimal allocation of soil organic layer C samples and layer thickness to achieve the lowest variance of the estimator. The allocation is a function of the correlation between sample and auxiliary variable and cost ratio. In this example, the expenses are fixed at $1000. The x-axis shows the thickness multiplier (n samples of thickness for each organic layer C samples) against the correlation (y-axis). Shaded area indicates the 95% CI for the correlation between soil organic layer C and thickness observed in the study plots. If the correlation between the two observations is 0.85 and the cost of collecting one soil core is $50 compared to $1 for each thickness measurement, the variance of the estimator is minimized by collecting one soil core for each nine thickness measurements.

155

The strong association correlation and cost differences between physically handling soil cores and collecting data on soil thickness can be utilized by the surveyor to (1) Improve precision of the mean estimate without any additional costs, or (2) reduce the cost without loss in precision of the mean estimate.

In the first scenario, we use a fixed cost derived from sampling without horizon thickness measurements (Fig. 3B). If the target accuracy of the forest organic layer C inventory is ± 0.25 Mg C ha^{-1}, and the price of one sample is \$25, the cost of collecting organic layer samples totals \$1800 (not including plot and sub-plot expenses) (Fig. 3B). For the same price, this uncertainty can be reduced to only ± 0.15 Mg C ha^{-1} by collecting primary and auxiliary variables in a 1:7 ratio. Increasing soil sampling costs affects the optimal sampling allocation in two ways. First, it shifts the ideal allocation of sampling units towards more plots with fewer samples in each (Fig. 3A). Second, it becomes beneficial to collect less soil samples and more thickness measurements. The estimate precision remains largely unchanged because the increased costs of the sampling protocol enables the surveyor to collect more data on thickness.

In the second scenario, our primary concern is lowering inventory costs without any loss in estimate precision (± 0.25 Mg C ha^{-1}). Our data demonstrates that sampling costs can be reduced by 80 to 82% by incorporating horizon thickness measurements in our estimates (Fig. 6), which corresponds to a reduction of 14 to 22% of the overall inventory costs.

156
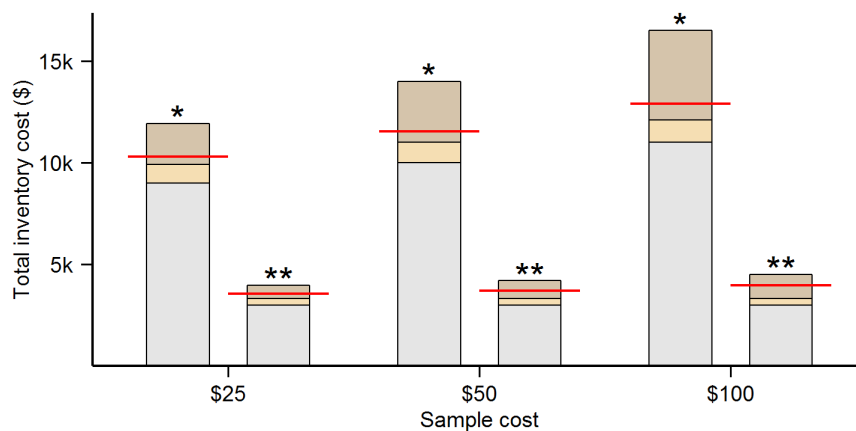
Figure 6. Reducing costs of soil organic layer C inventory. The cost of an inventory can be reduced by (1) lowering the desired precision of the estimate from ±0.25 Mg C ha^{-1} (*) to ± 0.5 Mg C ha^{-1} (**), or (2) including inexpensive measurements of organic layer thickness in a double sampling approach. The potential cost reduction of a double sampling procedure is illustrated by the horizontal line.

5.4. Discussion

The analysis of optimum sampling allocation allows us to make some plausible inferences about the sensitivity of sampling designs to both the scales of variability and costs for organic layer C inventories. There is a general awareness that robust planning of inventories and monitoring efforts requires empirical data on the magnitude of variability across scales. Improved knowledge of the variability can assist the surveyor in estimating the number of sampling units required, determine the distribution of sampling units, and ultimately decide upon the feasibility of the survey.

157

This study found that the majority (~70%) of organic layer C variability is due to the short-range variability confined in areas <100 m^2. Based on level of variability across the forest, our results suggest that the cost of estimating the organic layer C stock with a precision of ±0.25 Mg ha^{-1} is ~\$12,000. This may be lowered to only \$4,000 by increasing the estimate uncertainty to ±0.50 Mg C ha^{-1}. Further, our study demonstrates that the sampling costs may be significantly reduced (~80%) by incorporating inexpensive measurements of organic layer thickness in a double sampling procedure when conducting an organic layer C stock inventory.

5.4.1. Optimizing sampling allocation

Stratified sampling

In this study all survey plots were purposively located under forest cover, and our estimates may therefore not be a good indication of the mean C stock and its variance across the landscape as a whole, but should instead be considered a mean estimate of a stratum within a landscape. The fundamental method for stratification or scaling consists of subdividing the landscape into relatively homogenous patches, where variability is minimized (de Gruijter, 2006). Before stratification takes place the surveyor must utilize pre-existing knowledge on what features makes the organic layer C stock in one subarea more like or more dissimilar to other subareas within the landscape of interest (Peltoniemi et al., 2007). At landscape scales, vegetative patterns and the local topography are both known to influence the organic layer C stock (Binkley and Fisher,

2012; Shanin et al., 2013; Thompson and Kolka, 2005; Vesterdal et al., 2013). In the landscape containing the forest study plots, patches of peatland were present. Although they covered a relatively small proportion of the landscape, studies have shown they may contain a substantial amount of the organic C stock (Weishampel et al., 2009). Extrapolating our estimates to a landscape scale rather than an estimate from a stratum *within* the landscape may therefore underestimate the mean organic C stock in the area. It is essential that variance components are considered by the scales in use, and the stratum contribution to the overall variance strongly depends on what the '*overall*' entails.

We also recognize that a substantial amount of soil C exist below the top organic layer. In a study of 2100 podzols profiles in Sweden, Olsson et al (2009) reported that mineral soils had a C density of ~53 Mg C ha^{-1}. For studies aiming to present a full inventory of the forest soil C stock it essential that this large pool is considered when deciding on a sampling strategy. However, variables used for stratifying sampling for organic layer C stock might not be suitable when C in deeper soil horizons is of interest. For example, while vegetation cover can be considered a relevant stratifying variable for organic layer C stocks (Simonson, 1959; Vesterdal et al., 2013), studies have found that mineral C stocks in boreal and temperate regions may be more influenced by soil type and climate than by tree species (Marty et al., 2015; Prescott and Vesterdal, 2013). In a full soil C inventory across a landscape or region it is therefore essential that such differences are considered in the stratification process.

High resolution databases, such as national digital elevation models with resolutions of 30 m or better, and information on vegetation cover and soil type, provide opportunities for decreasing the landscape patches considered to be homogenous (Post et al., 2001). In turn, this may improve the stratification efficiency and increase the precision of C stock estimates for each patch (Post et al., 2001). Although stratification by relevant auxiliary variables is likely to improve the precision of the inventory estimate, there might still be substantial variability within each stratum.

5.4.2. *Variability within stratums*

When the area of interest is stratified, the number of plots are distributed evenly, proportional to stratum size, or based on stratum size and variance (Neyman, 1938). Unbiased estimates of the mean can then be obtained as a weighted average of the stratum means. Obtaining a representative sample within each plot to estimate the means for each stratum is therefore essential for all studies aiming to assess soil C stocks. In comparative studies of soil C, this is usually done by establishing as many plots as economically feasible to increase inference space, while simultaneously collecting as few measurements as possible within each of the plots. However, when the within-plot variability is large, collecting only a few samples within each plot reduces the accuracy of the mean estimate. The low accuracy of the mean estimate will in turn contribute to a poor estimation of the variance between plots (Shaw et al., 2008). Thus, in areas where

the within-plot variability is large, gains in the overall precision of the estimated mean for each stratum can be achieved by improving the plot mean estimates.

From our results it is clear that clustering subplots within plots did not add as much information as adding new plots or collecting more samples within each subplot. Similar conclusions were drawn by Bradford et al. (2009) in a study of five small landscapes (1 km^2) located in northern hardwood, northern mixed, and subalpine forest types across central and eastern United States. This implies that sampling large plots may be less effective than scattering smaller plots across the landscape. However, as we demonstrated in this study, the optimal allocation of sampling units also depends on the cost constraints included in the model (Fig. 3). Although we did not model different costs of plots and subplots explicitly, our model gives a general impression of how optimal sampling allocation may shift with the cost input. When conducting inventories of over larger areas, other considerations such as travel cost may therefore shift the optimal sampling allocation.

Although this study focuses on the scales of variability for inventory and monitoring purposes, information on variability across scales can also assist in identifying processes influencing the spatial heterogeneity of organic soil C. For example, if the majority of the nested effects are found at a sub-plot level, the processes that influence the accumulation of organic layer C may situated within a short distance from the sampling point. In this case, we might be able to reduce the number of sampling

161

plots across the forest, and instead intensify the sampling within smaller subplots. In the opposite case, if the majority of variance can be attributed to the plots, we are likely seeing the results of larger processes, such as topographical influences on the C accumulation.

For a full soil C inventory, the surveyor must consider the absolute estimate errors. Although the standard error of the organic layer mean may be large in relative terms, its absolute size must be contrasted to the absolute error of mineral soil C. The number of plots required to achieve a similar level of precision in a full soil C inventory may therefore be higher than for organic layer C stock alone. As pointed out by Bradford et al. 2009, estimating sample size from standard error will fail to account for the absolute variability, resulting in large uncertainty of the estimates. As we illustrated in this study, the surveyor must therefore contrast the overall gains in precision by reducing the uncertainty of the organic layer C estimate from ± 0.5 Mg C ha^{-1} to ± 0.25 Mg C ha^{-1} at three times the cost, or whether cost-efficiency may be higher by intensifying mineral soil C sampling.

5.4.3. *Variability within plots*

The majority of the variance in our mean estimate was confined in areas less than 100 m^2. This suggests that when designing plot sizes for regional or even national inventories, the optimal plot size for organic layer C inventories, should not exceed our subplot area (100 m^2). Similarly, care must be taken to ensure that the sample spacing

162

within each plot exceeds the autocorrelation distance, which in our plots range from ~1 to 3 m (Kristensen et al. – *in review*, Chapter 3). Comparable autocorrelation distances have been reported from other boreal forest stands (Häkkinen et al., 2011; Liski, 1995; Muukkonen et al., 2009).

The importance of within plot variability for the overall estimate observed here are comparable to data from Homann et al. (2001) who found that the variability in organic layer C within plots (625 m^2) accounted for over half of the variance observed across a Pacific Northwest forest stand in the United States. In a study from Northumberland, United Kingdom, Conen et al. (2004) found that 54% of the variance found within an area of 5.78 km^2 was located within 300 m^2 plots. The importance of short-range variability have also been reported at even greater scales. In a study from Georgia, United States, Palmer et al. (2002) found that 21% of the total variance in forest floor C occurred at distances <1 m, while another 38% over 0.01 km^2 plots, and the remaining 41% over an area of more than 10,000 km^2. From these results it is clear that the short-range variability of organic layer C may contribute significantly to the overall uncertainty in estimates over larger areas, and care must therefore be taken to ensure that enough samples are collected within each plot.

To lower the effects of short-range variability and reduce the efforts required to detect changes in the organic layer C stock, the surveyor may choose to compositing a number of soil samples (Brus and Noij, 2008). By mixing samples from a subplot within

163

the area of interest, the composite sample is then assumed to be representative for the area of choice. Since only the composite sample is analyzed, one can expect lower measurement costs. Although compositing samples generally reduces the overall efforts required, additional uncertainty may rise from imperfect mixing of the aliquots and in the later laboratory analysis of the mixture. Bulking procedures reduce the number of samples required for later analysis, but substantial time must be allocated to drilling multiple cores. Thus, the balance of laboratory costs to field sampling costs shifts as the surveyor collects composite samples instead of single cores (Singh et al., 2013). While we cannot generalize from the one particular dataset presented here on organic layer C stocks, it is notable that that the short-range variability accounts for the majority of the observed variance across the forest. Using compositing samples on subplots may therefore substantially reduce the overall sampling costs. However, compositing samples are not recommended for monitoring individual entities, because the data does not contain any information on the within-plot variability. Lacking spatial information coupled with a low rate of change compared to the C stock at any given time (Liski et al., 2006; Pregitzer and Euskirchen, 2004) may prohibit detection of changes between baseline sampling and revisit. Nonetheless, it is clear that there are potential advantages by using an aggregate support when the objective is to sample to characterize estimate C stocks on a large scale, such as regional or even national soil C protocols, (Lark, 2012).

For example, Mäkipää et al. (2008) concluded that using composite samples can reduce the national soil C inventory program in Finland by one-third.

5.4.4. *Double sampling procedure*

As an alternative to composite sampling, we presented in this study a double sampling approach. A benefit of the double sampling procedure, in contrast to composite sampling, is that the double sampling method does not compromise the ability to detect changes at plot levels. A double sampling procedure which incorporates organic layer thickness measurements may be utilized to either reduce cost or minimize the estimate variance for a fixed cost. The procedure demonstrated a high applicability for estimating organic layer C stock in this forest for two reasons: (1) the measurement data of organic layer C stock and layer thickness have a linear relationship (Fig. 4a), and (2) the measurement data obtained for layer thickness is substantially less expensive than collecting and analyzing soil samples.

In many forestry applications, the optimal allocation between collecting measurements of the principal variable of interest and gathering data on an auxiliary variable is commonly estimated by regression or ratio estimators. These methods assume that the population means or total of the auxiliary variable are known. This may be the case in estimates of for example mean tree height, where height is only measured on a sample set, and the supplementary variable dbh measured on each tree within a given plot. For organic layer C stock this will unlikely be the case. In practice, the true

coefficient of determination between organic layer C stock and layer thickness is not known beforehand, and must therefore be estimated from a preliminary sampling (Cochran, 1977; Särndal et al., 2003). When sampling to determine the correlation, we recommend that a minimum of 20 samples are collected (Fig 4.). However, we hypothesize that the strong correlation demonstrated in this study represents a common pattern in boreal forests. For example, in a study across Swedish podzols, Olsson et al. (2009) found strong correlations between organic layer C stock and layer thickness in dry, fresh and slightly moist sites. Liski (1995) reported similar findings from boreal forest plots in Finland. Comparable patterns have also been documented outside of Fennoscandia, for example by Hunt et al. (2009) in a study conducted in managed conifer stands in Northern Ontario, Canada.

If the assumption of a strong correlation between these variables can be generalized, the optimal allocation primarily hinges on the costs differences between collecting soil cores and registering thickness measurements. From Fig. 5 it can be seen that the correlation between the principal variate of interest and auxiliary variable have pronounced effects on the allocation ratio, and the potential benefits of a double sampling procedure declines with both lower correlation and smaller cost ratios. Cost will likely vary between countries, regions and methods used for sample collection and analysis. Although few studies have reported explicitly on the cost of sampling organic layer samples, the different cost ratios used in this study should cover a range of realistic

166

sample costs. In a study from Finland, Mäkipää et al. (2008) estimated the cost of one organic layer C sample at ~ €30, while Mooney (2003) and Smith (2002) reports costs of $25 to $40 per sample (adjusted to 2015 value, not including cost of laboratory analysis). The analytical expenditures may be a significant contributor to the per sample costs. For example, Mäkipää et al. (2008) reported that ~44% of the labor costs (time) per sample were spent during the analysis phase.

Nevertheless, if our results of an 80 to 82% reduction in sampling costs can be generalized, the potential cost of estimating the soil organic layer C stock could be substantially reduced. Mäkipää et al. (2008) reported that the estimated cost of a full national inventory of organic layer C stock in Finland (3000 plots with 20 samples in each) was €1,770,000 (fixed costs excluded). According to our data, these costs could be reduced by a factor of 5 without any loss in estimate precision. Given the interest in soil C, these results represents considerable improvements in the feasibility of large scale soil inventories and monitoring efforts. For soils where such associations are strong, the cost-reductions of a double sampling by soil horizon questions the efficiency in the recommended guidelines of IPCC of sampling to a fixed depth of 30 cm (IPCC, 2006). Although the correlation reported here may vary, the potential savings of incorporating a double sampling procedure is encouraging. More work is required to develop a flexible, generic framework for utilizing a double sampling procedure to efficiently map organic layer C stocks at different scales. In countries where a monitoring network is already

established, the double-sampling procedure may still be incorporated in the resampling procedure, by using data from the inventory to determine the association. Further cost improvements may be also possible, as double sampling can be extended to include more than one auxiliary variable (Van Laar and Akça, 2007). In such cases the surveyor must take care to select auxiliary variables which have minimum correlation to avoid multi-collinearity.

5.4. Conclusion

Because field data is time consuming and costly to obtain, this study provides a case study for optimizing sampling protocols in boreal organic layer C inventories. Approximately 70% of the estimated variance across the forest was confined within just 100 m^2, which highlights the importance of considering the short-range variability when conducting a large scale inventory. This article demonstrates how optimal distribution of sampling units (plot, subplot and sample) is not only a function of the variance component within that dimension, but also changes with the sampling unit costs. We find that the costs of conducting an organic layer C inventory can be reduced by more than 60% by increasing the inventory uncertainty from $\pm$ 0.25 Mg C ha^{-1} to $\pm$ 0.5 Mg C ha^{-1}. Finally, we show that the sampling costs can be reduced with ~80%, by conducting a double sampling procedure that utilizes the strong correlation and cost difference between organic layer C stock and layer thickness.

The specific results in this study are concerned with the organic layer C stock situated under multilayered boreal forests cover. To form robust conclusions for sampling strategies across a landscape or at a national scale it would be necessary to conduct similar studies across a number of additional sites and regions, and to include a wider range of soil types and other ecological variables. This paper sets out the methods and shows the considerations by which such studies should be conducted. It is encouraging that the sampling effort required for establishing precise estimates or organic layer C across a large forested area appears feasible.

Chapter 6: Conclusion

The primary goal of this dissertation was to assess the distribution and spatial heterogeneity of organic C in a boreal forest ecosystem using high density field sampling and airborne remote sensing. In so doing, it also sought to examine how this variability influences sampling strategies aiming to map and monitor the C across forests. Our main findings are: (1) Lidar can provide relevant information on C stocks in trees, field layer vegetation and the soil organic layer, (2) Organic layer C are autocorrelated at distances <3 m, (3) To effectively monitor organic layer C, paired samples must be located within 30 cm of the baseline sample, and (4) inexpensive measurements of organic layer thickness can lower the number soil samples collected, and thus substantially reduce the overall costs of soil sampling.

The majority of measured C was found in the trees, about a third in the soil organic layer, while a small portion was stored in the understory vegetation (comprised of field layer vegetation and mosses). By not measuring the C stock in mineral soils, a substantial portion of the full C stock was left out of the inventory. Using data related to stand structure, lidar proved to accurately estimate the C stocks in trees (above and belowground) and the field layer. We also found a consistent relationship between topographical data derived from lidar ground echoes and organic layer C stock at a plot scale. Though, while efforts to associate individual organic layer C measurements with 1 m^2 topographic lidar data did not yield any significant relationships. Together these

findings suggest that remote sensing data may contain information useful for forest C storage over large areas, and may assist surveyors in stratifying sampling efficiently across a landscape or region.

We observed great variability in the organic layer C stock both within individual plots and across the forest as a whole. Our results indicate that ~70% of the organic layer C stock variability was confined within only small blocks of the investigated forest, with spatial autocorrelation distances <3 m. The short-range variability has profound effects on sampling requirements necessary to detect a change, where substantially larger samples sizes must be specified to compensate for the additional uncertainty resulting from small shifts (<30 cm) in sample location. We found that 20 to 25 random samples are needed to establish the plot mean of organic layer C within ± 0.5 kg C m^{-2}. In contrast, the number of samples required to detect a change of similar magnitude, depends on the accumulation rate, whether the accumulation is spatially correlated to existing patterns, the spatial sampling precision, and the variability present at time of baseline sampling.

This dissertation also provides a case study for optimizing the cost-efficiency of sampling protocols in boreal organic layer C inventories, showing how desired level of accuracy and unit costs affects sample requirements and distribution. Finally, we show how conducting a double sampling procedure, combining organic layer samples with inexpensive and correlated measurements of organic layer can reduce costs of sampling by 80%.

171

References

Ahern, F.J., Belward A., Churchill, P., Davis, R., Janetos, A., Justice, C., Loveland, T., Malingreau, J.-P., Maiden, M., Skole, D., Taylor, V., Yausuoka, Y., Zhu, Z., 1998. A strategy for global observation of forest cover, Canada Centre for Remote Sensing, Ottawa, Ontario, Canada.

Ahokas, E., Kaartinen, H., Hyyppä, J., 2003. A quality assessment of airborne laser scanner data, ISPRS WG III/3 Workshop '3-D reconstruction from airborne laser scanner and InSAR data, Dresden, Germany.

Akselsson, C., Berg, B., Meentemeyer, V., Westling, O., 2005. Carbon sequestration rates in organic layers of boreal and temperate forest soils — Sweden as a case study. Global Ecology and Biogeography 14(1), 77-84.

Alaback, P.B., 1982. Dynamics of understory biomass in Sitka Spruce-Western Hemlock forests of southeast Alaska. Ecology 63(6), 1932-1948.

Alexander, C., Moeslund, J.E., Bøcher, P.K., Arge, L., Svenning, J.-C., 2013. Airborne laser scanner (LiDAR) proxies for understory light conditions. Remote Sensing of Environment 134(0), 152-161.

Allen, D.E., A Pringle, M.J., Page, K.L., Dalal, R.C. , 2010. A review of sampling designs for the measurement of soil organic carbon in Australian grazing lands. The Rangeland Journal 32(2), 227-246.

Atkinson, P.M., Webster, R., Curran, P.J., 1992. Cokriging with ground-based radiometry. Remote Sensing of Environment 41(1), 45-60.

Barbier, S., Gosselin, F., Balandier, P., 2008. Influence of tree species on understory vegetation diversity and mechanisms involved—A critical review for temperate and boreal forests. Forest Ecology and Management 254(1), 1-15.

Baritz, R., Seufert, G., Montanarella, L., Van Ranst, E., 2010. Carbon concentrations and stocks in forest soils of Europe. Forest Ecology and Management 260(3), 262-277.

Beets, P.N., Brandon, A., Fraser, B.V., Goulding, C.J., Lane, P.M., Stephens, P.R., 2010. New Zealand. In: E. Tomppo, T. Gschwantner, M. Lawrence, R.E. McRoberts (Eds.), National forest inventories - Pathways for common reporting. Springer, pp. 391-410.

Bens, O., Buczko, U., Sieber, S., Hüttl, R.F., 2006. Spatial variability of O layer thickness and humus forms under different pine beech-forest transformation stages in NE Germany. Journal of Plant Nutrition and Soil Science 169(1), 5-15.

Berg, B., 2000. Litter decomposition and organic matter turnover in northern forest soils. Forest Ecology and Management 133(1–2), 13-22.

Besag, J., 1977. Discussion of Dr Ripley's paper. Journal of the Royal Statistical Society Series B(39), 193-195.

Beven, K.J., Kirkby, M.J., 1979. A physically based, variable contributing area model of basin hydrology. Hydrological Sciences Bulletin 24(1), 43-69.

Binkley, D., Fisher, R., 2012. Ecology and management of forest soils. John Wiley & Sons, New York.

Birdsey, R., 2004. Data gaps for monitoring forest carbon in the United States: An inventory perspective. Environmental Management 33(1), S1-S8.

Bitterlich, W., 1984. The relascope idea: relative measurements in forestry. Commonwealth Agricultural Bureaux.

Bjune, A.E., Ohlson, M., Birks, H.J.B., Bradshaw, R.H.W., 2009. The development and local stand-scale dynamics of a Picea abies forest in southeastern Norway. The Holocene 19(7), 1073-1082.

Block, R., Van Rees, K., Pennock, D., 2002. Quantifying harvesting impacts using soil compaction and disturbance regimes at a landscape scale. Soil Science Society of America Journal 66(5), 1669-1676.

Bollandsås, O.M., Hanssen, K.H., Marthiniussen, S., Næsset, E., 2008. Measures of spatial forest structure derived from airborne laser data are associated with natural regeneration patterns in an uneven-aged spruce forest. Forest Ecology and Management 255(3), 953-961.

Bonan, G.B., 2008. Forests and climate change: Forcings, feedbacks, and the climate benefits of forests. Science 320(5882), 1444-1449.

Bradford, J., Weishampel, P., Smith, M.-L., Kolka, R., Birdsey, R.A., Ollinger, S.V., Ryan, M.G., 2009. Detrital carbon pools in temperate forests: magnitude and potential for landscape-scale assessment. Canadian Journal of Forest Research 39(4), 802-813.

Bradshaw, C.J.A., Warkentin, I.G., Sodhi, N.S., 2009. Urgent preservation of boreal carbon stocks and biodiversity. Trends in Ecology & Evolution 24(10), 541-548.

Brus, D., Te Riele, W., 2001. Design-based regression estimators for spatial means of soil properties: the use of two-phase sampling when the means of the auxiliary variables are unknown. Geoderma 104(3), 257-279.

Brus, D.J., Noij, I.G.A.M., 2008. Designing sampling schemes for effect monitoring of nutrient leaching from agricultural soils. European Journal of Soil Science 59(2), 292-303.

Cajander, A.K., 1926. The theory of forest types. Printing office of Society for the Finnish litterature.

Cajander, A.K., 1949. Forest types and their significance. Suomen metsätieteellinen seura.

Callesen, I., Liski, J., Raulund-Rasmussen, K., Olsson, M.T., Tau-Strand, L., Vesterdal, L., Westman, C.J., 2003. Soil carbon stores in Nordic well-drained forest soils—relationships with climate and texture class. Global Change Biology 9(3), 358-370.

Cambardella, C.A., Moorman, T.B., Novak, J.M., Parkin, T.B., Turco, R.F., Konopka, A.E., 1994. Field scale variability of soil properties in central Iowa soils. Soil Science Society of America Journal 58, 1501-1511.

Chang, Y.-C., Yeh, H.-D., 2007. Optimum allocation for soil contamination investigations in Hsinchu, Taiwan, by double sampling. Soil Science Society of America Journal 71(5), 1585-1592.

Chapin, F.S.I., Chapin, C., Matson, P.A., Vitousek, P., 2011. Principles of terrestrial ecosystem ecology. 2 ed. Springer Science & Business Media.

Chapin, F.S.I., McGuire, A., Randerson, J., Pielke, R., Baldocchi, D., Hobbie, S., Roulet, N., Eugster, W., Kasischke, E., Rastetter, E., 2000. Arctic and boreal ecosystems of western North America as components of the climate system. Global Change Biology 6(S1), 211-223.

Chatterjee, A., Lal, R., Wielopolski, L., Martin, M.Z., Ebinger, M.H., 2009. Evaluation of different soil carbon determination methods. Critical Reviews in Plant Sciences 28(3), 164-178.

Cliff, A.D., Ord, J.K., 1981. Spatial processes: Models & applications. Pion, London.

Cochran, W.G., 1977. Sampling techniques. 3 ed. John Wiley & Sons, New York.

Conant, R., Paustian, K., 2002. Spatial variability of soil organic carbon in grasslands: implications for detecting change at different scales. Environmental Pollution 116, S127-S135.

Conen, F., Yakutin, M.V., Sambuu, A.D., 2003. Potential for detecting changes in soil organic carbon concentrations resulting from climate change. Global Change Biology 9(11), 1515-1520.

175

Cressie, N., 1985. Fitting variogram models by weighted least squares. Mathematical Geology 17(5), 563-586.

Cressie, N., 1993. Statistics for spatial data: Wiley series in probability and statistics. John Wiley & Sons, New York.

Dale, M.R., 1999. Spatial pattern analysis in plant ecology. Cambridge, United Kingdom.

de Gruijter, J.J., 2006. Sampling for natural resource monitoring. Springer.

de Wit, H.A., Palosuo, T., Hylen, G., Liski, J., 2006. A carbon budget of forest biomass and soils in southeast Norway calculated using a widely applicable method. Forest Ecology and Management 225(1–3), 15-26.

Don, A., Schumacher, J., Scherer-Lorenzen, M., Scholten, T., Schulze, E.-D., 2007. Spatial and vertical variation of soil carbon at two grassland sites — Implications for measuring soil carbon stocks. Geoderma 141(3–4), 272-282.

Dunn, O.J., 1964. Multiple comparisons using rank sums. Technometrics 6(3), 241-252.

FAO, 2006. Global forest assessment 2005, Food and Agriculture Organization of the United Nations, Rome.

Finer, L., Mannerkoski, H., Piirainen, S., Starr, M., 2003. Carbon and nitrogen pools in an old-growth, Norway spruce mixed forest in eastern Finland and changes associated with clear-cutting. Forest Ecology and Management 174(1), 51-63.

Games, P.A., Howell, J.F., 1976. Pairwise multiple comparison procedures with unequal N's and/or variances: A Monte Carlo study. Journal of Educational and Behavioral Statistics 1(2), 113-125.

Gangodagamage, C., Rowland, J.C., Hubbard, S.S., Brumby, S.P., Liljedahl, A.K., Wainwright, H., Wilson, C.J., Altmann, G.L., Dafflon, B., Peterson, J., Ulrich, C., Tweedie, C.E., Wullschleger, S.D., 2014. Extrapolating active layer thickness measurements across Arctic polygonal terrain using LiDAR and NDVI data sets. Water Resources Research 50(8), 6339-6357.

Gaudinski, J., Trumbore, S., Davidson, E., Zheng, S., 2000. Soil carbon cycling in a temperate forest: radiocarbon-based estimates of residence times, sequestration rates and partitioning of fluxes. Biogeochemistry 51, 33-69.

Gaulton, R., Malthus, T.J., 2010. LiDAR mapping of canopy gaps in continuous cover forests: a comparison of canopy height model and point cloud based techniques. International Journal of Remote Sensing 31(5), 1193-1211.

Gessler, P.E., Moore, I., McKenzie, N., Ryan, P., 1995. Soil-landscape modelling and spatial prediction of soil attributes. International Journal of Geographical Information Systems 9(4), 421-432.

Goidts, E., Van Wesemael, B., Crucifix, M., 2009. Magnitude and sources of uncertainties in soil organic carbon (SOC) stock assessments at various scales. European Journal of Soil Science 60(5), 723-739.

Goovaerts, P., 1998. Geostatistical tools for characterizing the spatial variability of microbiological and physico-chemical soil properties. Biol Fertil Soils 27(4), 315-334.

Goovaerts, P., 1999. Geostatistics in soil science: State-of-the-art and perspectives. Geoderma 89(1-2), 1-45.

Goreaud, F., Pélissier, R., 1999. On explicit formulas of edge effect correction for Ripley's K-function. Journal of Vegetation Science 10(3), 433-438.

Grubbs, F.E., 1969. Procedures for detecting outlying observations in samples. Technometrics 11(1), 1-21.

Grömping, U., 2006. Relative importance for linear regression in R: the package relaimpo. Journal of statistical software 17(1), 1-27.

Guisan, A., Weiss, S.B., Weiss, A.D., 1999. GLM versus CCA spatial modeling of plant species distribution. Plant Ecology 143(1), 107-122.

177

Hansson, K., Olsson, B.A., Olsson, M., Johansson, U., Kleja, D.B., 2011. Differences in soil properties in adjacent stands of Scots pine, Norway spruce and silver birch in SW Sweden. Forest Ecology and Management 262(3), 522-530.

Havas, P., Kubin, E., 1983. Structure, growth and organic matter content in the vegetation cover of an old spruce forest in northern Finland. Annales Botanici Fennici 20, 115-149.

Hedde, M., Aubert, M., Decaëns, T., Bureau, F., 2008. Dynamics of soil carbon in a beechwood chronosequence forest. Forest Ecology and Management 255(1), 193-202.

Heim, A., Wehrli, L., Eugster, W., Schmidt, M.W.I., 2009. Effects of sampling design on the probability to detect soil carbon stock changes at the Swiss CarboEurope site Lägeren. Geoderma 149(3–4), 347-354.

Helmisaari, H.-S., Hallbäcken, L., 1999. Fine-root biomass and necromass in limed and fertilized Norway spruce (Picea abies (L.) Karst.) stands. Forest Ecology and Management 119(1–3), 99-110.

Hill, R.A., Broughton, R.K., 2009. Mapping the understorey of deciduous woodland from leaf-on and leaf-off airborne LiDAR data: A case study in lowland Britain. ISPRS Journal of Photogrammetry and Remote Sensing 64(2), 223-233.

Hill, R.A., Thomson, A.G., 2005. Mapping woodland species composition and structure using airborne spectral and LiDAR data. International Journal of Remote Sensing 26(17), 3763-3779.

Hilli, S., Stark, S., Derome, J., 2008. Carbon quality and stocks in organic horizons in boreal forest soils. Ecosystems 11(2), 270-282.

Hilli, S., Stark, S., Derome, J., 2010. Litter decomposition rates in relation to litter stocks in boreal coniferous forests along climatic and soil fertility gradients. Applied Soil Ecology 46(2), 200-208.

Hoffmann, U., Hoffmann, T., Jurasinski, G., Glatzel, S., Kuhn, N., 2014. Assessing the spatial variability of soil organic carbon stocks in an alpine setting (Grindelwald, Swiss Alps). Geoderma 232, 270-283.

Hogberg, P., Nordgren, A., Buchmann, N., Taylor, A.F.S., Ekblad, A., Hogberg, M.N., Nyberg, G., Ottosson-Lofvenius, M., Read, D.J., 2001. Large-scale forest girdling shows that current photosynthesis drives soil respiration. Nature 411(6839), 789-792.

Hogberg, P., Read, D.J., 2006. Towards a more plant physiological perspective on soil ecology. Trends in Ecology & Evolution 21(10), 548-554.

Holm, S., 1979. A simple sequentially rejective multiple test procedure. Scandinavian Journal of Statistics 6(2), 65-70.

Holmgren, J., 2004. Prediction of tree height, basal area and stem volume in forest stands using airborne laser scanning. Scandinavian Journal of Forest Research 19(6), 543-553.

Holmgren, J., Nilsson, M., Olsson, H., 2003. Estimation of tree height and stem volume on plots using airborne laser scanning. Forest Science 49(3), 419-428.

Holmgren, J., Persson, Å., 2004. Identifying species of individual trees using airborne laser scanner. Remote Sensing of Environment 90(4), 415-423.

Holmgren, J., Persson, Å., Södermand, U., 2008. Species identification of individual trees by combining high resolution LiDAR data with multi-spectral images. Int. J. Remote Sens. 29(5), 1537-1552.

Homann, P.S., Bormann, B.T., Boyle, J.R., 2001. Detecting treatment differences in soil carbon and nitrogen resulting from forest manipulations. Soil Sci. Soc. Am. J. 65(2), 463-469.

Hudak, A.T., Strand, E.K., Vierling, L.A., Byrne, J.C., Eitel, J.U., Martinuzzi, S., Falkowski, M.J., 2012. Quantifying aboveground forest carbon pools and fluxes from repeat LiDAR surveys. Remote Sensing of Environment 123, 25-40.

Hunt, S.L., Gordon, A.M., Morris, D.M., 2010. Carbon stocks in managed conifer forests in northern Ontario, Canada. Silva Fennica 44(4), 563-582.

Huntington, T.G., Johnson, C.E., Johnson, A.H., Siccama, T.G., Ryan, D.F., 1989. Carbon, organic matter, and bulk density relationships in a forested Spodosol. Soil Science 148(5), 380-386.

Husch, B., Beers, T.W., Kershaw, J.A., 2002. Forest mensuration. John Wiley & Sons.

Hyyppä, H., Yu, X., Hyyppä, J., Kaartinen, H., Kaasalainen, S., Honkavaara, E., Rönnholm, P., 2005. Factors affecting the quality of DTM generation in forested areas. International Archives of Photogrammetry, Remote Sensing and Spatial Information Sciences 36(3/W19), 85-90.

Hyyppä, J., Hyyppä, H., Leckie, D., Gougeon, F., Yu, X., Maltamo, M., 2008. Review of methods of small-footprint airborne laser scanning for extracting forest inventory data in boreal forests. Int. J. Remote Sens. 29(5), 1339-1366.

Häkkinen, M., Heikkinen, J., Mäkipää, R., 2011. Soil carbon stock increases in the organic layer of boreal middle-aged stands. Biogeosciences Discussions 8(1), 1015-1042.

Högberg, P., Ekblad, A., 1996. Substrate-induced respiration measured in situ in a C3-plant ecosystem using additions of C4-sucrose. Soil Biology and Biochemistry 28(9), 1131-1138.

IPCC, 2006. Agriculture, forestry and other land uses (AFOLU): 2006 IPCC guidelines for national greenhouse gas inventories, Institute for Global Environmental Strategies, Hayama, Japan.

Jandl, R., Rodeghiero, M., Martinez, C., Cotrufo, M.F., Bampa, F., van Wesemael, B., Harrison, R.B., Guerrini, I.A., Richter Jr, D.d., Rustad, L., Lorenz, K., Chabbi, A., Miglietta, F., 2014. Current status, uncertainty and future needs in soil organic carbon monitoring. Science of The Total Environment 468–469, 376-383.

Janzen, H.H., 2005. Soil carbon: a measure of ecosystem response in a changing world? Canadian Journal of Soil Science 85(4), 467-480.

Jungqvist, G., Oni, S.K., Teutschbein, C., Futter, M.N., 2014. Effect of climate change on soil temperature in Swedish boreal forests. PLoS ONE 9(4), e93957.

Kankare, V., Vastaranta, M., Holopainen, M., Räty, M., Yu, X., Hyyppä, J., Hyyppä, H., Alho, P., Viitala, R., 2013. Retrieval of forest aboveground biomass and stem volume with airborne scanning LiDAR. Remote Sensing 5(5), 2257-2274.

Kielland-Lund, J., 1981. Die Waldgesellschaften SO-Norwegens. Phytocoenologia, 53-250.

Kolari, P., Pumpanen, J., Rannik, Ü., Ilvesniemi, H., Hari, P., Berninger, F., 2004. Carbon balance of different aged Scots pine forests in Southern Finland. Global Change Biology 10(7), 1106-1119.

Kolka, R., Steber, A., Brooks, K., Perry, C.H., Powers, M., 2012. Relationships between Soil Compaction and Harvest Season, Soil Texture, and Landscape Position for Aspen Forests. Northern Journal of Applied Forestry 29(1), 21-25.

Korhonen, L., Korpela, I., Heiskanen, J., Maltamo, M., 2011. Airborne discrete-return LIDAR data in the estimation of vertical canopy cover, angular canopy closure and leaf area index. Remote Sensing of Environment 115(4), 1065-1080.

Korpela, I.S., 2008. Mapping of understory lichens with airborne discrete-return LiDAR data. Remote Sensing of Environment 112(10), 3891-3897.

Korsmo, H., 1995. Weight equations for determining biomass fractions of young hardwoods from natural regenerated stands. Scandinavian Journal of Forest Research 10(1-4), 333-346.

Koven, C.D., 2013. Boreal carbon loss due to poleward shift in low-carbon ecosystems. Nature Geosci 6(6), 452-456.

Kozlowski, T.T., Pallardy, S.G., 1997. Physiology of woody plants. Academic Press.

Krankina, O.N., Harmon, M.E., Griazkin, A.V., 1999. Nutrient stores and dynamics of woody detritus in a boreal forest: modeling potential implications at the stand level. Canadian Journal of Forest Research 29(1), 20-32.

Kristensen, T., Næsset, E., Ohlson, M., Bolstad, P.V., Kolka, R., 2015a. Mapping above- and below-ground carbon pools in boreal forests: The case for airborne lidar (*in review*).

Kristensen, T., Ohlson, M., Bolstad, P.V., Nagy, Z., 2015b. Spatial variability of organic layer thickness and carbon stocks in mature boreal forests stands – Implications and suggestions for sampling designs (*in review*).

Kulmatiski, A., Beard, K.H., 2004. Reducing sampler error in soil research. Soil Biology and Biochemistry 36(2), 383-385.

Kunkel, M.L., Flores, A.N., Smith, T.J., McNamara, J.P., Benner, S.G., 2011. A simplified approach for estimating soil carbon and nitrogen stocks in semi-arid complex terrain. Geoderma 165(1), 1-11.

Kurz, W.A., Stinson, G., Rampley, G., 2008. Could increased boreal forest ecosystem productivity offset carbon losses from increased disturbances? Philosophical Transactions of the Royal Society B: Biological Sciences 363(1501), 2259-2268.

Laiho, R., Prescott, C.E., 2004. Decay and nutrient dynamics of coarse woody debris in northern coniferous forests: a synthesis. Canadian Journal of Forest Research 34(4), 763-777.

Lark, R.M., 2009. Estimating the regional mean status and change of soil properties: two distinct objectives for soil survey. European Journal of Soil Science 60(5), 748-756.

Lark, R.M., 2012. Some considerations on aggregate sample supports for soil inventory and monitoring. European Journal of Soil Science 63(1), 86-95.

Lefsky, M.A., Cohen, W.B., Acker, S.A., Parker, G.G., Spies, T.A., Harding, D., 1999. Lidar remote sensing of the canopy structure and biophysical properties of

Douglas-fir western hemlock forests. Remote Sensing of Environment 70(3), 339-361.

Lefsky, M.A., Hudak, A.T., Cohen, W.B., Acker, S., 2005. Geographic variability in lidar predictions of forest stand structure in the Pacific Northwest. Remote Sensing of Environment 95(4), 532-548.

Legendre, P., Fortin, M.J., 1989. Spatial pattern and ecological analysis. Vegetatio 80(2), 107-138.

Lie, M.H., Arup, U., Grytnes, J.-A., Ohlson, M., 2009. The importance of host tree age, size and growth rate as determinants of epiphytic lichen diversity in boreal spruce forests. Biodivers Conserv 18(13), 3579-3596.

Lie, M.H., Josefsson, T., Storaunet, K.O., Ohlson, M., 2012. A refined view on the "Green lie": Forest structure and composition succeeding early twentieth century selective logging in SE Norway. Scandinavian Journal of Forest Research 27(3), 270-284.

Lin, H., Wheeler, D., Bell, J., Wilding, L., 2005. Assessment of soil spatial variability at multiple scales. Ecological Modelling 182(3–4), 271-290.

Lindholm, T., Vasander, H., 1987. Vegetation and stand development of mesic forest after prescribed burning. Silva Fennica 21(3), 259-278.

Lindner, M., Karjalainen, T., 2007. Carbon inventory methods and carbon mitigation potentials of forests in Europe: a short review of recent progress. European Journal of Forest Research 126(2), 149-156.

Liski, J., 1995. Variation in soil organic carbon and thickness of soil horizons within a boreal forest stand - effect of trees and implications for sampling. Silva Fennica 29(4), 255-266.

Liski, J., Lehtonen, A., Palosuo, T., Peltoniemi, M., Eggers, T., Muukkonen, P., Mäkipää, R., 2006. Carbon accumulation in Finland's forests 1922–2004 – an estimate

obtained by combination of forest inventory data with modelling of biomass, litter and soil. Ann. For. Sci. 63(7), 687-697.

Liski, J., Perruchoud, D., Karjalainen, T., 2002. Increasing carbon stocks in the forest soils of western Europe. Forest Ecology and Management 169(1–2), 159-175.

Liski, J., Westman, C.J., 1995. Density of organic carbon in soil at coniferous forest sites in southern Finland. Biogeochemistry 29(3), 183-197.

Liu, C., Westman, C.J., 2009. Biomass in a Norway spruce-Scots pine forest: a comparison of estimation methods. Boreal Environment Research 15(5), 875-888.

Lundström, U.S., van Breemen, N., Bain, D., 2000. The podzolization process. A review. Geoderma 94(2–4), 91-107.

Lutz, J.A., Larson, A.J., Swanson, M.E., Freund, J.A., 2012. Ecological importance of large-diameter trees in a temperate mixed-conifer forest. PLoS One 7(5), e36131.

Luyssaert, S., Inglima, I., Jung, M., Richardson, A., Reichstein, M., Papale, D., Piao, S., Schulze, E.D., Wingate, L., Matteucci, G., 2007. CO_2 balance of boreal, temperate, and tropical forests derived from a global database. Global change biology 13(12), 2509-2537.

Luyssaert, S., Schulze, E.D., Borner, A., Knohl, A., Hessenmoller, D., Law, B.E., Ciais, P., Grace, J., 2008. Old-growth forests as global carbon sinks. Nature 455(7210), 213-215.

Magnussen, S., Eggermont, P., LaRiccia, V.N., 1999. Recovering tree heights from airborne laser scanner data. Forest Science 45(3), 407-422.

Makkonen, K., Helmisaari, H.S., 2001. Fine root biomass and production in Scots pine stands in relation to stand age. Tree physiology 21(2-3), 193-198.

Malhi, Y., Baldocchi, D.D., Jarvis, P.G., 1999. The carbon balance of tropical, temperate and boreal forests. Plant, Cell & Environment 22(6), 715-740.

Maltamo, M., Peuhkurinen, J., Malinen, J., Vauhkonen, J., Packalén, P., Tokola, T., 2009. Predicting tree attributes and quality characteristics of Scots pine using airborne laser scanning data, 43.

Marchant, B.P., Lark, R.M., 2006. Adaptive sampling and reconnaissance surveys for geostatistical mapping of the soil. European Journal of Soil Science 57(6), 831-845.

Marklund, L.G., 1988. Biomassafunktioner för tall, gran och björk i Sverige: biomass functions for pine, spruce and birch in Sweden. Sveriges lantbruksuniversitet, Institutionen för skogstaxering.

Martinuzzi, S., Vierling, L.A., Gould, W.A., Falkowski, M.J., Evans, J.S., Hudak, A.T., Vierling, K.T., 2009. Mapping snags and understory shrubs for a LiDAR-based assessment of wildlife habitat suitability. Remote Sensing of Environment 113(12), 2533-2546.

Marty, C., Houle, D., Gagnon, C., 2015. Variation in stocks and distribution of organic C in soils across 21 eastern Canadian temperate and boreal forests. Forest Ecology and Management 345(0), 29-38.

McBratney, A.B., Mendonça Santos, M.d.L., Minasny, B., 2003. On digital soil mapping. Geoderma 117(1), 3-52.

McBratney, A.B., Webster, R., 1983. Optimal interpolation and isarithmic mapping of soil properties. Journal of Soil Science 34(1), 137-162.

McBratney, A.B., Webster, R., Burgess, T.M., 1981. The design of optimal sampling schemes for local estimation and mapping of of regionalized variables—I: Theory and method. Computers & Geosciences 7(4), 331-334.

McTiernan, K.B., Couteaux, M.M., Berg, B., Berg, M.P., Calvo de Anta, R., Gallardo, A., Kratz, W., Piussi, P., Remacle, J., Virzo De Santo, A., 2003. Changes in chemical composition of Pinus sylvestris needle litter during decomposition along

a European coniferous forest climatic transect. Soil Biology and Biochemistry 35(6), 801-812.

Messier, C., Parent, S., Bergeron, Y., 1998. Effects of overstory and understory vegetation on the understory light environment in mixed boreal forests. Journal of Vegetation Science 9(4), 511-520.

Miesch, A., 1975. Variograms and variance components in geochemistry and ore evaluation. Geological Society of America Memoirs 142, 333-340.

Moen, A., 1999. National Atlas of Norway: Vegetation. Norwegian Mapping Authority, Hønefoss.

Molinari, C., Bradshaw, R.H.W., Risbøl, O., Lie, M., Ohlson, M., 2005. Long-term vegetational history of a Picea abies stand in south-eastern Norway: Implications for the conservation of biological values. Biological Conservation 126(2), 155-165.

Mooney, S., Antle, J., Capalbo, S., Paustian, K., 2004. Influence of project scale and carbon variability on the costs of measuring soil carbon credits. Environmental Management 33(1), S252-S263.

Morvan, X., Saby, N.P.A., Arrouays, D., Le Bas, C., Jones, R.J.A., Verheijen, F.G.A., Bellamy, P.H., Stephens, M., Kibblewhite, M.G., 2008. Soil monitoring in Europe: A review of existing systems and requirements for harmonisation. Science of The Total Environment 391(1), 1-12.

Mueller, K., Eissenstat, D., Hobbie, S., Oleksyn, J., Jagodzinski, A., Reich, P., Chadwick, O., Chorover, J., 2012. Tree species effects on coupled cycles of carbon, nitrogen, and acidity in mineral soils at a common garden experiment. Biogeochemistry 111(1-3), 601-614.

Mueller, T., Pierce, F., 2003. Soil Carbon Maps: Enhancing spatial estimates with simple terrain attributes at multiple scales. Soil Science Society of America Journal 67(1), 258-267.

Muir, A., 1961. The podzol and podzolic soils. In: A.G. Norman (Ed.), Advances in Agronomy. Academic Press, pp. 1-56.

Mulder, V.L., de Bruin, S., Schaepman, M.E., Mayr, T.R., 2011. The use of remote sensing in soil and terrain mapping — A review. Geoderma 162(1–2), 1-19.

Muukkonen, P., Häkkinen, M., Mäkipää, R., 2009. Spatial variation in soil carbon in the organic layer of managed boreal forest soil—implications for sampling design. Environmental Monitoring and Assessment 158(1), 67-76.

Muukkonen, P., Mäkipää, R., 2006. Empirical biomass models of understorey vegetation in boreal forests according to stand and site attributes. Boreal Environment Research 11(5), 355-369.

Mäkipää, R., 1995. Effect of nitrogen input on carbon accumulation of boreal forest soils and ground vegetation. Forest Ecology and Management 79(3), 217-226.

Mäkipää, R., 1999. Response patterns of Vaccinium myrtillus and V. vitis-idaea along nutrient gradients in boreal forest. Journal of Vegetation Science 10(1), 17-26.

Mäkipää, R., Häkkinen, M., Muukkonen, P., Peltoniemi, M., 2008. The costs of monitoring changes in forest soil carbon stocks. Boreal Env. Res. 13(Suppl. B), 120-130.

Nabuurs, G.J., Masera, O., Andrasko, K., Benitez-Ponce, P., Boer, R., Dutschke, M., Elsiddig, E., Ford-Robertson, J., Frumhoff, P., T.Karjalainen, Krankina, O., Kurz, W.A., Matsumoto, M., Oyhantcabal, W., Ravindranath, N.H., Sanchez, M.J.S., Zhang, X., 2007. Forestry. In Climate Change 2007: Mitigation. Contribution of Working Group III to the Fourth Assessment Report of the Intergovernmental Panel on Climate Change [B. Metz, O.R. Davidson, P.R. Bosch, R. Dave, L.A. Meyer (eds)] (Cambridge University Press, Cambridge, United Kingdom and New York, NY, USA.), 541-584.

Neyman, J., 1938. Contribution to the theory of sampling human populations. Journal of the American Statistical Association 33(201), 101-116.

Nielsen, A., Totland, Ø., Ohlson, M., 2007. The effect of forest management operations on population performance of Vaccinium myrtillus on a landscape-scale. Basic and Applied Ecology 8(3), 231-241.

Nijland, W., Nielsen, S.E., Coops, N.C., Wulder, M.A., Stenhouse, G.B., 2014. Fine-spatial scale predictions of understory species using climate- and LiDAR-derived terrain and canopy metrics. APPRES 8(1), 083572-083572.

Nilsson, M.-C., Wardle, D.A., 2005. Understory vegetation as a forest ecosystem driver: evidence from the northern Swedish boreal forest. Frontiers in Ecology and the Environment 3(8), 421-428.

Nilsson, M., 1996. Estimation of tree heights and stand volume using an airborne lidar system. Remote Sensing of Environment 56(1), 1-7.

Næsset, E., 1997a. Determination of mean tree height of forest stands using airborne laser scanner data. ISPRS Journal of Photogrammetry and Remote Sensing 52(2), 49-56.

Næsset, E., 1997b. Estimating timber volume of forest stands using airborne laser scanner data. Remote Sensing of Environment 61(2), 246-253.

Næsset, E., 2002. Predicting forest stand characteristics with airborne scanning laser using a practical two-stage procedure and field data. Remote Sensing of Environment 80(1), 88-99.

Næsset, E., 2004. Effects of different flying altitudes on biophysical stand properties estimated from canopy height and density measured with a small-footprint airborne scanning laser. Remote Sensing of Environment 91(2), 243-255.

Næsset, E., 2007. Airborne laser scanning as a method in operational forest inventory: Status of accuracy assessments accomplished in Scandinavia. Scandinavian Journal of Forest Research 22(5), 433-442.

Næsset, E., Gobakken, T., 2005. Estimating forest growth using canopy metrics derived from airborne laser scanner data. Remote sensing of environment 96(3), 453-465.

Næsset, E., Gobakken, T., 2008. Estimation of above- and below-ground biomass across regions of the boreal forest zone using airborne laser. Remote Sensing of Environment 112(6), 3079-3090.

Næsset, E., Økland, T., 2002. Estimating tree height and tree crown properties using airborne scanning laser in a boreal nature reserve. Remote Sensing of Environment 79(1), 105-115.

Olsson, M.T., Erlandsson, M., Lundin, L., Nilsson, T., Nilsson, A., Stendahl, J., 2009. Organic carbon stocks in Swedish Podzol soils in relation to soil hydrology and other site characteristics. Silva Fennica 43(2), 209-222.

Ortiz, C.A., Liski, J., Gärdenäs, A.I., Lehtonen, A., Lundblad, M., Stendahl, J., Ågren, G.I., Karltun, E., 2013. Soil organic carbon stock changes in Swedish forest soils—A comparison of uncertainties and their sources through a national inventory and two simulation models. Ecological Modelling 251(0), 221-231.

Palmer, C., Smith, W., Conkling, B., 2002. Development of a protocol for monitoring status and trends in forest soil carbon at a national level. Environmental Pollution 116, S209-S219.

Palviainen, M., Finér, L., Kurka, A.M., Mannerkoski, H., Piirainen, S., Starr, M., 2004. Decomposition and nutrient release from logging residues after clear-cutting of mixed boreal forest. Plant and Soil 263(1), 53-67.

Pan, Y., Birdsey, R.A., Fang, J., Houghton, R., Kauppi, P.E., Kurz, W.A., Phillips, O.L., Shvidenko, A., Lewis, S.L., Canadell, J.G., Ciais, P., Jackson, R.B., Pacala, S.W., McGuire, A.D., Piao, S., Rautiainen, A., Sitch, S., Hayes, D., 2011. A large and persistent carbon sink in the world's forests. Science 333(6045), 988-993.

Pase, C.P., Hurd, R.M., 1958. Understory vegetation as related to basal area, crown cover and litter produced by immature ponderosa pine stands in the Black Hills. Proceedings of the Society of American Forester's meeting 1957.

Payandeh, B., 1981. Choosing regression models for biomass prediction equations. Forestry Chronicle 57.

Pearson, T.R., Brown, S.L., Birdsey, R.A., 2007. Measurement guidelines for the sequestration of forest carbon.

Peckham, S.D., Ahl, D.E., Gower, S.T., 2009. Bryophyte cover estimation in a boreal black spruce forest using airborne lidar and multispectral sensors. Remote Sensing of Environment 113(6), 1127-1132.

Pei, T., Qin, C.Z., Zhu, A.X., Yang, L., Luo, M., Li, B., Zhou, C., 2010. Mapping soil organic matter using the topographic wetness index: A comparative study based on different flow-direction algorithms and kriging methods. Ecological Indicators 10(3), 610-619.

Pelt, R.V., Franklin, J.F., 2000. Influence of canopy structure on the understory environment in tall, old-growth, conifer forests. Canadian Journal of Forest Research 30(8), 1231-1245.

Peltoniemi, M., Mäkipää, R., Liski, J., Tamminen, P., 2004. Changes in soil carbon with stand age – an evaluation of a modelling method with empirical data. Global Change Biology 10(12), 2078-2091.

Peltoniemi, M., Thürig, E., Ogle, S., Palosuo, T., Schrump, M., Wutzler, T., Butterbach-Bahl, K., Chertov, O., Komarov, A., Mikhailov, A., 2007. Models in country scale carbon accounting of forest soils. Silva Fennica 41(3), 575.

Penne, C., Ahrends, B., Deurer, M., Böttcher, J., 2010. The impact of the canopy structure on the spatial variability in forest floor carbon stocks. Geoderma 158(3–4), 282-297.

Pesonen, A., Maltamo, M., Eerikäinen, K., Packalèn, P., 2008. Airborne laser scanning-based prediction of coarse woody debris volumes in a conservation area. Forest Ecology and Management 255(8–9), 3288-3296.

Petersson, H., Ståhl, G., 2006. Functions for below-ground biomass of Pinus sylvestris, Picea abies, Betula pendula and Betula pubescens in Sweden. Scandinavian Journal of Forest Research 21(S7), 84-93.

Pfeifer, N., Gorte, B., Elberink, S.O., 2004. Influences of vegetation on laser altimetry–analysis and correction approaches. International Archives of Photogrammetry, Remote Sensing and Spatial Information Sciences 36(part 8), W2.

Polyakova, O., Billor, N., 2007. Impact of deciduous tree species on litterfall quality, decomposition rates and nutrient circulation in pine stands. Forest Ecology and Management 253(1), 11-18.

Post, W.M., Izaurralde, R.C., Mann, L.K., Bliss, N., 2001. Monitoring and verifying changes of organic carbon in soil. Climatic Change 51(1), 73-99.

Poussart, J.-N., Ardö, J., Olsson, L., 2004. Verification of soil carbon sequestration—Sample requirements. Environmental Management 33(0), S416-S425.

Pregitzer, K.S., Euskirchen, E.S., 2004. Carbon cycling and storage in world forests: biome patterns related to forest age. Global Change Biology 10(12), 2052-2077.

Prescott, C.E., Vesterdal, L., 2013. Tree species effects on soils in temperate and boreal forests: emerging themes and research needs. Forest Ecology and Management 309, 1-3.

Price, O.R., Oliver, M.A., Walker, A., Wood, M., 2009. Estimating the spatial scale of herbicide and soil interactions by nested sampling, hierarchical analysis of variance and residual maximum likelihood. Environmental Pollution 157(5), 1689-1696.

R Core Team, 2013. R: A language and environment for statistical computing. R Foundation for Statistical Computing, Vienna, Austria.

Rawlins, B.G., Scheib, A.J., Lark, R.M., Lister, T.R., 2009. Sampling and analytical plus subsampling variance components for five soil indicators observed at regional scale. European Journal of Soil Science 60(5), 740-747.

Reich, P.B., Peterson, D.W., Wedin, D.A., Wrage, K., 2001. Fire and vegetation effects on productivity and nitrogen cycling across a forest-grassland continuum. Ecology 82(6), 1703-1719.

Rice, W.R., 1989. Analyzing tables of statistical tests. Evolution 43(1), 223-225.

Riley, S.J., DeGloria, S.D., Elliot, R., 1999. A terrain ruggedness index that quantifies topographic heterogeneity. intermountain Journal of sciences 5(1-4), 23-27.

Ripley, B.D., 1977. Modelling spatial patterns. Journal of the Royal Statistical Society. Series B (Methodological), 172-212.

Rossi, J., Govaerts, A., De Vos, B., Verbist, B., Vervoort, A., Poesen, J., Muys, B., Deckers, J., 2009. Spatial structures of soil organic carbon in tropical forests—A case study of Southeastern Tanzania. Catena 77(1), 19-27.

Schulp, C.J.E., Nabuurs, G.J., Verburg, P.H., de Waal, R.W., 2008. Effect of tree species on carbon stocks in forest floor and mineral soil and implications for soil carbon inventories. Forest Ecology and Management 256(3), 482-490.

Schöning, I., Totsche, K.U., Kögel-Knabner, I., 2006. Small scale spatial variability of organic carbon stocks in litter and solum of a forested Luvisol. Geoderma 136(3–4), 631-642.

Seedre, M., Shrestha, B., Chen, H.H., Colombo, S., Jõgiste, K., 2011. Carbon dynamics of North American boreal forest after stand replacing wildfire and clearcut logging. J For Res 16(3), 168-183.

Seibert, J., Stendahl, J., Sørensen, R., 2007. Topographical influences on soil properties in boreal forests. Geoderma 141(1–2), 139-148.

Shanin, V., Komarov, A., Mäkipää, R., 2013. Tree species composition affects productivity and carbon dynamics of different site types in boreal forests. European Journal of Forest Research, 1-14.

Shapiro, S.S., Wilk, M.B., 1965. An analysis of variance test for normality (complete samples). Biometrika 52(3-4), 591-611.

192

Shaw, C., Boyle, J., Omule, A., 2008. Estimating forest soil carbon and nitrogen stocks with double sampling for stratification. Soil Science Society of America Journal 72(6), 1611-1620.

Siitonen, J., Martikainen, P., Punttila, P., Rauh, J., 2000. Coarse woody debris and stand characteristics in mature managed and old-growth boreal mesic forests in southern Finland. Forest Ecology and Management 128(3), 211-225.

Simbahan, G.C., Dobermann, A., Goovaerts, P., Ping, J., Haddix, M.L., 2006. Fine-resolution mapping of soil organic carbon based on multivariate secondary data. Geoderma 132(3–4), 471-489.

Simonson, R.W., 1959. Outline of a generalized theory of soil genesis. Soil Science Society of America Journal 23(2), 152-156.

Singh, K., Murphy, B.W., Marchant, B.P., 2013. Towards cost-effective estimation of soil carbon stocks at the field scale. Soil Research 50(8), 672-684.

Soja, A.J., Tchebakova, N.M., French, N.H.F., Flannigan, M.D., Shugart, H.H., Stocks, B.J., Sukhinin, A.I., Parfenova, E.I., Chapin III, F.S., Stackhouse Jr, P.W., 2007. Climate-induced boreal forest change: Predictions versus current observations. Global and Planetary Change 56(3-4), 274-296.

Sokal, R.R., Rohlf, F.J., 1995. Biometry: the principles and practice ofstatistics in biological research. State University of New Yorkat Stony Brook. 3 ed. W. H. Freeman, New York.

Solberg, S., Brunner, A., Hanssen, K.H., Lange, H., Næsset, E., Rautiainen, M., Stenberg, P., 2009. Mapping LAI in a Norway spruce forest using airborne laser scanning. Remote Sensing of Environment 113(11), 2317-2327.

Stage, A.R., 1976. Notes: An expression for the effect of aspect, slope, and habitat type on tree growth. Forest Science 22(4), 457-460.

Stendahl, J., Johansson, M., Eriksson, E., Langvall, O., 2010. Soil organic carbon in Swedish Spruce and Pine forests - differences in stock levels and regional patterns. Silva Fennica 44(1), 5-21.

Stephens, P.R., Kimberley, M.O., Beets, P.N., Paul, T.S., Searles, N., Bell, A., Brack, C., Broadley, J., 2012. Airborne scanning LiDAR in a double sampling forest carbon inventory. Remote Sensing of Environment 117, 348-357.

Stockmann, U., Adams, M.A., Crawford, J.W., Field, D.J., Henakaarchchi, N., Jenkins, M., Minasny, B., McBratney, A.B., Courcelles, V.d.R.d., Singh, K., Wheeler, I., Abbott, L., Angers, D.A., Baldock, J., Bird, M., Brookes, P.C., Chenu, C., Jastrow, J.D., Lal, R., Lehmann, J., O'Donnell, A.G., Parton, W.J., Whitehead, D., Zimmermann, M., 2013. The knowns, known unknowns and unknowns of sequestration of soil organic carbon. Agriculture, Ecosystems & Environment 164(0), 80-99.

Ståhl, G., 2004. Methodological options for quantifying changes in carbon pools in Swedish forests.

Särndal, C.-E., Swensson, B., Wretman, J., 2003. Model assisted survey sampling. Springer Science & Business Media.

Tenenbein, A., 1970. A double sampling scheme for estimating from binomial data with misclassifications. Journal of the American Statistical Association 65(331), 1350-1361.

Thompson, J.A., Kolka, R.K., 2005. Soil carbon storage estimation in a forested watershed using quantitative soil-landscape modeling. Soil Science Society of America Journal 69(4), 1086-1093.

Thompson, S.K., 2012. Sampling. John Wiley & Sons, New York.

Throop, H.L., Archer, S.R., Monger, H.C., Waltman, S., 2012. When bulk density methods matter: Implications for estimating soil organic carbon pools in rocky soils. Journal of Arid Environments 77(0), 66-71.

Trumbore, S., 2009. Radiocarbon and soil carbon dynamics. Annual Review of Earth and Planetary Sciences 37, 47-66.

Upchurch, D.R., Edmonds, W.J., 1991. Statistical procedures for specific objectives. Spatial variabilities of soils and landforms (spatialvariabil), 49-71.

van der Hoeven, N., 2008. Calculation of the minimum significant difference at the NOEC using a non-parametric test. Ecotoxicology and environmental safety 70(1), 61-66.

van Groenigen, J.W., 2000. The influence of variogram parameters on optimal sampling schemes for mapping by kriging. Geoderma 97(3–4), 223-236.

van Groenigen, J.W., Siderius, W., Stein, A., 1999. Constrained optimisation of soil sampling for minimisation of the kriging variance. Geoderma 87(3–4), 239-259.

Van Laar, A., Akça, A., 2007. Forest mensuration, 13. 2 ed. Springer Science & Business Media, Netherlands.

Van Leeuwen, M., Nieuwenhuis, M., 2010. Retrieval of forest structural parameters using LiDAR remote sensing. European Journal of Forest Research 129(4), 749-770.

VandenBygaart, A.J., Gregorich, E.G., Angers, D.A., McConkey, B.G., 2007. Assessment of the lateral and vertical variability of soil organic carbon. Canadian Journal of Soil Science 87(4), 433-444.

Vehmas, M., Eerikäinen, K., Peuhkurinen, J., Packalén, P., Maltamo, M., 2009. Identification of boreal forest stands with high herbaceous plant diversity using airborne laser scanning. Forest Ecology and Management 257(1), 46-53.

Vehmas, M., Packalén, P., Maltamo, M., Eerikäinen, K., 2011. Using airborne laser scanning data for detecting canopy gaps and their understory type in mature boreal forest. Annals of Forest Science 68(4), 825-835.

Vepakomma, U., St-Onge, B., Kneeshaw, D., 2008. Spatially explicit characterization of boreal forest gap dynamics using multi-temporal lidar data. Remote Sensing of Environment 112(5), 2326-2340.

Vesterdal, L., Clarke, N., Sigurdsson, B.D., Gundersen, P., 2013. Do tree species influence soil carbon stocks in temperate and boreal forests? Forest Ecology and Management 309(0), 4-18.

Wahba, G., 1990. Spline models for observational data, 59. Siam.

Wardle, D.A., Bardgett, R.D., Klironomos, J.N., Setälä, H., van der Putten, W.H., Wall, D.H., 2004. Ecological linkages between aboveground and belowground Biota. Science 304(5677), 1629-1633.

Wardle, D.A., Jonsson, M., Bansal, S., Bardgett, R.D., Gundale, M.J., Metcalfe, D.B., 2012. Linking vegetation change, carbon sequestration and biodiversity: insights from island ecosystems in a long-term natural experiment. Journal of Ecology 100(1), 16-30.

Webster, R., Oliver, M.A., 1992. Sample adequately to estimate variograms of soil properties. Journal of Soil Science 43(1), 177-192.

Webster, R., Oliver, M.A., 2001. Geostatistics for environmental scientists. John Wiley & Sons, Chichester.

Weishampel, P., Kolka, R., King, J.Y., 2009. Carbon pools and productivity in a 1-km 2 heterogeneous forest and peatland mosaic in Minnesota, USA. Forest Ecology and Management 257(2), 747-754.

Wirth, C., Gleixner, G., Heimann, M., 2009. Old-growth forests: function, fate, and value, 1. 1 ed. Springer, Berlin Heidelberg.

Worsham, L., Markewitz, D., Nibbelink, N.P., West, L.T., 2012. A comparison of three field sampling methods to estimate soil carbon content. Forest Science 58(5), 513-522.

Yanai, R.D., Stehman, S.V., Arthur, M.A., Prescott, C.E., Friedland, A.J., Siccama, T.G., Binkley, D., 2003. Detecting change in forest floor carbon. Soil Sci. Soc. Am. J. 67(5), 1583-1593.

Yarwood, S.A., Myrold, D.D., Högberg, M.N., 2009. Termination of belowground C allocation by trees alters soil fungal and bacterial communities in a boreal forest. FEMS Microbiology Ecology 70(1), 151-162.

Youden, W., Mehlich, A., 1937. Selection of efficient methods for soil sampling. Contributions of the Boyce Thompson institute for plant research 9, 59-70.

Zar, J.H., 2010. Biostatistical analysis. 5 ed. Prentice Hall, Boston.

Zevenbergen, L.W., Thorne, C.R., 1987. Quantitative analysis of land surface topography. Earth Surface Processes and Landforms 12(1), 47-56.

Ziadat, F.M., 2005. Analyzing digital terrain attributes to predict soil attributes for a relatively large area. Soil Science Society of America Journal 69(5), 1590-1599.

Ørka, H.O., Næsset, E., Bollandsås, O.M., 2009. Classifying species of individual trees by intensity and structure features derived from airborne laser scanner data. Remote Sensing of Environment 113(6), 1163-1174.

Ågren, G., Hyvönen, R., Nilsson, T., 2007. Are Swedish forest soils sinks or sources for CO_2—model analyses based on forest inventory data. Biogeochemistry 82(3), 217-227.

Appendix

Table A1. Lidar variables

Id	From	Name	Short	First/both	Reference/Note
1	Field	Basal area	Ba	Both	
2	Lidar ground	Elevation	Elev	Both	
3	Lidar ground	Slope	Slope	Both	
4	Lidar ground	Aspect	Aspect	Both	
5	Lidar ground	Slope Degrees	SlopeDeg	Both	Stage (1976)
6	Lidar ground	Aspect Degrees	AspectDeg	Both	Stage (1976)
7	Lidar ground	Topographic Ruggedness Index	TRI	Both	Riley et al. (1999)
8	Lidar ground	Topographic Position Index	TPI	Both	Guisan et al. (1999)
9	Lidar ground	Curvature	Curvature	Both	Zevenbergen and Thorne (1987)
10	Lidar ground	Topographic Wetness Index	TWI	Both	Gessler et al. (1995)
11	Lidar Overstory	Height Percentile$_{10}$	h_{10}	First	
12	Lidar Overstory	Height Percentile$_{20}$	h_{20}	First	
13	Lidar Overstory	Height Percentile$_{30}$	h_{30}	First	
14	Lidar Overstory	Height Percentile$_{40}$	h_{40}	First	

15	Lidar Overstory	Height Percentile$_{50}$	h_{50}	First
16	Lidar Overstory	Height Percentile$_{60}$	h_{60}	First
17	Lidar Overstory	Height Percentile$_{70}$	h_{70}	First
18	Lidar Overstory	Height Percentile$_{80}$	h_{80}	First
19	Lidar Overstory	Height Percentile$_{90}$	h_{90}	First
20	Lidar Overstory	Height Percentile$_{95}$	h_{95}	First
21	Lidar Overstory	Height Percentile$_{mean}$	h_{mean}	First
22	Lidar Overstory	Height$_{CV}$	h_{CV}	First
23	Lidar Overstory	Canopy Density$_0$	Cd_0	First
24	Lidar Overstory	Canopy Density$_{10}$	Cd_{10}	First
25	Lidar Overstory	Canopy Density$_{20}$	Cd_{20}	First
26	Lidar Overstory	Canopy Density$_{30}$	Cd_{30}	First
27	Lidar Overstory	Canopy Density$_{40}$	Cd_{40}	First
28	Lidar Overstory	Canopy Density$_{50}$	Cd_{50}	First
29	Lidar Overstory	Canopy Density$_{60}$	Cd_{60}	First
30	Lidar Overstory	Canopy Density$_{70}$	Cd_{70}	First
31	Lidar Overstory	Canopy Density$_{80}$	Cd_{80}	First
32	Lidar Overstory	Canopy Density$_{90}$	Cd_{90}	First

33	Lidar Overstory	Stratum 1	$Strat_1$	First	From 1.5 - 2.5
34	Lidar Overstory	Stratum 2	$Strat_2$	First	From 2.5 - 5
35	Lidar Overstory	Stratum 3	$Strat_3$	First	From 5 - 10
36	Lidar Overstory	Stratum 4	$Strat_4$	First	From 10 - 20
37	Lidar Overstory	Stratum 5	$Strat_5$	First	From >20
38	Lidar Understory	Height Percentile$_{10}$ - Filter 1	$UhF1B_{10}$	Both	From 0.01
39	Lidar Understory	Height Percentile$_{20}$ - Filter 1	$UhF1B_{20}$	Both	From 0.01
40	Lidar Understory	Height Percentile$_{30}$ - Filter 1	$UhF1B_{30}$	Both	From 0.01
41	Lidar Understory	Height Percentile$_{40}$ - Filter 1	$UhF1B_{40}$	Both	From 0.01
42	Lidar Understory	Height Percentile$_{50}$ - Filter 1	$UhF1B_{50}$	Both	From 0.01
43	Lidar Understory	Height Percentile$_{60}$ - Filter 1	$UhF1B_{60}$	Both	From 0.01
44	Lidar Understory	Height Percentile$_{70}$ - Filter 1	$UhF1B_{70}$	Both	From 0.01
45	Lidar Understory	Height Percentile$_{80}$ - Filter 1	$UhF1B_{80}$	Both	From 0.01
46	Lidar Understory	Height Percentile$_{90}$ - Filter 1	$UhF1B_{90}$	Both	From 0.01
47	Lidar Understory	Height Percentile$_{mean}$	UhB_{mean}	Both	From 0.01
48	Lidar Understory	Height Percentile$_{10}$ - Filter 2	$UhF2B_{10}$	Both	From 0.2
49	Lidar Understory	Height Percentile$_{20}$ - Filter 2	$UhF2B_{20}$	Both	From 0.2
50	Lidar Understory	Height Percentile$_{30}$ - Filter 2	$UhF2B_{30}$	Both	From 0.2

51	Lidar Understory	Height Percentile$_{40}$ - Filter 2	UhF2B$_{40}$	Both	From 0.2
52	Lidar Understory	Height Percentile$_{50}$ - Filter 2	UhF1B$_{50}$	Both	From 0.2
53	Lidar Understory	Height Percentile$_{60}$ - Filter 2	UhF2B$_{60}$	Both	From 0.2
54	Lidar Understory	Height Percentile$_{70}$ - Filter 2	UhF2B$_{70}$	Both	From 0.2
55	Lidar Understory	Height Percentile$_{80}$ - Filter 2	UhF$_2$B$_{80}$	Both	From 0.2
56	Lidar Understory	Height Percentile$_{90}$ - Filter 2	UhF$_2$B$_{90}$	Both	From 0.2
57	Lidar Understory	Height Percentile$_{mean}$ - Filter 2	UhF$_2$B$_{mean}$	Both	From 0.2
58	Lidar Understory	Height Percentile$_{10}$ - Filter 1	UhF1F$_{10}$	First	From 0.01
59	Lidar Understory	Height Percentile$_{20}$ - Filter 1	UhF1F$_{20}$	First	From 0.01
60	Lidar Understory	Height Percentile$_{30}$ - Filter 1	UhF1F$_{30}$	First	From 0.01
61	Lidar Understory	Height Percentile$_{40}$ - Filter 1	UhF1F$_{40}$	First	From 0.01
62	Lidar Understory	Height Percentile$_{50}$ - Filter 1	UhF1F$_{50}$	First	From 0.01
63	Lidar Understory	Height Percentile$_{60}$ - Filter 1	UhF1F$_{60}$	First	From 0.01
64	Lidar Understory	Height Percentile$_{70}$ - Filter 1	UhF1F$_{70}$	First	From 0.01
65	Lidar Understory	Height Percentile$_{80}$ - Filter 1	UhF1F$_{80}$	First	From 0.01
66	Lidar Understory	Height Percentile$_{90}$ - Filter 1	UhF1F$_{90}$	First	From 0.01
67	Lidar Understory	Height Percentile$_{mean}$	UhF1F$_{mean}$	First	From 0.01
68	Lidar Understory	Height Percentile$_{10}$ - Filter 2	UhF2F$_{10}$	First	From 0.2

69	Lidar Understory	Height Percentile$_{20}$ - Filter 2	UhF2F$_{20}$	First	From 0.2
70	Lidar Understory	Height Percentile$_{30}$ - Filter 2	UhF2F$_{30}$	First	From 0.2
71	Lidar Understory	Height Percentile$_{40}$ - Filter 2	UhF2F$_{40}$	First	From 0.2
72	Lidar Understory	Height Percentile$_{50}$ - Filter 2	UhF2F$_{50}$	First	From 0.2
73	Lidar Understory	Height Percentile$_{60}$ - Filter 2	UhF2F$_{60}$	First	From 0.2
74	Lidar Understory	Height Percentile$_{70}$ - Filter 2	UhF2F$_{70}$	First	From 0.2
75	Lidar Understory	Height Percentile$_{80}$ - Filter 2	UhF2F$_{80}$	First	From 0.2
76	Lidar Understory	Height Percentile$_{90}$ - Filter 2	Uh$_{F2}$F$_{90}$	First	From 0.2
77	Lidar Understory	Height Percentile$_{mean}$ - Filter 2	UhF2F$_{mean}$	First	From 0.2
78	Lidar Understory	Density Stratum 1 - Filter 1	UdF1B$_1$	Both	From 0.01 - 0.5
79	Lidar Understory	Density Stratum 2 - Filter 1	UdF1B$_2$	Both	From 0.5 to 1
80	Lidar Understory	Density Stratum 3 - Filter 1	UdF1B$_3$	Both	From 1 to 1.5
81	Lidar Understory	Density Stratum 1 - Filter 2	UdF2B$_1$	Both	From 0.2 - 0.5
82	Lidar Understory	Density Stratum 2 - Filter 2	UdF2B$_2$	Both	From 0.5 to 1
83	Lidar Understory	Density Stratum 3 - Filter 2	UdF2B$_3$	Both	From 1 to 1.5
84	Lidar Understory	Density Stratum 1 - Filter 1	UdF1F$_1$	First	From 0.01 - 0.2
85	Lidar Understory	Density Stratum 2 - Filter 1	UdF1F$_2$	First	From 0.2 to 1
86	Lidar Understory	Density Stratum 3 - Filter 1	UdF1F$_3$	First	From 1 to 1.5

87	Lidar Understory	Density Stratum 1 - Filter 2	$UdF2F_1$	First	From 0.01 - 0.2
88	Lidar Understory	Density Stratum 2 - Filter 2	$UdF2F_2$	First	From 0.2 to 1
89	Lidar Understory	Density Stratum 3 - Filter 2	$UdF2F_3$	First	From 1 to 1.5
90	Lidar Understory	Proportion Non Ground - Filter 1	$UF1B_i$	Both	From 0.01 to 1.5
91	Lidar Understory	Proportion Non Ground - Filter 2	$UF2B_i$	Both	From 0.2 to 1.5
92	Lidar Understory	Proportion Non Ground - Filter 1	$UF1F_i$	First	From 0.01 to 1.5
93	Lidar Understory	Proportion Non Ground - Filter 2	$UF2F_i$	First	From 0.2 to 1.5

Note: To explore the use of lidar data in mapping and quantifying forest C stocks we used echoes from the *first* returns only and a combination of *both* first and last returns. *From* represent the cutoff height or bin range (in m) of lidar echo.
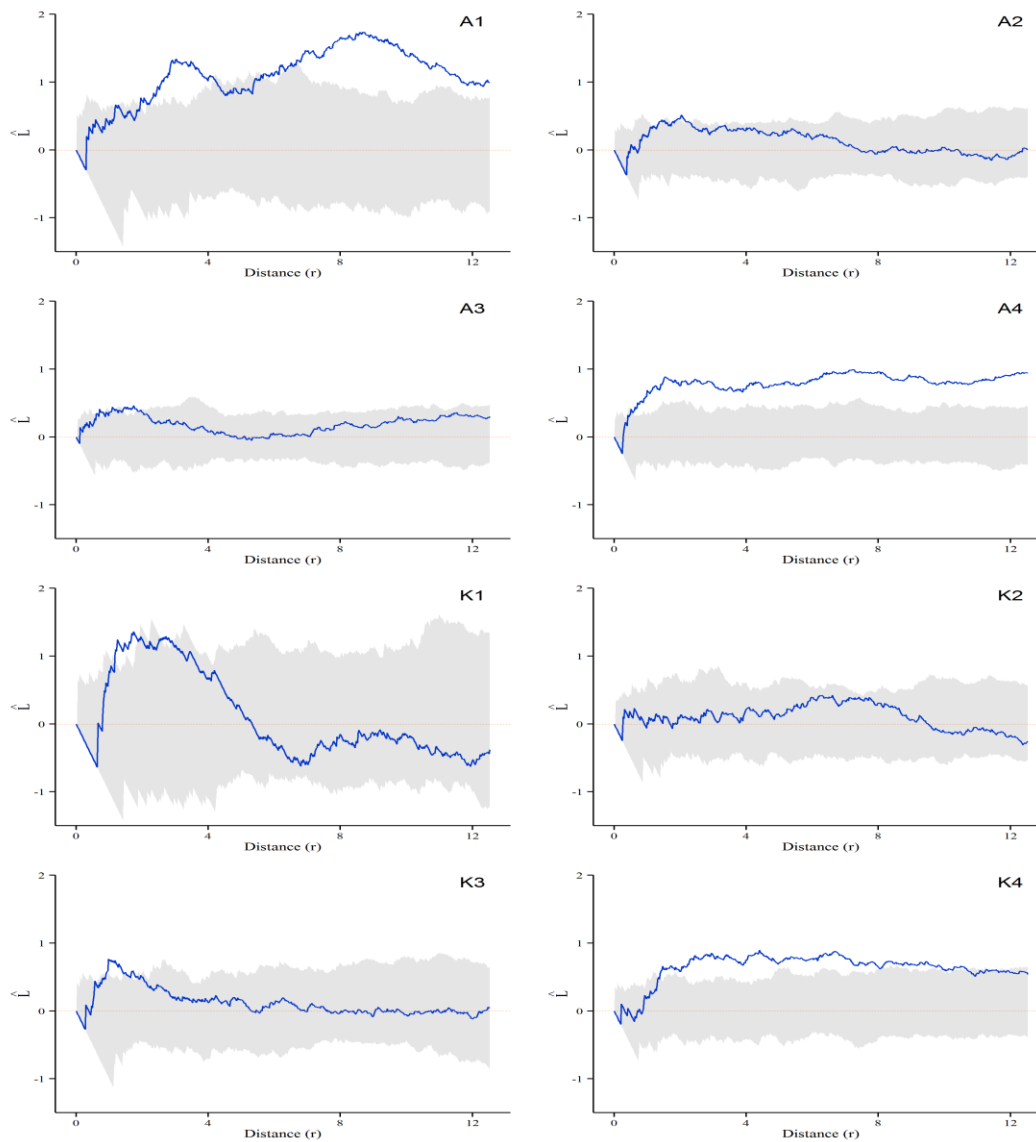
Figure A1. Spatial distribution of stems. Solid line represents the $\hat{L}(r)$ statistics for the observed pattern; where distance is the inter-tree distance in meters. Positive values of $\hat{L}(r)$ indicate spatial aggregation, while negative values indicate spatial regularity. The shaded area corresponds to confident envelopes calculated by 999 Monte-Carlo simulations.